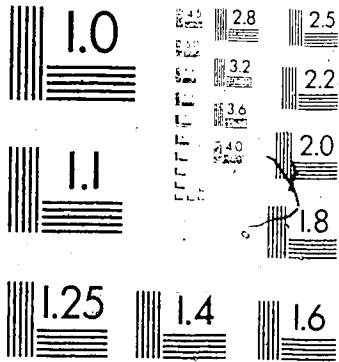


# 1



**MICRO**



National Library  
of Canada

Bibliothèque nationale  
du Canada

Canadian Theses Service

Service des thèses canadiennes

Ottawa, Canada  
K1A 0N4

## NOTICE

The quality of this microform is heavily dependent upon the quality of the original thesis submitted for microfilming. Every effort has been made to ensure the highest quality of reproduction possible.

If pages are missing, contact the university which granted the degree.

Some pages may have indistinct print especially if the original pages were typed with a poor typewriter ribbon or if the university sent us an inferior photocopy.

Previously copyrighted materials (journal articles, published tests, etc.) are not filmed.

Reproduction in full or in part of this microform is governed by the Canadian Copyright Act, R.S.C. 1970, c. C-30.

## AVIS

La qualité de cette microforme dépend grandement de la qualité de la thèse soumise au microfilmage. Nous avons tout fait pour assurer une qualité supérieure de reproduction.

S'il manque des pages, veuillez communiquer avec l'université qui a conféré le grade.

La qualité d'impression de certaines pages peut laisser à désirer, surtout si les pages originales ont été dactylographiées à l'aide d'un ruban usé ou si l'université nous a fait parvenir une photocopie de qualité inférieure.

Les documents qui ont déjà l'objet d'un droit d'auteur (articles de revue, tests publiés, etc.) ne sont pas microfilmés.

La reproduction, même partielle, de cette microforme est soumise à la Loi canadienne sur le droit d'auteur, SRC 1970, c. C-30.

THE UNIVERSITY OF ALBERTA

THE CONFORMATIONAL PROPERTIES OF MALTOSE,  
MALTOTRIOSE AND AMYLOSE

by



Eugenio Alvarado

A THESIS

SUBMITTED TO THE FACULTY OF GRADUATE STUDIES AND RESEARCH  
IN PARTIAL FULFILMENT OF THE REQUIREMENTS FOR THE DEGREE  
OF DOCTOR OF PHILOSOPHY

DEPARTMENT OF CHEMISTRY

EDMONTON, ALBERTA

FALL, 1987

Permission has been granted to the National Library of Canada to microfilm this thesis and to lend or sell copies of the film.

The author (copyright owner) has reserved other publication rights, and neither the thesis nor extensive extracts from it may be printed or otherwise reproduced without his/her written permission.

L'autorisation a été accordée à la Bibliothèque nationale du Canada de microfilmer cette thèse et de prêter ou de vendre des exemplaires du film.

L'auteur (titulaire du droit d'auteur) se réserve les autres droits de publication; ni la thèse ni de longs extraits de celle-ci ne doivent être imprimés ou autrement reproduits sans son autorisation écrite.

ISBN 0-315-41054-X

# THE UNIVERSITY OF ALBERTA

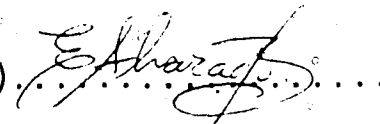
## RELEASE FORM

NAME OF AUTHOR: Eugenio Alvarado  
TITLE OF THESIS: The Conformational Properties of Maltose,  
Maltotriose and Amylose.  
DEGREE FOR WHICH THESIS WAS PRESENTED:  
Doctor of Philosophy  
YEAR THIS DEGREE GRANTED: 1987

Permission is hereby granted to THE UNIVERSITY OF ALBERTA LIBRARY to reproduce single copies of this thesis and to lend or sell such copies for private, scholarly or scientific research purposes only.

The author reserves other publications rights, and neither the thesis nor extensive extracts from it may be printed or otherwise reproduced without the author's written permission.

(Signed) .....



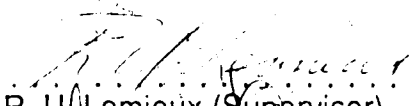
Permanent address:  
Heredia; Avenida Central,  
Calles 6 - 8,  
COSTA RICA.

DATED: May 27, 1987.

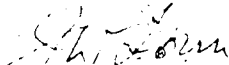
# THE UNIVERSITY OF ALBERTA

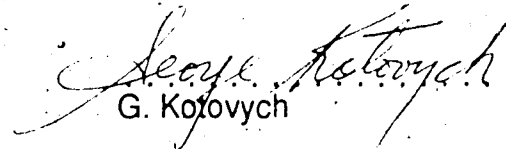
## FACULTY OF GRADUATE STUDIES AND RESEARCH

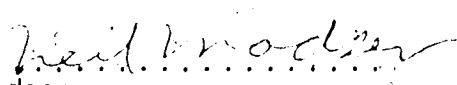
The undersigned certify that they have read, and recommend to the Faculty of Graduate Studies and Research, for acceptance, a thesis entitled "*The Conformational Properties of Maltose, Maltotriose and Amylose*" submitted by Eugenio Alvarado in partial fulfilment of the requirements for the degree of Doctor of Philosophy.


  
R. U. Lemieux (Supervisor)

  
H. J. Liu

  
J. W. Lown

  
G. Kotovych

  
N. Madsen

  
C. E. Ballou (External Examiner)

DATE: *May 27*, 1987

*To my parents.*

## ABSTRACT

The conformational preference of methyl  $\alpha$ -maltoside and related compounds in deuterium oxide and dimethyl sulfoxide- $d_6$  solutions was studied by nuclear magnetic resonance spectroscopy including the determination of nuclear Overhauser enhancements and deuterium isotope shifts. The compounds studied were; methyl  $\beta$ -maltoside, methyl  $\alpha$ -maltoside, 1,2-dideoxymaltose, methyl 3-deoxy- $\alpha$ -maltoside, methyl 6,6'-dideoxy- $\alpha$ -maltoside, methyl 6-deoxy- $\beta$ -maltoside, methyl 4-O-( $\alpha$ -D-glucopyranosyl)- $\alpha$ -D-mannopyranoside, methyl 4-O-( $\alpha$ -D-glucopyranosyl)- $\alpha$ -D-xylopyranoside and methyl  $\alpha$ -maltotrioside.

It was demonstrated that HSEA calculations yield conformations that are close to the experimental values provided by the nuclear Overhauser enhancements. Calculation of conformational preference without inclusion of the *exo*-anomeric effect did not reproduce the experimental nuclear Overhauser enhancements.

The nuclear Overhauser enhancements require different conformational preferences in water than in dimethyl sulfoxide solution. For the maltoside in dimethyl sulfoxide, the abundant conformers are favorable to intramolecular hydrogen bonding between OH-2' and OH-3. In the case of the xyloside, an intramolecular hydrogen bond between OH-2' and O-1' is formed. The different conformational preferences exhibited by methyl  $\alpha$ -maltoside and  $\alpha$ -xyloside suggest that, for the maltosides, non-bonded interactions between H-5' and the hydroxymethyl group dominate the *exo*-anomeric effect. The preferred conformer for the maltosides both in water and in dimethyl sulfoxide



differ from those found in the crystal structures of  $\alpha$ -maltose and methyl  $\beta$ -maltoside but are close to those of methyl  $\alpha$ -maltotrioside,  $V_h$ -amylose and B-amylose.

The results of this study are in accord with the expectation that solvation of glycosides by water strengthens the *exo*-anomeric effect.

## ACKNOWLEDGEMENTS

The author wishes to express his sincere gratitude to his research director, Professor R. U. Lemieux, for his invaluable guidance and encouragement during the course of this work and also for his interest and assistance in the preparation of this thesis.

The author would also like to thank Dr. U. Spohr, Mr. M. Ralitsch and Ms. A. Morales for their help and support during the preparation of this thesis, Professor K. Bock provided samples of compounds necessary in the development of this investigation as well as helpful discussions. The invaluable ideas, discussions and the continuous encouragement and friendship provided by Dr. O. Hindsgaul are deeply appreciated.

The author would also like to thank the Department of Chemistry of The University of Alberta for financial support and the Alberta Heritage Foundation for Medical Research for the award of a studentship (June, 1984 to May, 1987).

## TABLE OF CONTENTS

Abstract . . . . .	v
Acknowledgements . . . . .	vii
List of Tables . . . . .	x
List of Figures . . . . .	xii
List of Schemes . . . . .	xvii
I. INTRODUCTION . . . . .	1
1. Historical Overview . . . . .	1
2. Objectives of this study . . . . .	4
3. Conformational analysis . . . . .	5
3.1. X-ray studies . . . . .	6
3.2. Optical rotation studies . . . . .	10
3.3. Nuclear magnetic resonance spectroscopy . . . . .	12
3.3.1. Chemical shifts . . . . .	13
3.3.2. Coupling constants . . . . .	14
3.3.3. Spin-Lattice relaxation times . . . . .	16
3.3.4. Nuclear Overhauser enhancements . . . . .	17
3.4. Theoretical calculations . . . . .	20
3.4.1. Quantum mechanical procedures . . . . .	20
3.4.2. Semi-empirical calculations . . . . .	21
3.4.2.1. Force field calculations for maltose and methyl maltosides . . . . .	26
3.4.2.2. Hard-sphere <i>exo</i> -anomeric calculations (HSEA) . . . . .	29

II. EXPERIMENTAL .....	32
1. General methods .....	32
2. NMR spectroscopy .....	32
3. The calculation of conformational preference .....	34
4. Synthesis .....	35
III. DISCUSSION .....	48
1. Synthesis .....	48
2. The model compounds .....	58
3. HSEA calculations .....	61
4. Chemical Shifts .....	67
5. Nuclear Overhauser enhancements .....	78
5.1. Theoretical relative nuclear Overhauser enhancements .....	78
5.2. Experimental nuclear Overhauser enhancements .....	80
6. Hydrogen bonding studies .....	90
7. Conclusions .....	104
IV. REFERENCES .....	114

## LIST OF TABLES

<u>Table</u>	<u>Title</u>	<u>Page</u>
1	Observed solid state conformations about intersugar bonds of maltose analogs. . . . .	7
2	Conformational distribution for methyl $\alpha$ -maltoside obtained by Kochetkov <i>et al.</i> <sup>56</sup> . . . . .	27
3	Conformational distribution for $\beta$ -maltose obtained by Melberg and Rasmussen. <sup>90</sup> . . . . .	28
4	The conformational equilibrium for maltose calculated by Tvaroska and Pérez <sup>92</sup> . . . . .	29
5	Structures of the model compounds that were used in the development of this thesis. . . . .	59
6	Conformational preferences and energies as indicated by HSEA calculations setting $\omega = -90^\circ$ and $\tau = 117^\circ$ . . . . .	62
7	The $^1\text{H}$ -n.m.r. chemical shifts ( $\delta$ , ppm) for the compounds listed in Table 5. . . . .	68
8	The $^1\text{H}$ -n.m.r. coupling constants ( $^3J$ , Hz) for the compounds listed in Table 5. . . . .	69
9	The $^1\text{H}$ -n.m.r. chemical shifts ( $\delta$ , ppm) for the compounds listed in Table 5. . . . .	70
10	The $^1\text{H}$ -n.m.r. coupling constants ( $^3J$ , Hz) for the compounds listed in Table 5. . . . .	71
11	Specific interunit deshielding of the anomeric hydrogen of $\alpha$ -linked disaccharides because of non-bonded interaction with an oxygen atom. . . . .	72
12	$^1\text{H}$ -n.m.r. chemical shifts and vicinal coupling constants for methyl $\alpha$ -maltoside (13) and methyl $\alpha$ -maltotrioside (4) in $\text{D}_2\text{O}$ at 295 °K. . . . .	73
13	The $^{13}\text{C}$ -n.m.r. chemical shifts (ppm) in $\text{D}_2\text{O}$ at 305 °K for the compounds listed in Table 5. . . . .	74
14	The $^{13}\text{C}$ -n.m.r. chemical shifts (ppm) in $\text{DMSO}-d_6$ at 305 °K for the compounds listed in Table 5. . . . .	75
15	Theoretical relative nuclear Overhauser enhancements . . . . .	79

<u>Table</u>	<u>Title</u>	<u>Page</u>
16	Carbon-13 spin-lattice relaxation times $T_1$ (s) of methyl $\beta$ -maltoside (18) in $D_2O$ and in $DMSO-d_6$ .....	81
17	Experimental relative nuclear Overhauser enhancements.....	82
18	Comparison of theoretical and experimental n.O.e.'s when H-3eq of methyl 3-deoxy- $\alpha$ -maltoside (1) was saturated.....	89
19	Experimental n.O.e.'s obtained when $CH_3$ -6 of methyl 6-deoxy- $\beta$ -maltoside (2) was saturated.....	90
20	Deuterium isotope shifts in $DMSO-d_6$ , ppm.....	93
21	Comparison of calculated and experimental linkage coupling constants for methyl maltosides.....	108
22	Comparison of experimental and calculated nuclear Overhauser enhancements.....	109
23	Comparison of the experimental relative n.O.e. with those calculated for methyl $\alpha$ -maltoside, using the results of Kochetkov <i>et al.</i> <sup>56</sup> and of HSEA calculations.....	112

## LIST OF FIGURES

<u>Figure</u>	<u>Title</u>	<u>Page</u>
1	Partial chemical-structure of amylose. ....	1
2	Partial chemical structure of amylopectin. ....	2
3	$\alpha$ -Maltose ( 4-O-( $\alpha$ -D-glucopyranosyl)- $\alpha$ -D-glucopyranoside ) and designations for torsion angles. ....	3
4	Observed solid state conformations of maltose and analogs in relation to the internuclear distances between O-3 and O-2'. The numbers correspond to the compounds listed in Table 1. The shadowed area indicates the conformations that give rise to an intramolecular hydrogen bond between O-3 and O-2'. ....	8
5	Experimental evidence <sup>52,54</sup> for the Karplus-type relationship between <sup>13</sup> C to vicinal <sup>1</sup> H coupling and the torsion angles these atoms define. ....	15
6	Measurement of the <sup>1</sup> H-n.m.r. spectrum of methyl $\alpha$ -maltoside with saturation of H-1' may lead to major enhancement of the signals for hydrogens in close vicinity such as H-4 and H-2'. ....	18
7	The interaction between two atoms depending on their separation as provided by the Lennard-Jones potential. ....	23
8	The changes in bond energy expected by <i>ab initio</i> calculation <sup>66</sup> as the orientation of the aglycon is changed by rotation about the glycosidic bond of a glycopyranoside. The <sup>0</sup> ° torsion angle is that for which the bond to the anomeric hydrogen is eclipsed to the aglycon. ....	30
9	The <sup>1</sup> H-n.m.r. spectrum of compound 10 in CDCl <sub>3</sub> at 200 MHz. ....	41
10	The <sup>1</sup> H-n.m.r. spectrum of compound 11 in CDCl <sub>3</sub> . ....	41
11	The <sup>1</sup> H-n.m.r. spectrum of compound 14 in CDCl <sub>3</sub> . ....	45
12	The <sup>1</sup> H-n.m.r. spectrum of compound 15 in CDCl <sub>3</sub> . ....	45
13	The <sup>1</sup> H-n.m.r. spectrum in D <sub>2</sub> O of a) methyl $\beta$ -maltoside (18) at 295 °K, b) methyl $\alpha$ -maltoside (13) at 310 °K and c) methyl $\alpha$ -maltotrioside (4) at 310 °K. ....	49

<u>Figure</u>	<u>Title</u>	<u>Page</u>
14	The $^1\text{H}$ -n.m.r. spectrum in $\text{D}_2\text{O}$ at 295 °K of a) 1,2-dideoxy-maltose (7), b) methyl 6-deoxy- $\beta$ -maltoside (2) and c) methyl 6,6'-dideoxy- $\alpha$ -maltoside (16).....	52
15	The $^1\text{H}$ -n.m.r. spectrum in $\text{D}_2\text{O}$ at 295 °K of a) methyl 3-deoxy- $\alpha$ -maltoside (1), b) methyl 4- $\text{O}$ -( $\alpha$ -D-glucopyranosyl)- $\alpha$ -D-mannopyranoside (3) and c) methyl 4- $\text{O}$ -( $\alpha$ -D-glucopyranosyl)- $\alpha$ -D-xylopyranoside (12).....	54
16	Computer drawn structures for methyl $\alpha$ -maltoside (13) and the derivatives 1 and 12. The formula for compound 13 is reproduced in the more usual form to assist in the interpretation of the molecular models.....	60
17	Variation in conformational energy with rotation about the C-5 — C-6 bond of methyl $\alpha$ -maltoside in the conformation -30°/-25°.....	63
18	HSEA calculated energy contour map of methyl $\alpha$ -maltoside (13) with $\omega = -90^\circ$ and $\tau = 117^\circ$ . Each contour represents 0.5 kcal/mol.....	64
19	Overlap of the HSEA and HS calculated energy contour maps of methyl $\alpha$ -maltoside (13) to display the influence of the <i>exo</i> -anomeric effect on the conformational preference.....	64
20	Overlap of the HSEA calculated energy contour maps of methyl $\alpha$ -maltoside (13) and methyl 4- $\text{O}$ -( $\alpha$ -D-glucopyranosyl)- $\alpha$ -D-xylopyranoside (12) to display the effect of replacing the hydroxymethyl group of the reducing unit on the conformational preference of 13.....	65
21	Overlap of the HSEA calculated energy contour maps of methyl $\alpha$ -maltoside (13) and methyl 3-deoxy- $\alpha$ -maltoside (1) to display the effect of deoxygenation at C-3 on the conformational preference of 13.....	65
22	Change of the $^{13}\text{C}$ -n.m.r. chemical shifts of methyl $\alpha$ -maltoside (13) with change in the molar percent of $\text{DMSO-}d_6$ in $\text{H}_2\text{O}$ .....	76
23	Comparison of the $^{13}\text{C}$ -n.m.r. chemical shifts of methyl $\alpha$ -maltoside (13) and methyl $\alpha$ -maltotrioside (4) a) in $\text{D}_2\text{O}$ and b) in $\text{DMSO-}d_6$ at 305 °K.....	77
24	Partial $^1\text{H}$ -n.m.r. spectrum of methyl $\alpha$ -maltoside (13) in $\text{D}_2\text{O}$ (lower trace) and n.o.e. difference spectrum (top trace) obtained upon saturation of H-1'.....	83



<u>Figure</u>	<u>Title</u>	<u>Page</u>
25	Partial $^1\text{H}$ -n.m.r. spectrum of 1,2-dideoxymaltose (7) in $\text{D}_2\text{O}$ (lower trace) and n.O.e. difference spectrum (top trace) obtained upon saturation of H-1' . . . . .	83
26	Partial $^1\text{H}$ -n.m.r. spectrum of methyl 3-deoxy- $\alpha$ -maltoside (1) in $\text{D}_2\text{O}$ (lower trace) and n.O.e. difference spectrum (top trace) obtained upon saturation of H-1' . . . . .	84
27	Partial $^1\text{H}$ -n.m.r. spectrum of methyl 6,6'-dideoxy- $\alpha$ -maltoside (16) in $\text{D}_2\text{O}$ (lower trace) and n.O.e. difference spectrum (top trace) obtained upon saturation of H-1' . . . . .	84
28	Partial $^1\text{H}$ -n.m.r. spectrum of methyl 6-deoxy- $\beta$ -maltoside (2) in $\text{D}_2\text{O}$ (lower trace) and n.O.e. difference spectrum (top trace) obtained upon saturation of H-1' . . . . .	85
29	Partial $^1\text{H}$ -n.m.r. spectrum of methyl 4-O-( $\alpha$ -D-glucopyranosyl)- $\alpha$ -D-mannopyranoside (3) in $\text{D}_2\text{O}$ (lower trace) and n.O.e. difference spectrum (top trace) obtained upon saturation of H-1' . . . . .	85
30	Partial $^1\text{H}$ -n.m.r. spectrum of methyl 4-O-( $\alpha$ -D-glucopyranosyl)- $\alpha$ -D-xylopyranoside (12) in $\text{D}_2\text{O}$ (lower trace) and n.O.e. difference spectrum (top trace) obtained upon saturation of H-1' . . . . .	86
31	Partial $^1\text{H}$ -n.m.r. spectrum of methyl 3-deoxy- $\alpha$ -maltoside (1) in $\text{D}_2\text{O}$ (lower trace) and n.O.e. difference spectrum (top trace) obtained upon saturation of H-3eq. . . . .	86
32	Partial $^1\text{H}$ -n.m.r. spectrum of methyl 6-deoxy- $\beta$ -maltoside (2) in $\text{D}_2\text{O}$ (lower trace) and n.O.e. difference spectrum (top trace) obtained upon saturation of the methyl group. . . . .	87
33	Deuterium-induced isotope shifts in the $^1\text{H}$ -n.m.r. spectrum in $\text{DMSO}-d_6$ of systems containing hydroxyl groups that form intramolecular hydrogen bonds. . . . .	92
34	Partial $^1\text{H}$ -n.m.r. spectrum of methyl $\beta$ -maltoside (18) in $\text{DMSO}-d_6$ at 295 $^\circ\text{K}$ before (lower trace) and after (top trace) the addition of enough $\text{D}_2\text{O}$ to half-exchange the hydroxyl protons with deuterium. . . . .	94
35	Partial $^1\text{H}$ -n.m.r. spectrum of methyl $\alpha$ -maltoside (13) in $\text{DMSO}-d_6$ at 301 $^\circ\text{K}$ before (lower trace) and after (top trace) the addition of enough $\text{D}_2\text{O}$ to half-exchange the hydroxyl protons with deuterium. . . . .	94
36	Partial $^1\text{H}$ -n.m.r. spectrum of 1,2-dideoxymaltose (7) in $\text{DMSO}-d_6$ at 293 $^\circ\text{K}$ before (lower trace) and after (top trace) the addition of enough $\text{D}_2\text{O}$ to half-exchange the hydroxyl protons with deuterium. . . . .	95

<u>Figure</u>	<u>Title</u>	<u>Page</u>
37	Partial $^1\text{H}$ -n.m.r. spectrum of methyl 6,6'-dideoxy- $\alpha$ -maltoside (16) in $\text{DMSO}-d_6$ at 305 $^\circ\text{K}$ before (lower trace) and after (top trace) the addition of enough $\text{D}_2\text{O}$ to half-exchange the hydroxyl protons with deuterium. . . . .	95
38	Partial $^1\text{H}$ -n.m.r. spectrum of methyl 6-deoxy- $\beta$ -maltoside (2) in $\text{DMSO}-d_6$ at 315 $^\circ\text{K}$ before (lower trace) and after (top trace) the addition of enough $\text{D}_2\text{O}$ to half-exchange the hydroxyl protons with deuterium. . . . .	96 <sup>a</sup>
39	Partial $^1\text{H}$ -n.m.r. spectrum of methyl 4- $O$ -( $\alpha$ -D-glucopyranosyl)- $\alpha$ -D-mannopyranoside (3) in $\text{DMSO}-d_6$ at 297 $^\circ\text{K}$ before (lower trace) and after (top trace) the addition of enough $\text{D}_2\text{O}$ to half-exchange the hydroxyl protons with deuterium. . . . .	96
40	Partial $^1\text{H}$ -n.m.r. spectrum of methyl 4- $O$ -( $\alpha$ -D-glucopyranosyl)- $\alpha$ -D-xylopyranoside (12) in $\text{DMSO}-d_6$ at 295 $^\circ\text{K}$ before (lower trace) and after (top trace) the addition of enough $\text{D}_2\text{O}$ to half-exchange the hydroxyl protons with deuterium. . . . .	97
41	Partial $^1\text{H}$ -n.m.r. spectrum of methyl $\alpha$ -maltotrioside (4) in $\text{DMSO}-d_6$ at 307 $^\circ\text{K}$ before (lower trace) and after (top trace) the addition of enough $\text{D}_2\text{O}$ to half-exchange the hydroxyl protons with deuterium. . . . .	97
42	Computer drawn structure for methyl $\alpha$ -maltoside (13) to display the hydrogen bond network $\text{HO}-3' \rightarrow \text{HO}-2' \rightarrow \text{HO}-3$ . . . . .	99
43	Dependence of the $^1\text{H}$ -n.m.r. chemical shifts of methyl $\alpha$ -maltoside (13) in $\text{DMSO}-d_6$ with changes in temperature. . . . .	100
44	Dependence of the $^1\text{H}$ -n.m.r. chemical shifts of methyl 4- $O$ -( $\alpha$ -D-glucopyranosyl)- $\alpha$ -D-xylopyranoside (12) in $\text{DMSO}-d_6$ with changes in temperature. . . . .	101
45	Computer drawn structure for methyl 4- $O$ -( $\alpha$ -D-glucopyranosyl)- $\alpha$ -D-xylopyranoside (12) to display the hydrogen bond $\text{O}-1' \rightarrow \text{HO}-2'$ . . . . .	103

<u>Figure</u>	<u>Title</u>	<u>Page</u>
46	Conformational energy contour plot of methyl $\alpha$ -maltoside (13). The vertically shaded area indicates the range of conformations that would give rise to the occurrence of an intramolecular hydrogen bond between O-2' and O-3 (interatomic distance = 2.7 - 3.0 Å). The horizontally shaded area encloses the conformations that produce a n.O.e. ratio close to the one found in DMSO- $d_6$ (H-4 / H-2' = 1.15 - 1.35). The intersection shows the region where the conformation of the molecule is expected to occur in DMSO solution. . . . .	105
47	Conformational energy contour plot of methyl $\alpha$ -maltoside (13). The horizontally shaded area shows the conformations that produce a n.O.e. ratio close to the one found in D <sub>2</sub> O (H-4 / H-2' = 0.90 - 1.10). The cross-hatched area shows the region where the conformation of the molecule is expected to occur in water. Indicated in the map are the solid state conformations of 1) $\alpha$ -maltose <sup>13</sup> , 2)methyl $\alpha$ -maltotriose <sup>37</sup> , 3)V <sub>h</sub> -amylose <sup>48</sup> , 4)B-amylose <sup>44</sup> , and 5)maltoheptaose <sup>155</sup> . . . . .	106
48	Structure of methyl $\alpha$ -maltoside to illustrate that partial delocalization of the lone electron pair of the ring oxygen of glycosides by way of hydrogen bonding to a molecule of water strengthens the <i>exo</i> -anomeric effect. . . . .	110

## LIST OF SCHEMES

Scheme 1	47
Scheme 2	48
Scheme 3	50
Scheme 4	53

## I. INTRODUCTION

### 1. Historical overview

Starch is the chief reserve carbohydrate of plants<sup>1</sup> and is, therefore, one of the most widely distributed substances in the vegetable kingdom. It is found in nature in granular form in seeds, fruits, leaves and tubers in amounts that vary from a few percent to over 75% in cereal grains. It forms the major source of carbohydrates in the human diet and is therefore of great economic importance.

Starch can be separated in two components; namely, amylose and amylopectin.<sup>5</sup> Amylose is a water soluble linear polymer of  $\alpha$ -D-glucopyranose units with 1,4-linkages, (Figure 1). Its average molecular weight ranges<sup>2</sup> from  $4.4 \times 10^4$  to  $6.2 \times 10^5$  corresponding to degrees of polymerization of 270-380. Amylopectin, the water insoluble main component of starch, consists of chains of  $\alpha$ -1,4-glucopyranose to which branches are attached in  $\alpha$ -1,6 linkages, (Figure 2). An even higher molecular weight from  $4.5 \times 10^4$  to  $2.4 \times 10^8$  was found<sup>2</sup> corresponding to degrees of polymerization of 280 -  $1.45 \times 10^6$ .

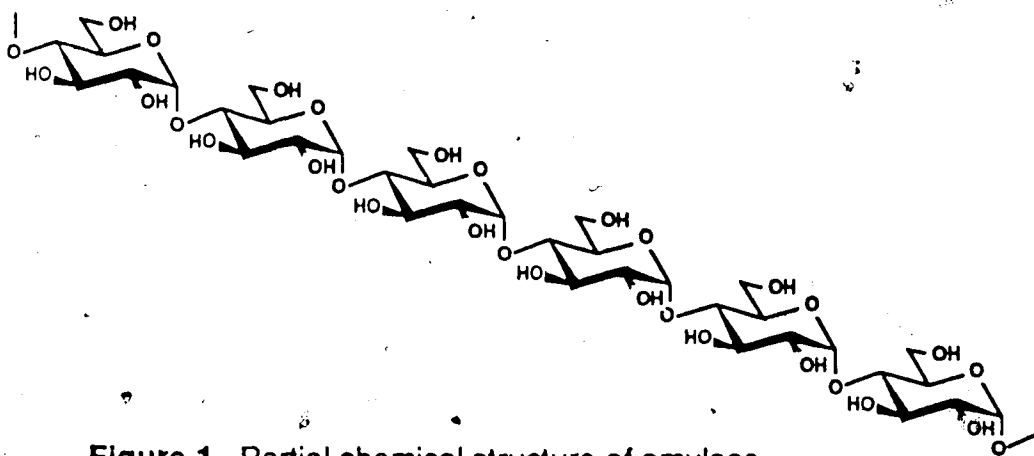


Figure 1. Partial chemical structure of amylose.

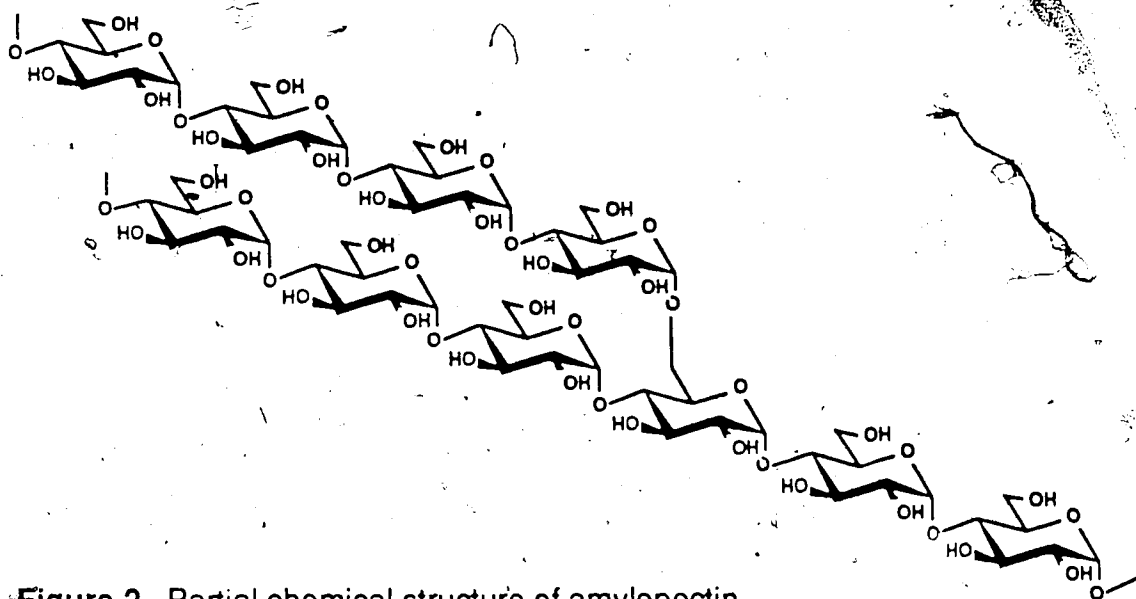
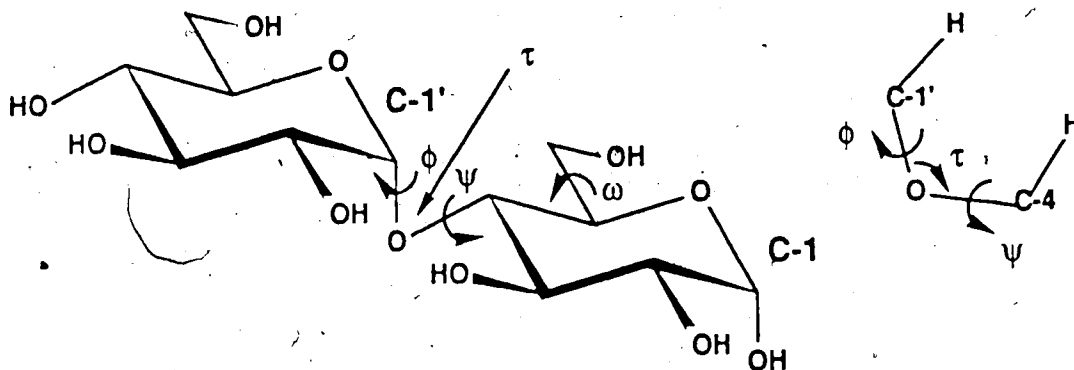


Figure 2. Partial chemical structure of amylopectin.

The structure of glycogen (animal starch) that functions as a food reserve for animal cells is similar to that of amylopectin.

The disaccharide  $\alpha$ -maltose is the basic building unit of starch (Figure 3). The compound was first obtained in 1811 by Kirchoff<sup>3</sup> by the action of acid hydrolysis on starch. Saussure<sup>4</sup> made further investigations, but it remained for Dubrunfaut<sup>5</sup> to recognize it as a new sugar, different from grape-sugar (D-glucose). It was named maltose because it had been obtained from the action of malt diastase on starch. Meiss<sup>6</sup> deduced that it was composed of two molecules of glucose joined through the loss of a molecule of water. However, the position of the linkage between the two units remained unsolved until 1919 when Haworth and Leicht<sup>7</sup> finally found, by methylation of the molecule followed by hydrolysis, that the linkage is either 1 $\rightarrow$ 4 or 1 $\rightarrow$ 5. The unambiguous assignment of pyranose structures to the glucose units was also made by Haworth<sup>8,9</sup> and based on the methylation analysis of oxidized maltose to establish the 1 $\rightarrow$ 4 linkage. The  $\alpha$ -configuration for the glycosidic linkages

was assigned because maltose is hydrolysed by maltase, an enzyme specific for the so-called  $\alpha$ -glucosides following Hudson's rules of isorotation.<sup>10</sup> The establishment of the configurations of anomeric glycosides was reviewed in 1951 by Ballou, Roseman and Link<sup>11</sup> and more recently by Lemieux and Koto.<sup>12</sup> The configuration of  $\alpha$ -maltose (Figure 3) and its  $\beta$ -methyl glycoside have been confirmed by X-ray crystallography.<sup>13,14</sup>



**Figure 3.**  $\alpha$ -maltose ( 4-O-( $\alpha$ -D-glucopyranosyl)- $\alpha$ -D-glucopyranoside ) and designations for torsion angles.

The notations for the labelling of atoms presented in Figure 3 and used throughout this thesis are as follows. It is seen that unprimed numbers refer to the atoms of the reducing unit and primed numbers to the atoms of the non-reducing unit. Also indicated are the torsion angles each involving an hydrogen atom that define the conformation of maltose<sup>12</sup>, where  $\phi$  is the angle described by the torsion of the segment H-1' — C-1' — O-1' — C-4, similarly  $\psi$  is described by C-1' — O-1' — C-4 — H-4, and  $\omega$  by H-5 — C-5 — C-6 — O-6. The glycosidic linkage angle  $\tau$  is the valence angle defined by the segment C-1' — O-1' — C-4. In the present work the signs of  $\phi$  and  $\psi$  are positive or negative according to IUPAC recommendations.<sup>15,16</sup>

## 2. Objectives of this study

In view of the importance of starch as one of man's main sources of energy, many studies have been made to determine its properties in solution. Of primary concern in biological processes is the nature of enzyme-substrate interactions and lectin-cell surface carbohydrate recognition.<sup>17,18</sup> In order to better understand the characteristics of these interactions it is necessary to have a good understanding of the conformational properties of the substrate in solution since it has been demonstrated that oligosaccharides dissolved in water have well defined conformational preferences<sup>19</sup> and, therefore, a subject of importance to their recognition by proteins such as lectins, antibodies and enzymes.

Several studies have been carried out to determine the conformation of amylose in solution.<sup>20-23</sup> However, it seemed advantageous to choose a simpler molecule as a model compound for conformational studies. Ideally, this molecule would reflect the conformation of amylose in solution. The models chosen for the present study were methyl  $\alpha$ -maltoside (methyl 4-O-( $\alpha$ -D-glucopyranosyl)- $\alpha$ -D-glucopyranoside), since it contains the basic glycosidic linkage that allows variations of conformation in these molecules and methyl  $\alpha$ -maltotrioside which can be considered as made up of two  $\alpha$ -maltose units.

Maltose has recently received a great deal of attention. A wide range of conformer populations have been proposed based on X-ray diffraction data and theoretical calculations. However, the influence of the *exo-anomeric*<sup>24</sup> effect on its conformation was not recognized. The present study was undertaken to examine the magnitude of the effect on conformational analysis based on solid



state data or theoretical calculations without the consideration of the contribution by the *exo*-anomeric effect. The *exo*-anomeric effect has been very recently reviewed in detail by Praly and Lemieux.<sup>24</sup> These authors also presented evidence based in n.m.r. spectroscopy for the influence of the solvent on the relative magnitudes of the *endo* and *exo*-anomeric effects. Of major relevance to this thesis is the conclusion that water should strongly increase the *exo*-anomeric effect whereas Lipkind, Verovsky and Kochetkov have stated that the *exo*-anomeric effect "does not play a significant role under the conditions of an aqueous medium".<sup>25,26</sup>

For this study, it was desired to determine not only the preferred conformation of maltose in aqueous solution but also the structural and / or electronic features responsible for that conformation. Furthermore, it seems probable that oligosaccharides may be accepted by protein receptor sites partly in intramolecular hydrogen-bonded forms.<sup>27-32</sup> For this reason, this study is also directed toward an investigation of structural features within oligosaccharide structures that are conducive to intramolecular hydrogen bond formation.

### 3. Conformational analysis

Several methods have been used to obtain information about the conformational properties of oligosaccharides. Of these, the following will be considered.

- 3.1. X-Ray (or neutron) diffraction methods
- 3.2. Optical rotation studies
- 3.3. Nuclear magnetic resonance spectroscopy
- 3.4. Theoretical calculations

### 3.1. X-ray studies

With the advent of computer assistance, single crystal X-ray crystallography has provided a great deal of information about the structure of carbohydrates and their conformations in the crystalline state. A list of such crystal structures are reported periodically by Jeffrey and co-workers.<sup>33</sup> It may be considered that the crystal structure provides a correct description of the conformation that the molecule exhibits in solution. However, this may not be the case since the conformation adopted by a molecule in a microscopic environment is the result of the competing actions of both intra- and intermolecular forces and the kinds, magnitudes and directions of the intermolecular forces of the compound in solution may differ from those in the crystal lattice. Therefore, solid state conformations can only provide a starting point in the search for the solution conformation.

The crystal structures of a variety of compounds related to maltose have been reported and their conformations are presented in Table 1. It is seen that very substantial differences can occur between the orientations adopted about the glucosidic linkage depending upon the structure of the compound.

**Table 1.** Observed solid state conformations about intersugar bonds of maltose analogs.

Compounds	$\phi^\circ$	$\psi^\circ$	Reference
$\alpha$ -maltose (1)	-3.6	4.1	13
$\beta$ -maltose, H <sub>2</sub> O (2)	4.8	13.3	34
methyl $\beta$ -maltoside, H <sub>2</sub> O (3)	5.6	15.9	14
phenyl $\alpha$ -maltoside <sup>a</sup> (4)	-7.6	-15.8	35
	-8.1	-25.5	
$\beta$ -maltose octaacetate (5)	-29.0	-36.0	36
methyl $\alpha$ -maltotrioside, 4H <sub>2</sub> O (6)	-38.0	-29.0	37
	-38.0	-33.0	
maltoheptaose • phosphorylase complex (7)	-15.0	-15.0	17

<sup>a</sup>Two different conformers are present in the crystal.

An examination of molecular models for maltose and related compounds shows that, as reported in Figure 4, changes in the  $\phi$  and  $\psi$  torsion angles about the interunit glucosidic bond provides two zones in a conformational map depending on whether or not the internuclear distance between O-2' and O-3 is longer than 3.0 Å. When the data reported in Table 1 are examined in this context, it is seen that methyl  $\alpha$ -maltotrioside and  $\beta$ -maltose octaacetate occur in conformations that do not allow an intramolecular hydrogen bond to be established between these atoms. The conformations which fall into the shadowed zone in Figure 4 allow this type of intramolecular hydrogen bond. This matter is presented since there exists considerable speculation on the importance of intramolecular hydrogen bonding between the contiguous glucose units on the conformation of maltose. This arose because early

Quigley *et al.*<sup>40</sup> claimed that "This hydrogen bond appears to be one of the principal forces controlling the conformations which are based on  $\alpha$ -1,4 linked glucoses", while Pangborn *et al.*<sup>37</sup> stated "Therefore the occurrence of the intramolecular hydrogen bond between contiguous chain residues *i.e.* O-2' and O-3 is not an essential contributor to the establishment of the preferred conformations about the glycosidic bonds". In the present study an attempt is made to obtain information about the occurrence and significance of an intramolecular hydrogen bond in solution.

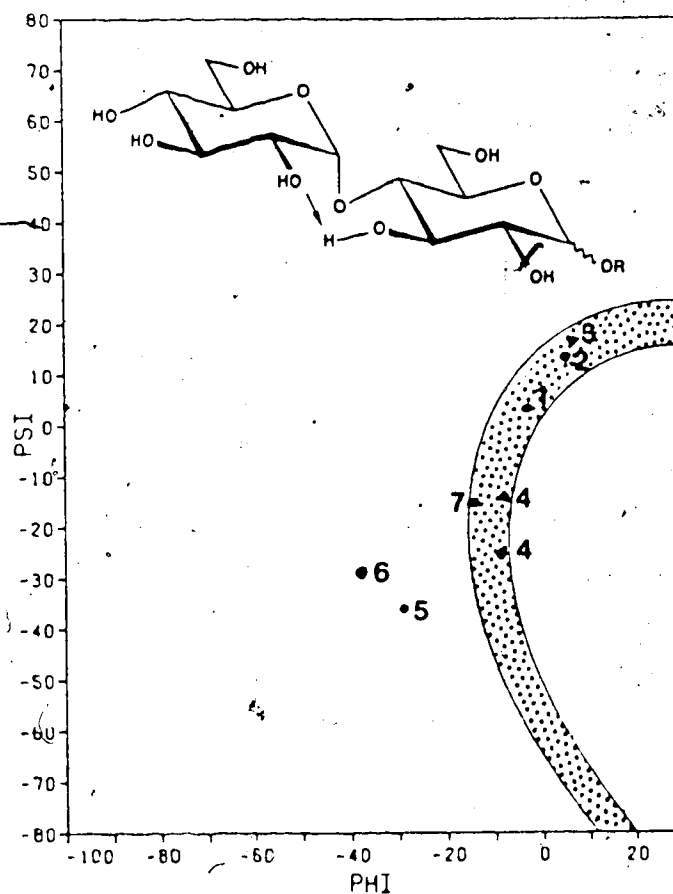


Figure 4. Observed solid state conformations of maltose and analogs in relation to the internuclear distances between O-3 and O-2'. The numbers correspond to the compounds listed in Table 1. The shadowed area indicates

The first X-ray diffraction patterns of native starch were published<sup>41</sup> in 1928, however, the crystalline structure of starch is not yet well understood.<sup>42</sup> Native starches give X-ray diffraction patterns which can be classified as three main types<sup>42,43</sup>: the A type, typical of cereal starches; the B type, characteristic of tuber and maize starches and the C type, an intermediate between A and B types, found in bean and root starches. Another pattern, the V type, is obtained when amylose is complexed with organic compounds, iodine or water. The crystalline V form exists in anhydrous,  $V_a$ , and hydrated,  $V_h$ , states. Of the naturally occurring crystalline forms of amylose, the B type has been more extensively studied. Its structure was considered<sup>44</sup> to be composed of six-fold, left-handed, single helices with torsion angles between contiguous units of approximately  $\phi = -20^\circ$  and  $\psi = -10^\circ$ . However, Wu and Sarko<sup>45,46</sup> later proposed a B type structure based on parallel stranded double helices after a suggestion made by Kainuma and French<sup>1,47</sup>. In this structure, the individual antiparallel strands are in a right-handed, six-fold helical conformation with approximate torsion angles of  $\phi = 30^\circ$  and  $\psi = 25^\circ$ , but even now, these double helical structures are being questioned.<sup>42</sup> The crystal structure of  $V_h$ -amylose has been recently studied by Rappenecker and Zugenmaier<sup>48</sup>. These authors proposed a structure of left-handed, six-fold, single helices with torsion angles  $\phi = -14.4^\circ$  and  $\psi = -7.5^\circ$ . These data are presented because they will be of interest when compared with the conformational preferences of methyl  $\alpha$ -maltoside and methyl  $\alpha$ -maltotrioxide obtained from this investigation.

### 3.2. Optical rotation studies

In 1970 Rees<sup>49</sup> proposed a method to estimate the torsion angle  $\phi$  and  $\psi$  of glycosidic linkages from the optical rotation of carbohydrates. The parameter he derived, known as the "linkage rotation",  $[\Lambda]_D$ , is defined as

$$[\Lambda_{\text{obs}}] = [M_{\text{NR}}] - \{[M_{\text{MeN}}] + [M_{\text{R}}]\}, \quad (1)$$

where,

$[\Lambda_{\text{obs}}]$  = observed linkage rotation,

$[M_{\text{NR}}]$  = molecular rotation for a given disaccharide which contains a non-reducing (N) and a reducing (R) residue,

$[M_{\text{MeN}}]$  = molecular rotation of the methyl glycoside of N having the same anomeric configuration as the disaccharide,

$[M_{\text{R}}]$  = rotation of the reducing sugar.

The linkage rotation represents the optical rotation due to interactions across the glycosidic linkage, minus any contributions from the individual monosaccharide units. Rees<sup>49</sup> attempted to correlate the linkage rotation with the torsion angles  $\phi$  and  $\psi$  based on the postulate of Brewster<sup>50</sup> that each four atom chain, in this case about the glycosidic linkage, makes a contribution to the rotation which depends on the sine of the torsion angle. The relationships for  $\alpha$ - and  $\beta$ - linked disaccharides are,

$$[\Lambda^{\alpha}_{\text{calc}}]_D = -105^{\circ} - 120(\sin \phi + \sin \psi)^{\circ} \quad \text{and} \quad (2)$$

$$[\Lambda^{\beta}_{\text{calc}}]_D = 105^{\circ} - 120(\sin \phi + \sin \psi)^{\circ}. \quad (3)$$

Using torsion angles obtained from X-ray studies, Rees predicted the linkage rotations of several disaccharides with very good accuracy. For example, the torsion angles for  $\beta$ -cellobiose in its crystal structure are  $\phi = 42^{\circ}$

and  $\psi = -18^\circ$ , which leads to  $[\Lambda_{\text{calc}}^{\beta}]_{\text{D}} = 62^\circ$  as compared with  $[\Lambda_{\text{obs}}^{\beta}]_{\text{D}} = 59^\circ$ . For  $\beta$ -lactose,  $\phi = 31^\circ$  and  $\psi = -25^\circ$  and thus  $[\Lambda_{\text{calc}}^{\beta}]_{\text{D}} = 94^\circ$  in excellent agreement with  $[\Lambda_{\text{obs}}]_{\text{D}} = 95^\circ$ . However, the close agreement between the calculated and observed optical linkage rotations must be interpreted with caution. As mentioned earlier, intermolecular hydrogen bonding and crystal packing forces can influence the conformation of the molecule and, thus, the torsion angles found in the solid state may well deviate from those found in solution. That this can be in fact the case is well demonstrated as follows. Although the linkage rotation for methyl  $\beta$ -cellobioside in aqueous solution ( $[\Lambda_{\text{obs}}]_{\text{D}} = 64^\circ$ ) agrees well with the theoretical value ( $[\Lambda_{\text{calc}}^{\beta}]_{\text{D}} = 62^\circ$ ) derived from the crystal conformation of cellobiose ( $\phi = 42^\circ$ ,  $\psi = -18^\circ$ ), it deviates considerably from the linkage rotation ( $[\Lambda_{\text{calc}}^{\beta}]_{\text{D}} = 128^\circ$ ) based on the crystal structure of methyl  $\beta$ -cellobioside itself ( $\phi = 25^\circ$ ,  $\psi = -38^\circ$ ). Furthermore, Rees' description of the linkage rotation assumes that the same values of the torsion angles defined by O-6 — C-6 — C-5 — H-5 ( $\omega$ ) of the individual monosaccharide residues in the crystal structures are preserved in the case of a disaccharide. A variation of the values for  $\omega$  in the disaccharide in solution from those of the constituent monosaccharides in the solid state thus may lead to serious errors when interpreting  $[\Lambda_{\text{obs}}]_{\text{D}}$  in terms of only  $\phi$  and  $\psi$  as in Equations (2) and (3). The consequences of neglecting an additional term in those equations to account for variations of the torsion angle of the hydroxymethyl groups can be especially misleading in the case of maltose since molecular modelling studies suggest<sup>51</sup> that changes of the  $\phi$  and  $\psi$  torsion angles are likely to influence the orientation of the hydroxymethyl group of the reducing unit. In this regard it is of interest to compare the angles for methyl  $\beta$ -maltoside<sup>14</sup> ( $\omega = 176.4^\circ$ ) and  $\beta$ -maltose<sup>34</sup> ( $\omega = 31.5^\circ$ ) with the angles in methyl  $\beta$ -D-glucopyranoside<sup>52</sup> ( $\omega = -50.5^\circ$ ) and in methyl  $\alpha$ -D-gluc-

pyranoside<sup>53</sup> ( $\omega = -44.6^\circ$ ). Lemieux and Brewer<sup>54</sup> presented a study about the conformational preferences of hydroxymethyl groups of hexopyranoses in different solvents.

In conclusion, the close agreement between  $[\Lambda_{\text{calc}}]_{\text{D}}$  and  $[\Lambda_{\text{obs}}]_{\text{D}}$  for the cases cited must be considered as fortuitous and therefore the use of the optical linkage rotation in predicting the average conformation about glycosidic bonds is not acceptable. Despite the previous considerations, Tvaroska<sup>55</sup> and more recently Kochetkov<sup>25,26,56</sup> have employed the linkage optical rotations of maltose and methyl maltosides as an important factor to assess the conformational properties of these compounds in solution. Rees and coworkers<sup>57-59</sup> studied the effect that solvent plays on the conformational preference of methyl  $\beta$ -maltoside. The optical linkage rotations in dimethyl sulfoxide (DMSO) and dioxane ( $[\Lambda_{\text{obs}}]_{\text{D}} = -19^\circ$  and  $-23^\circ$ , respectively) were interpreted as an indication that in these solvents, the time-averaged conformation is displaced from the crystal structure, but still, a high proportion of the molecules exists in conformations in which intramolecular hydrogen bonding is possible. In aqueous solution, the linkage optical rotation ( $[\Lambda_{\text{obs}}]_{\text{D}} = +46^\circ$ ) indicated that the molecule spends a larger proportion of its time in a "folded conformation" with torsion angles  $\phi = 70^\circ$  and  $\psi = -40^\circ$  corresponding to  $[\Lambda_{\text{calc}}]_{\text{D}} = +85^\circ$  which had been suggested<sup>60</sup> to account for the specific thermal expansion of maltose in aqueous solution.

### 3.3. Nuclear magnetic resonance spectroscopy

Proton and carbon-13 nuclear magnetic resonance spectroscopies are the most powerful methods of obtaining information about the preferred



conformation of oligosaccharides in solution. Bock<sup>61</sup> has recently presented a detailed review of these developments which were made possible by the advent of modern computer-assisted, high field FT n.m.r. spectrometers.

The n.m.r. parameters which yield conformational information are:

- 3.3.1. Chemical shifts
- 3.3.2. Coupling constants
- 3.3.3. Spin-lattice relaxation times
- 3.3.4. Nuclear Overhauser enhancements

These parameters will now be discussed as applied to the study of the conformation of maltose derivatives.

### 3.3.1. Chemical shifts

Proton chemical shifts have proven useful in the conformational analysis of oligosaccharides because these tend to be very similar ( $\pm 0.1$  ppm) to those found for the simple methyl glycosides of the component sugars. However, on occasions, for specific protons, much larger changes in chemical shift occur. This was first noticed for the signal for H-5 of the fucose unit in the Lewis a trisaccharide<sup>62</sup> and subsequently observed on several occasions.<sup>51,63</sup> In each case, it became apparent that the specific deshielding occurred because of a nonbonded interaction of the hydrogen with an oxygen atom of another sugar unit. These deshielding effects are similar to those observed for hydrogen atoms that are *syn*-axial to oxygen atoms and surely result from electrostatic interactions.<sup>61</sup> An example is the downfield shift of ca. 0.25 ppm which is

observed for H-3 and H-5 of methyl glucopyranoside when the anomeric configuration is changed from  $\beta$  to  $\alpha$ .

The main use of  $^{13}\text{C}$ -chemical shifts in conformational studies has been for the comparison of similar structural units in different compounds.<sup>63,64</sup> Since these shifts appear to be highly sensitive to slight changes in carbon hybridization, their calibration for the prediction of conformational preferences will be very difficult.

### 3.3.2. Coupling constants

In the conformational analysis of oligosaccharides, proton-proton spin-spin coupling constants are used mainly to confirm the chair conformations for the sugar units.

In this study, the coupling constants that yield information about the conformation are the so-called "linkage" coupling constants,  $J^P$  and  $J^N$ , which are the vicinal coupling constants for the terminal atoms of the fragments  $\text{H-1}' - \text{C-1}' - \text{O-1}' - \text{C-4}$  and for  $\text{C-1}' - \text{O-1}' - \text{C-4} - \text{H-4}$ , respectively. These parameters have been used more than any other n.m.r. parameter for the study of the conformation of maltose. Their application as a conformational tool is based on a Karplus-type relationship for the system  $^{13}\text{C} - \text{O} - \text{C} - ^1\text{H}$ . There exists both experimental<sup>65</sup> and theoretical<sup>66</sup> evidence for this relationship; however, the experimental values exhibit considerable scatter as can be appreciated in Figure 5. Most of these experimental values were assigned on the basis of torsion angles exhibited in the crystalline state and for a wide range of chemical structures. The experimental difficulties of measuring an accurate coupling constant also add to the uncertainty. It is to be expected that vicinal

$^{13}\text{C}$  to  $^1\text{H}$  coupling constants will be sensitive to electronegative effects as Altona and coworkers<sup>68</sup> have recently described in detail for vicinal  $^1\text{H}$  to  $^1\text{H}$  coupling.

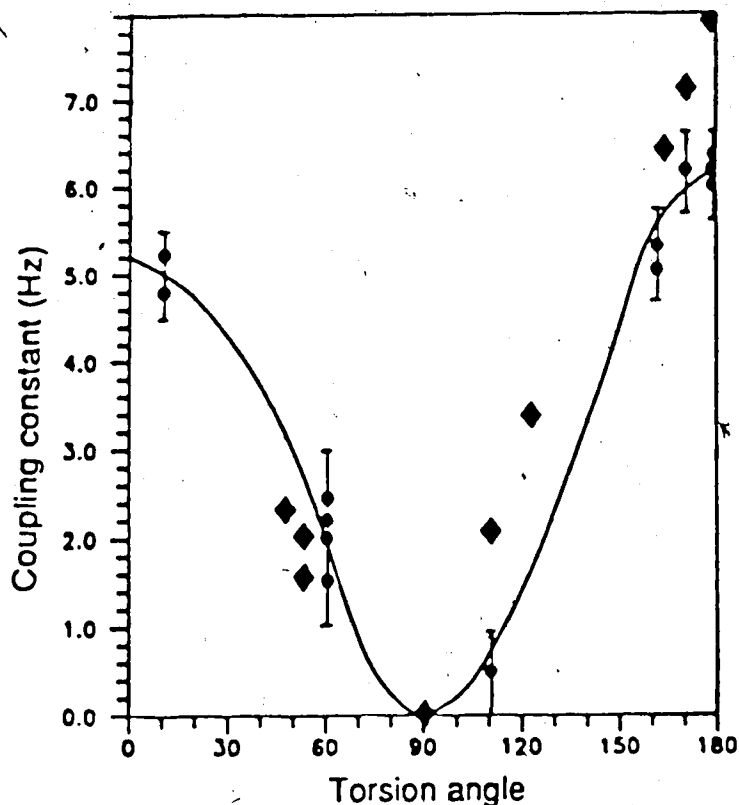


Figure 5. Experimental evidence<sup>65,67</sup> for the Karplus-type relationship between  $^{13}\text{C}$  to vicinal  $^1\text{H}$  coupling and the torsion angles these atoms define. The points  $\blacklozenge$ <sup>65</sup> were not used by Pérez *et al.*<sup>69</sup> in their estimation of the conformational preferences of glycosidic linkages.

Although the use of a Karplus relationship for the assignment of torsion angles may lead to serious errors, Pérez *et al.*<sup>69</sup> used the following relationships for the assignment of solution conformations of methyl  $\beta$ -maltoside,

$${}^3J_{\text{C-4},\text{H-1}} = \mathcal{J}^{\beta} = 4.3 \cos^2\phi + 0.6 \quad \text{and} \quad (4)$$

$${}^3J_{\text{C-1}',\text{H-4}} = \mathcal{J}^{\nu} = 4.8 \cos^2\psi + 0.7 \quad (5)$$

Similarly, Kochetkov<sup>25,26,56</sup> used "linkage" coupling constants for the conformational study of maltose. The measured coupling constants were

assigned to glycosidic angles according to an empirical curve proposed by Perlin and coworkers.<sup>67</sup>

### 3.3.3. Spin-Lattice relaxation times

The application of proton spin-lattice relaxation rates in the study of interglycosidic conformations relies on a dependence on intramolecular proton-proton distances according to the following equation,

$$(1/T_1)_i = \text{constant} \cdot \tau_c \cdot \sum r_{ij}^{-6}, \quad (6)$$

where  $r_{ij}$  is the distance between proton  $i$  and all other protons ( $j$ ) in the molecule and  $\tau_c$  is the correlation time.<sup>70</sup> The problem arising from the application of proton-relaxation rates is that it is generally difficult to determine the individual relaxation contributions and thus obtain a quantitative measure for the proton-proton interactions in neighbouring pyranose rings.

For carbons, spin-lattice relaxation occurs essentially through dipolar interactions with directly bonded protons, and is therefore a function of the number of protons attached to the observed carbon nucleus;

$$1/T_1 = \text{constant} \cdot N \cdot \tau_c. \quad (7)$$

Spin-lattice relaxation times are used mainly to obtain information about the mobility and tumbling properties of the molecules in solution<sup>61</sup> and provide the evidence for isotropic tumbling required for the use of expression 8 to be discussed below.

### 3.3.4. Nuclear Overhauser enhancements

The most widely used tool for the determination of the conformation of complex molecules in solution is the measurement of nuclear Overhauser enhancements.<sup>71</sup> In this technique the relative contributions of neighbouring protons to the relaxation of another proton are measured. Since the contribution depends on the interatomic distance the n.O.e.'s give a measure of the relative proton-proton distances within the molecule. Considering a homonuclear n.m.r. experiment in which a nuclear spin  $s$  is being saturated and a spin  $d$  is detected, the nuclear Overhauser enhancement on  $d$ ,  $f_d(s)$ , is well approximated by the following equation,<sup>72</sup>

$$f_d(s) = \frac{r_{ds}^{-6}}{2\sum r_{dj}^{-6}}, \quad (8)$$

where  $r_{ds}$  is the distance between protons  $d$  and  $s$  and  $r_{dj}$  are the distances between proton  $d$  and the other protons  $j$  in the molecule. Equation (8) is valid under the following conditions; the molecule must tumble isotropically in solution, the relaxation of spin  $d$  must occur exclusively by a dipole-dipole mechanism and spins  $d$  and  $s$  should not be tightly coupled with any other protons in the molecule.

The n.O.e. observed for a given  $^1\text{H}$ -signal (spin  $d$ ) gives a measure of the distance between the nuclei  $d$  and  $s$  and, for this reason, it can provide valuable information about molecular conformation and structure. The steady-state n.O.e. however, does not provide a direct or absolute indication of the distance, for it only determines the relative contributions of internuclear dipole-dipole relaxations, *i.e.* if all the distances in the molecule were doubled the measured n.O.e.'s would remain the same. The absolute value of the

enhancement is meaningless in quantitative studies not only for this reason but also because of experimental factors (like the presence of dissolved oxygen or paramagnetic impurities). To obtain information about distances two approaches can be taken: the measurement of the rate of growth of the n.O.e.<sup>73</sup> and the use of an "internal reference"<sup>74</sup>. The former provides direct information of distance but requires longer instrumental times making it often prohibitive. The latter takes advantage of an enhancement induced in another proton which is known to be at a fixed distance from s to calibrate the distance between s and d. In the case of maltose, the distance H-1' — H-4 provides an indication of the conformation about the glycosidic bond; namely,  $\phi$  and  $\psi$  torsion angles. In order to estimate this distance, H-1' is irradiated to induce an enhancement of H-2' which can be used as the "internal ruler" since it is known from vicinal coupling constants that the glucose units in solution are in the  ${}^4C_1$  conformation.<sup>63</sup> Should the signal for the aglyconic hydrogen, H-4, also be significantly enhanced, then its distance to H-1' can be estimated, (Figure 6).

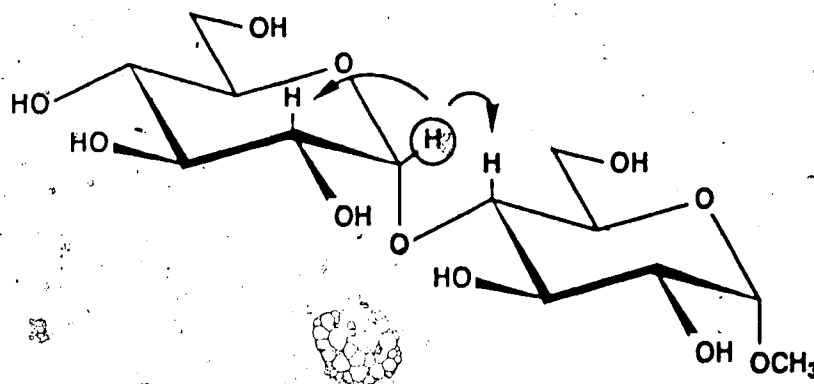


Figure 6. Measurement of the  ${}^1\text{H}$ -n.m.r. spectrum of methyl  $\alpha$ -maltoside with saturation of H-1' may lead to major enhancement of the signals for hydrogens in close vicinity such as H-4 and H-2'.

It is this method that was used for the preparation of this thesis. In all cases, the n.O.e. values which are reported are those found relative to H-2' since the distance between H-1' and H-2' can be derived from X-ray crystal data. The conformation obtained in this way is of course an average in the n.m.r. time scale of all populated conformers in the solution.

Recently, Kochetkov *et al.*<sup>56</sup> published the results of an n.O.e. determination on methyl  $\beta$ -maltoside in D<sub>2</sub>O. The observed enhancements on pre-irradiation of H-1' are: H-3 = 1.0%, H-4 = 5.9% and H-2' = 7.9%. These results were compared with those obtained from theoretical calculations as follows: the conformational preferences for maltose were assessed with the aid of semi-empirical calculations (to be discussed in the next section). Then, for each of the four afforded conformers a theoretical n.O.e. was calculated and the statistical average was calculated based on a Boltzman distribution of the conformers. The experimental ratios of n.O.e.'s, H-4/H-2' and H-3/H-2' were compared with the calculated ratios and a reasonable agreement was found. These authors therefore concluded that in order to account for the measured n.O.e.'s the compound must exist in aqueous solution as a mixture of the four conformers predicted by their calculations and not as a single conformer as predicted by HSEA calculations.<sup>75,76</sup> The conclusions were confirmed by similar comparisons of the calculated and experimental linkage optical rotations and <sup>13</sup>C - <sup>1</sup>H coupling constants. However, it must be noted that the quantitative measurement of the n.O.e.'s in methyl  $\beta$ -maltoside, even at 500 MHz, is precluded by the partial overlapping of H-4 and H-2' making the obtained values unreliable. Also, the enhancement on H-4 is sensitive to the orientation of the hydroxymethyl group and for this reason they chose to fix the C-6 group in the conformation generally found in the crystal structure of methyl glycosides ( $\omega = -60.0^\circ$ ).<sup>52,53</sup> The results obtained from similar experiments on

methyl  $\alpha$ -maltoside and derivatives in this laboratory<sup>75,76</sup> do not agree with those found by Kochetkov *et al.* and a comparison of the results will be presented in the discussion.

### 3.4. Theoretical calculations

Conformational energy calculations have been used over the last years to aid in the interpretation of experimental data and to obtain information that would not be possible to obtain otherwise.<sup>77,78</sup> Two kinds of approaches have been used:

3.4.1. Quantum mechanical procedures

3.4.2. Semi-empirical calculations

#### 3.4.1. Quantum mechanical procedures

Quantum mechanical calculations have not yet been widely applied to calculate the preferred conformation of oligosaccharides due to the fact that these calculations are very expensive and in general not practically possible on large molecules. In principle, the most direct way to calculate the conformation of a molecule would be by solution of the Schrödinger equation for a given nuclear configuration, followed by an adjustment of the nuclear configuration to minimize the energy of the molecule.<sup>77</sup> This is not possible for all molecules except the hydrogen molecule ion and consequently approximations are necessary. The most sophisticated methods used at present are the semi-empirical *ab initio* methods. However, since the amount of calculation required for a molecule is proportional to the fourth power of the number of orbitals, this



method has been applied to only a few simple model compounds. Of special interest to carbohydrate chemistry are the calculations performed by Pople and coworkers<sup>80</sup> on dimethoxymethane because this molecule can be used as a model of the acetal system of glycosides. Rasmussen and coworkers<sup>81</sup> performed an *ab initio* calculation to estimate the energy of maltose in a fixed conformation but, because of the high cost of the computer assistance, a conformational analysis was not done.

There are a number of other semi-empirical quantum mechanical methods which attempt to reduce the amount of computation involved. Among these are those<sup>78</sup> referred to as CNDO, INDO, MINDO and others which are faster than *ab initio*. Although the computation time is approximately proportional to the square of the number of orbitals, even this computational requirement is too large to render these methods of practical utility for most molecules of interest.

### 3.4.2. Semi-empirical calculations

Semi-empirical calculations or force field calculations have been extensively used for the determination of chemical structures<sup>79</sup>. For the evaluation of conformational energies these methods use different contributions to the total potential energy function (the force field) which include non-bonded interactions, bond and angle deformations, torsional terms, electrostatic interactions and hydrogen bonding. These calculations have the advantage that the amount of computational time is greatly reduced from the quantum mechanical calculations, being approximately proportional to the square of the number of atoms involved.

In order to simplify the procedure these calculations usually neglect the contribution of angle and bond deformations (stretching and bending) when applied to carbohydrates. The monosaccharide units of an oligosaccharide are thus considered as rigid bodies. This is justified by the crystallographic data for many sugars which indicate that crystal packing does not alter considerably the bond lengths or angles of related pyranose rings.<sup>82</sup> Arnott and Scott have also proposed the use of coordinates for an average pyranose ring.<sup>83</sup>

To assess the conformation of an oligosaccharide, the computer uses the atomic coordinates of the component sugar units (as determined from neutron diffraction and previously stored in a computer library) to generate the coordinates of the oligosaccharide. At this point the molecule possesses at least three degrees of freedom that must be specified before the potential energy can be determined. The size of the glycosidic angle  $\tau$  (as defined by C-1' — O-1 — C-4) is usually set at  $117.0^\circ$  which is the angle that occurs most frequently in crystallographic determinations of oligosaccharides.<sup>63</sup> The values of  $\phi$  and of  $\psi$  are, of course, the variables that will determine the orientation of an aglycon. The computer then calculates the total potential energy of the molecule at an initial conformation and iterates  $\phi$  and  $\psi$  in steps recalculating the energy for each conformer. The result is an energy map from which minimum energy conformers can be established.

In order to calculate the conformational energy, a potential energy function must be chosen. The two best known functions for the Van der Waal's forces are the Lennard-Jones potential:

$$E_{nb} = \frac{B}{r^{12}} - \frac{A}{r^6}, \quad (9)$$

and the Buckingham potential:

$$E_{nb} = Ce^{-\mu r} - \frac{A}{r^6}, \quad (10)$$

where A, B, C and  $\mu$  are parameters that have to be determined for each kind of pair of atoms present in the molecule and  $r$  is the internuclear separation. These equations represent the same general features of intermolecular potentials; at short distances the interaction energy is repulsive and increases very rapidly, roughly as an exponential of the atomic distance. The repulsion arises from nuclear - nuclear and electron - electron Coulombic interactions. At distances longer than at the minimum in energy, the forces involved are the so-called London dispersion forces which vary primarily as  $r^{-6}$  due to mutually induced fluctuating dipoles, *i.e.* distortion of the electron orbitals. The forces are attractive. The first part of Equations (9) and (10) describes the repulsive interactions and the second part the attractive interactions. Figure 7 illustrates these features.

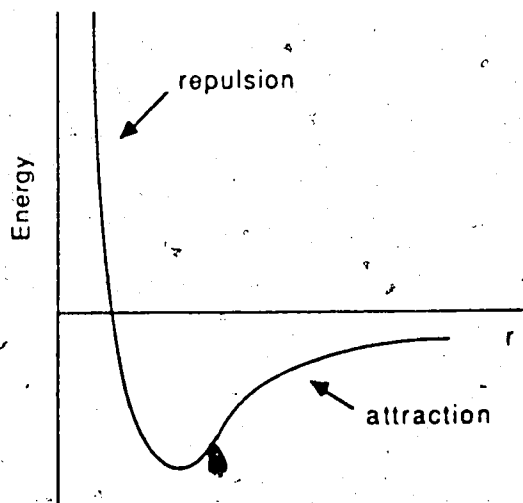


Figure 7. The interaction between two atoms depending on their separation as provided by the Lennard-Jones potential.

The next kind of force that is considered accounts for torsional terms. It is found that if the energy of a molecule such as ethane is calculated including only Van der Waal terms, the eclipsed conformation is less stable than the staggered form but not sufficiently less stable. In order to reproduce the experimental data, a torsional term is sometimes included, which for ethane has the form of Equation (11) (the Pitzer potential):

$$E_{\text{tors}} = (E_0/2)(1 - \cos 3\omega) \quad , \quad (11)$$

where;

$E_{\text{tors}}$  = the torsional energy,

$E_0$  = the barrier height of rotation,

$\omega$  = the H - C - C - H dihedral angle.

The barrier heights,  $E_0$ , may be found by way of microwave or n.m.r. spectroscopic measurements. The torsional energy is attributed to exchange interactions of electrons in bonds adjacent to the bond about which internal rotation occurs, following a theory developed by Pauling.<sup>84,85</sup> In his theory of internal rotation, Pauling adds some *d* and *f* character to his wavefunction for the carbon-bonding orbitals in addition to the usual *s* and *p* character. It is the small amount of *f* character which leads to the rotation barrier in his theory.

In order to achieve greater validity, an account is sometimes made of electrostatic interactions and of the energies of hydrogen bonds. The contribution of electrostatic interactions is usually approximated by considering the formation of partial point charges or monopoles on each of the atoms of the molecule and calculating the interaction energy according to the classical Coulomb potential:

$$E_c = \frac{k Q_i Q_j}{\epsilon r} \quad , \quad (12)$$

where,

$E_c$  = the electrostatic energy,

$k$  = a conversion constant,

$Q_i, Q_j$  = the partial charges on atoms  $i$  and  $j$ ,

$\epsilon$  = the dielectric constant of the medium,

$r$  = the separation between atoms  $i$  and  $j$ .

The residual charges can be calculated using quantum mechanical procedures.

The determination of a microscopic dielectric constant is more difficult and can only be estimated for a particular solvent. The energy potential for a hydrogen bond is also sensitive to the solvent and is usually assumed to follow the Morse potential:

$$E_{HB} = E_{diss} [ 1 - \exp(-\beta(r-r_e)^2) ] \quad , \quad (13)$$

where,

$E_{HB}$  = the hydrogen bond energy,

$E_{diss}$  = the dissociation energy of the bond,

$\beta$  = a constant related to the kind of hydrogen bond,

$r$  = the distance between  $-O \cdots HO-$ ,

$r_e$  = the equilibrium position of the bond.

The energy parametrization for hydrogen bonds is a difficult problem since data for aqueous solutions are not available and can only be roughly estimated based on data from work on peptides.<sup>86</sup>

From the previous paragraphs it can be appreciated that the actual form of the potential energy function used in a conformational calculation can take many different shapes according to which functions are used to describe each contribution to the total energy. At this point, the different implementations of the semi-empirical calculations used by some research groups and that have been applied to maltose will be described.

#### 3.4.2.1. Force field calculations for maltose and methyl maltosides

Kochetkov and coworkers<sup>28,26,56</sup> performed theoretical calculations on maltose and cellobiose using different models for the force field. They compared the results of calculations that use the potential functions proposed by Scott and Scheraga<sup>87</sup>, by Momany<sup>88</sup> and by Kitaigorodsky.<sup>89</sup> They included a torsional barrier around the glycosidic bond as described above. The influence of electrostatic interactions, hydrogen bonding and the *exo*-anomeric effect on the calculations was also studied. The results were then compared with the experimental data provided by the optical rotations and with the <sup>13</sup>C-n.m.r. coupling constants across the glycosidic bond. They concluded that conformational preferences in aqueous solutions could be described properly only when the non-bonded interactions were described by the parametrization of Scott and Scheraga and a torsional contribution for the constraint of rotation around the glycosidic bond was included. Allowance for electrostatic interactions, hydrogen bond or the *exo*-anomeric effect had no influence or yielded results which were in worse agreement with those expected from the speculations based on optical rotation. In fact, these calculations provide a complex conformational distribution for maltose consisting of four conformers

with different populations. The results for methyl  $\alpha$ -maltoside are presented in Table 2.

**Table 2.** Conformational distribution for methyl  $\alpha$ -maltoside obtained by Kochetkov *et al.*<sup>56</sup>

Conformer	$\phi$	$\psi$	E(kcal/mol)	population
A	-70°	-40°	-4.2	60%
B	-20°	-20°	-3.1	30%
C	20°	30°	-2.4	7%
D	-30°	-160°	-2.6	3%

These conclusions appeared supported by experimental data related to linkage optical rotations,  $^{13}\text{C}$ -coupling constants and nuclear Overhauser effects. These conclusions will be criticized later on in connection with the similar studies to be presented in this thesis.

Rees and Smith<sup>57</sup> performed calculations on maltose taking into account Van der Waal's interactions using a Lennard-Jones potential function with the parameters of Scott and Scheraga and invoking electrostatic interactions, a torsional term and hydrogen bond energies. Two conformers were obtained; namely, conformer M with  $\phi = -32^\circ$  and  $\psi = -13^\circ$  and the higher energy conformer R with  $\phi = -67^\circ$  and  $\psi = -38^\circ$ . On the basis of the optical linkage rotations for methyl  $\beta$ -maltoside, they concluded that the conformation in DMSO and dioxan is within  $5^\circ$  of the overall energy minimum, M, while in aqueous solution, an important contribution from conformer R is in effect.

A similar calculation was performed by Melberg and Rasmussen<sup>90,91</sup> to provide the four minimum energy conformers for  $\beta$ -maltose which are presented in Table 3.

**Table 3.** Conformational distribution for  $\beta$ -maltose obtained by Melberg and Rasmussen.<sup>90</sup>

Conformer	$\phi$	$\psi$	E(kcal/mol)	Population
A	-66°	-50°	0.00	86%
B	-18°	-31°	0.91	8%
C	3°	33°	1.65	5%
D	-41°	-162°	2.61	1%

Tvaroska<sup>55</sup> accepted the four conformers of Melberg and Rasmussen<sup>90</sup> and made theoretical calculations to anticipate how solvents may affect the conformation of  $\beta$ -maltose. It was concluded that a change of solvent may induce a redistribution of populations of the four conformers. The results were compared with the linkage optical rotations and the linkage coupling constants in several solvents and a qualitative agreement between the calculated and experimental data was found. The author concluded that the conformational equilibrium for  $\beta$ -maltose depends on electrostatic solvent-solute interactions.

In a collaboration with Pérez, Tvaroska<sup>92</sup> recently introduced a new methodology (MM2CARB which is a modified version of MM2<sup>77</sup> for the molecular modelling of carbohydrates) to approximate to the potential energy functions for dimethoxymethane and maltose. Based on a comparison of the results of their theoretical calculations with experimental data for



dimethoxymethane, it was concluded that MM2CARB is the preferred method. The calculations provided five conformers of maltose, three of these being most abundant (see Table 4). *They recommended that HSEA calculations be avoided.*

**Table 4.** The conformational equilibrium for maltose calculated by Tvaroska and Pérez<sup>92</sup>.

Conformer	$\phi$	$\psi$	E(kcal/mol)	Population
A	-58°	-42°	21.3	22%
B	-30°	-29°	21.0	38%
C	-30°	-170°	20.9	39%
D	26°	24°	24.1	0.2%
E	-49°	164°	24.0	0.2%

#### 3.4.2.2. Hard-sphere *exo*-anomeric calculations (HSEA)

The HSEA method of Lemieux *et al.*<sup>74</sup> is the simplest of all the calculations discussed so far and is based on the procedure used by Venkatachalam and Ramachandran<sup>93</sup> to estimate conformational preferences for polypeptides. It adopts a Buckingham equation modified by Kitaigorodsky<sup>89</sup> for the non-bonded interactions (Equation 14), in which  $z = r_{ij}/r_0$ .

$$E_{nb} = 3.5 ( -0.04 / z^6 + 8.5 \times 10^3 \exp( -13z ) ) \text{ kcal/mole} . \quad (14)$$

The term,  $r_{ij}$ , refers to the distance which separates the nuclei of the two interacting atoms and  $r_0$  is the equilibrium distance between these nuclei. The value of  $r_0$  is  $1.11(r_i + r_j)$ , where  $r_i$  and  $r_j$  are the Van der Waal's radii for the

atoms involved in the interaction. A torsional bonding energy, termed the *exo-anomeric effect*<sup>24</sup>, is added to the sum of the nonbonded energies. This energy function is that derived by *ab initio* calculation for dimethoxymethane<sup>80</sup> and has the form

$$E_{\text{exo},\alpha} = 1.58(1 - \cos\phi^{0.5}) - 0.74(1 - \cos 2\phi^{0.5}) - 0.70(1 - \cos 3\phi^{0.5}) + 1.72, \quad (15)$$

$$E_{\text{exo},\beta} = 2.61(1 - \cos\phi^{0.5}) - 1.21(1 - \cos 2\phi^{0.5}) - 1.18(1 - \cos 3\phi^{0.5}) + 2.86, \quad (16)$$

where  $E_{\text{exo},\alpha}$  and  $E_{\text{exo},\beta}$  are the *exo-anomeric effect* energies (in kcal/mol) for  $\alpha$ - and  $\beta$ - anomeric configurations. The form of these potentials is illustrated in Figure 8.

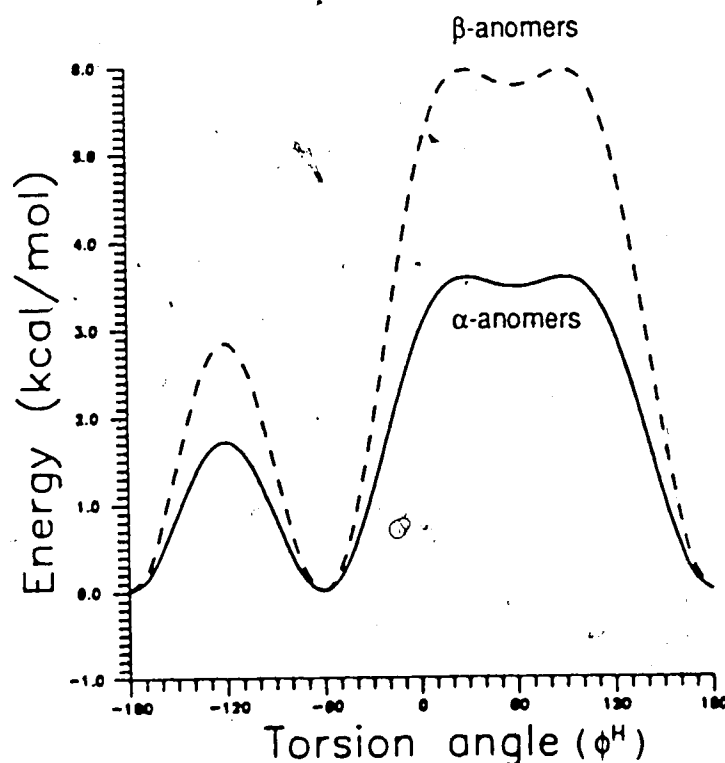


Figure 8. The changes in bond energy expected by *ab initio* calculation<sup>80</sup> as the orientation of the aglycon is changed by rotation about the glycosidic bond of a glycopyranoside. The  $0^\circ$  torsion angle is that for which the bond to the anomeric hydrogen is eclipsed to the aglycon.

No other terms are included in the force field. Although very simple, this method has been applied successfully to a variety of oligosaccharides, including the human blood group B trisaccharide ( $\alpha$ -L-Fuc(1 $\rightarrow$ 2)[ $\alpha$ -D-Gal(1 $\rightarrow$ 3)]- $\beta$ -D-Gal-OMe), since the results are verified by n.m.r.<sup>74</sup> and, in the case of the B blood group determinant, by X-ray crystallography.<sup>94</sup> A major advantage is the short computer times required to perform calculations that produce excellent results whenever the interactions between the sugar units do not involve strongly solvated groups such as hydroxyl groups.<sup>95</sup> The shape of Kitaigorodsky's potential produces a deep, well-defined energy well which reflects a conformational equilibrium with the most stable conformer in agreement with the experimental data to within  $\pm 10^\circ$  for the  $\phi$  and  $\psi$  torsion angles. The success of the HSEA calculations probably results from the fact that the most important forces controlling the orientation of aglycons in aqueous solution are Van der Waal's interactions and the *exo*-anomeric effect.<sup>63</sup>

Lemieux and Bock<sup>51</sup> performed HSEA calculations for maltose and methyl maltosides using different atomic coordinates for the glucosidic units and found that the conformational preferences and energies were sensitive to the orientation of the C-5 hydroxymethyl group. They interpreted this situation as arising mainly from the interaction between the hydroxymethyl group of the reducing end and H-5' of the other unit. Because the conformational preference of maltose in solution is strongly influenced by the orientation of the C-5 hydroxymethyl group a gearing effect<sup>96</sup> was proposed. It is largely these considerations which led to the research for this thesis which is in part a collaboration between the laboratories of Professors Lemieux and Bock.

## II. EXPERIMENTAL

### 1. General methods

All solvents and reagents were reagent grade and, if further purification was required, standard procedures<sup>97</sup> were followed. Anhydrous solution transfers were done under nitrogen using standard syringe techniques.<sup>98</sup>

Thin layer chromatography (tlc) was performed on precoated silica gel 60-F254 plates (E. Merck, Darmstadt) and developed by quenching fluorescence and/or charring after spraying with 5% sulfuric acid in ethanol. Silica gel 60H (E. Merck, No. 7736) or silica gel 60 (E. Merck, No. 9385, 0.040-0.063 mm) were used for medium pressure chromatography.

Melting points were determined on a Fisher-Johns melting point apparatus and are uncorrected. Optical rotations were measured with a Perkin-Elmer 241 polarimeter at 589 nm in a 1 dm cell at room temperature (23±1 °C). Elemental analyses were performed by the departmental Analytical Service Laboratory under the supervision of Mr. R. Swindlehurst.

### 2. NMR spectroscopy

<sup>1</sup>H-n.m.r. spectra were obtained at 295 °K on a Bruker WM-360 spectrometer operating at 360 MHz. The acquisition parameters consisted typically of spectral widths of 1.5 kHz, with a data memory of 16 K to give a digital resolution of 0.09 Hz/pt. Pulse widths employed were 4.5 μs (45°). Acetone was used as internal reference ( $\delta = 2.225$  ppm) in D<sub>2</sub>O and DMSO-*d*<sub>6</sub> solutions and tetramethylsilane (TMS,  $\delta = 0.000$  ppm) in CDCl<sub>3</sub> solutions.

Assignments were done using (a) double resonance experiments in connection with partially relaxed spectra, (b) 2D n.m.r. spectra (COSY,  $J$ -resolved), (c) nuclear Overhauser enhancement experiments.

The steady state n.O.e. experiments were performed in specially-treated glassware<sup>99</sup> and the solutions were previously degassed by bubbling dry nitrogen through for 5 min. Usually 400 scans or more were recorded. The  $D_2O$  used was purchased from Aldrich (99.96% D, low in paramagnetic impurities). Anhydrous  $DMSO-d_6$  was prepared by drying it over  $CaH_2$ <sup>100</sup> for several days under nitrogen, followed by distillation from freshly activated molecular sieves (BDH, 4Å, activated by heating overnight at 300°C at high vacuum) in a Kugelrohr "bulb-to-bulb" distillation apparatus at high vacuum. The solvent was then stored in the presence of molecular sieves under nitrogen.

Measurement of the nuclear Overhauser enhancements in  $DMSO-d_6$  was performed in the same way as for the  $D_2O$  solutions but approximately 1 mg of a basic resin (Dowex 1X2-200, hydroxide form) previously stirred in  $D_2O$  and freeze-dried twice was added to the solution prior to bubbling with nitrogen. The n.m.r. tube was then capped and sealed with parafilm (American Can Company) and kept at room temperature for at least two days with occasional stirring before the measurement was made. The spectra obtained following this procedure were generally free from any residual water signal that often precludes the measurement of the desired n.O.e.'s.

The deuterium induced isotope shifts were measured by dissolving a known amount (ca. 0.015 mmol) of the compound in  $DMSO-d_6$  (0.50 mL) and adding small aliquots of a standard solution of  $D_2O$  in  $DMSO-d_6$  with a microsyringe directly to the n.m.r. tube (capped with a rubber septum) to

provide a calculated ratio of OD/OH = 1.0. The addition of a few mg of calcined calcium sulphate to the DMSO- $d_6$  solution usually helped to slow down the rate of proton exchange and thus to sharpen the signals of the hydroxyl groups.

$^{13}\text{C}$ -n.m.r. spectra were obtained at 310-315 °K on the same instrument operating at 90.5 MHz. The acquisition parameters consisted typically of spectral widths of 10 KHz with a data memory of 16K and zero-filling<sup>101</sup> to 32K to give a digital resolution of 0.31 Hz/pt. The pulse widths employed were approximately 10  $\mu\text{s}$  (45°). Dioxane was used as internal reference ( $\delta = 67.40$  ppm) in  $\text{D}_2\text{O}$  and DMSO- $d_6$  solutions and tetramethylsilane ( $\delta = 0.00$  ppm) in  $\text{CDCl}_3$  solutions. Assignments were done using (a) 2D-nmr spectroscopy (heteronuclear COSY's) and (b) selective proton irradiation.

Spin-lattice relaxation times were measured by inversion recovery<sup>102</sup> and processed with the subroutines provided by Bruker's DISNMR program<sup>103</sup>.

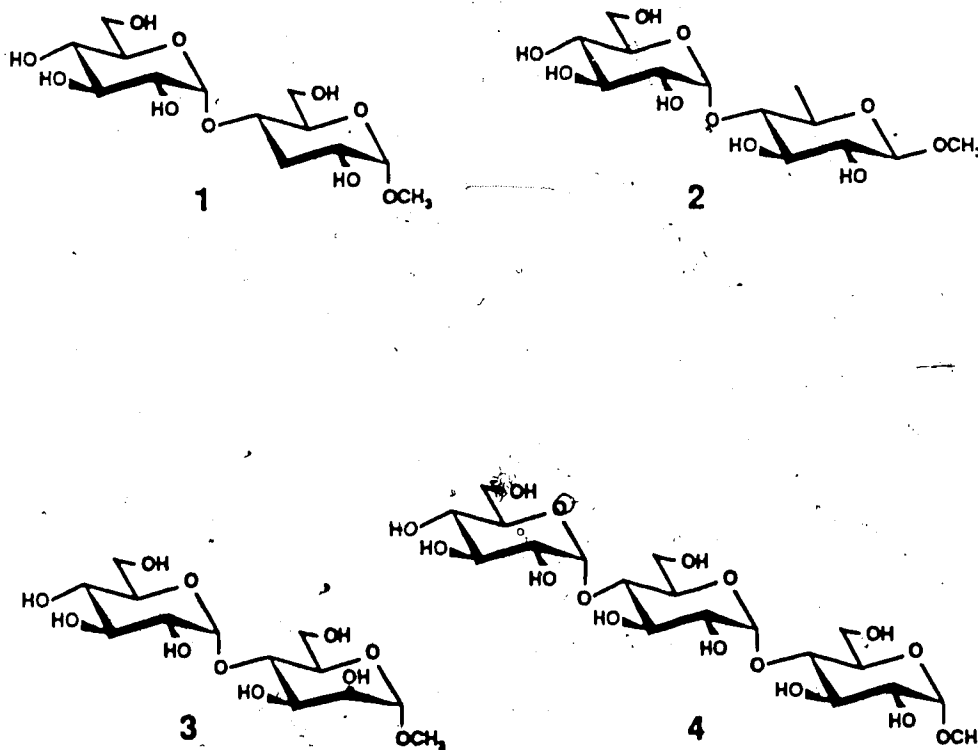
### 3. The calculation of conformational preference

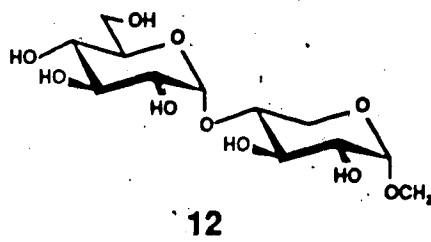
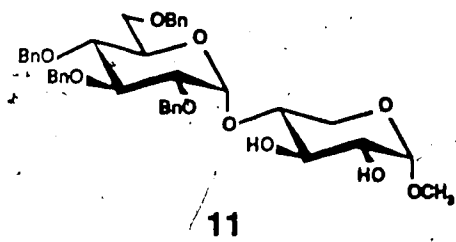
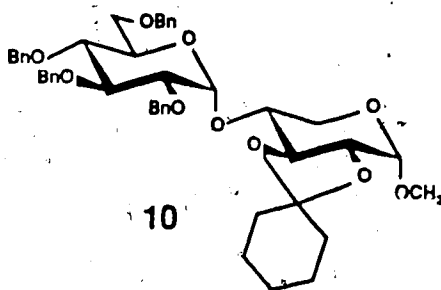
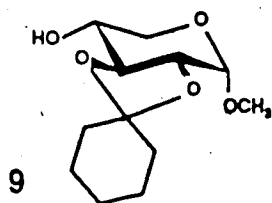
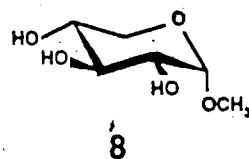
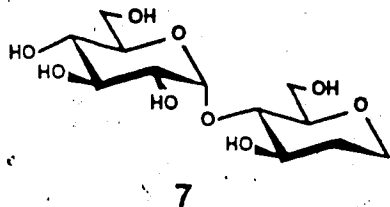
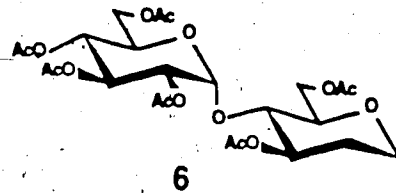
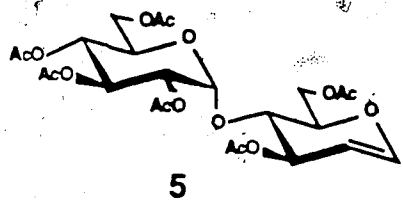
All molecular modelling presented in this thesis was obtained by application of the HSEA (hard sphere *exo*-anomeric effect) method<sup>74</sup>. As previously stated, this method uses the potential energy function of Kitaigorodsky<sup>89</sup> with the parametrization of Venkatachalan and Ramachandran<sup>93</sup> for the calculation of nonbonded interactions and a torsional potential energy function for rotation about the torsion angle  $\phi$  representing the *exo*-anomeric effect. The atomic coordinates were obtained from appropriate crystal structures; namely, the results of the neutron diffraction studies of methyl  $\alpha$ -D-glucopyranoside and methyl  $\alpha$ -D-mannopyranoside.<sup>53</sup> In the case

of deoxygenated glucopyranoses and  $\alpha$ -D-xylopyranoside, the coordinates were generated by bond modification of methyl  $\alpha$ -D-glucopyranoside using a C—H bond length of 1.10 Å. The internuclear distances generated by the HSEA program for a specific conformer provided the input for the determination of the theoretical nuclear Overhauser enhancements, for which purpose the computer program developed by H. Beierbeck was utilized.<sup>104</sup>

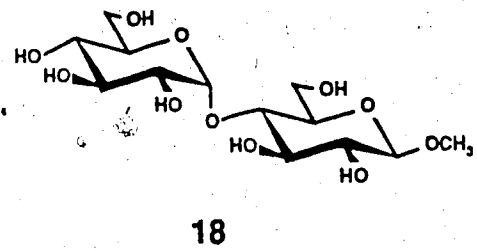
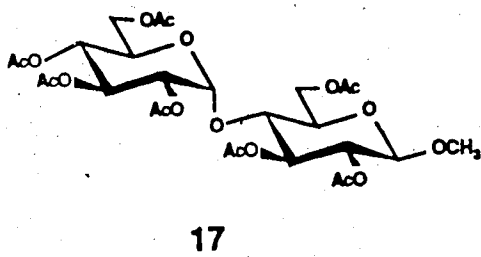
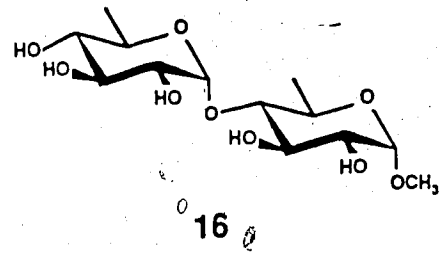
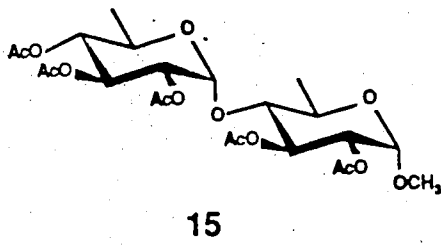
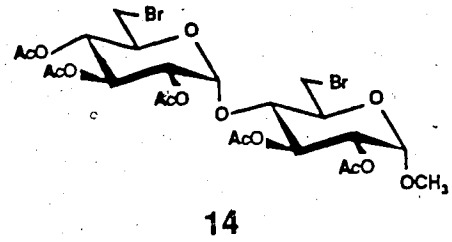
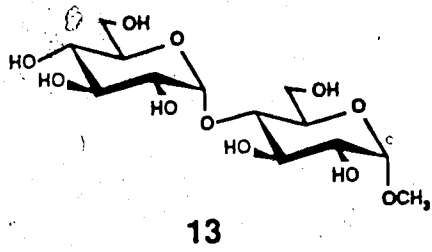
#### 4. Synthesis

This section deals with the following structures.









Samples of methyl 3-deoxy- $\alpha$ -maltoside (1), methyl 6-deoxy- $\beta$ -maltoside (2) and methyl 4-*O*-( $\alpha$ -D-glucopyranosyl)- $\alpha$ -D-mannopyranoside (3) were obtained from Professor Bock of The Technical University of Denmark, and used without further purification. Methyl  $\alpha$ -maltotriose (4) was synthesized by A. Ragauskas\*, m.p. 147-8°C,  $[\alpha]_D +200$  (c 1.4, H<sub>2</sub>O); lit.<sup>105</sup>, m.p. 145-7°C,  $[\alpha]_D +202$ .

*1,5-anhydro-2-deoxy-4-O- $\alpha$ -D-glucopyranosyl-D-arabino-hexitol* (7). — Maltal hexaacetate (3,6-di-*O*-acetyl-1,5-anhydro-2-deoxy-4-*O*-(2,3,4,6-tetra-*O*-acetyl- $\alpha$ -D-glucopyranosyl)-D-arabino-hex-1-enitol) (5) was prepared according to a published procedure,<sup>106</sup>  $[\alpha]_D +66.6$  (c 2.0, CHCl<sub>3</sub>); lit.<sup>106</sup>  $[\alpha]_D^{20} +68$  (c 0.8, CHCl<sub>3</sub>). This compound (4.30 g 7.68 mmol) was dissolved in methanol (50 mL) and treated with 10 mL of a solution of sodium methoxide in methanol (50 mg of sodium in 10 mL of methanol) at room temperature.<sup>107</sup> After 1 hr, 0.5 g of 5% palladium on charcoal, were added and the mixture was hydrogenated at 100 psi for 36 hr. Neutralization of the mixture with Amberlite IRC-50 (H<sup>+</sup>) followed by filtration of the catalyst and evaporation of the solvent under reduced pressure afforded 2.24 g of the title compound (7.22 mmol, 94% yield).  $[\alpha]_D +114.4$  (c 2.6, water). The <sup>1</sup>H-n.m.r. spectrum is reproduced in Figure 14a.

<sup>1</sup>H-n.m.r. (D<sub>2</sub>O):  $\delta$  5.36 (d,  $J_{1,2} = 4.0$  Hz, 1 H, H-1'), 3.96 (ddd,  $J_{1ax,1eq} = 12.0$  Hz,  $J_{1ax,2ax} = 12.0$  Hz,  $J_{1ax,2eq} = 2.0$  Hz, 1 H, H-1ax), 3.91 (ddd,  $J_{2ax,3} = 9.0$  Hz,  $J_{2eq,3} = 2.0$  Hz,  $J_{3,4} = 9.0$  Hz, 1 H, H-3), 3.90 (m, 1 H, H-5'), 3.75 (4 H, H-6a, H-6b, H-6a' and H-6b'), 3.69 (dd,  $J_{2,3} = 10.0$  Hz,  $J_{3,4'} = 9.5$  Hz, 1 H, H-3'), 3.59 (dd,  $J_{1,2} = 4.0$  Hz,  $J_{2,3} = 10.0$  Hz, 1 H, H-2'), 3.52 (ddd,  $J_{1ax,1eq} = 12.0$  Hz,

\*University of Alberta postdoctoral fellow (1985-86) in the laboratory of Professor Lemieux.

$J_{1ax,2ax} = 12.0$  Hz,  $J_{1ax,2eq} = 2.0$  Hz, 1 H, H-1ax), 3.48 (dd,  $J_{3,4} = 9.0$  Hz,  $J_{4,5} = 9.0$  Hz, 1 H, H-4), 3.41 (dd,  $J_{3,4} = J_{4,5} = 9.5$  Hz, 1 H, H-4'), 3.40 (m, 1 H, H-5), 2.01 (dddd,  $J_{1ax,2eq} = 2.0$  Hz,  $J_{1eq,2eq} = 1.5$  Hz,  $J_{2ax,2eq} = 13.0$  Hz,  $J_{2eq,3} = 2.0$  Hz, 1 H, H-2eq), 1.66 (dddd,  $J_{1ax,2ax} = 12.0$  Hz,  $J_{1eq,2ax} = 5.0$  Hz,  $J_{2ax,2eq} = 13.0$  Hz,  $J_{2ax,3} = 9.0$  Hz, 1 H, H-2ax).

Compound 7 could be purified by acetylation to afford its hexaacetate 6 which was easily crystallized from ethanol, m.p. 134-5°C. *Anal. Calc.* for  $C_{24}H_{34}O_{15}$ : C 51.24, H 6.09; found: C 51.51, 6.20.

*Methyl 2,3-O-cyclohexylidene-4-O-(2,3,4,6-tetra-O-benzyl- $\alpha$ -D-glucopyranosyl)- $\alpha$ -D-xylopyranoside (10).* — Methyl  $\alpha$ -D-xylopyranoside<sup>108</sup> (8) (0.60 g, 3.66 mmol), 1,1-dimethoxycyclohexane (1.0 mL, 0.94 g, 6.53 mmol) and p-toluenesulfonic acid monohydrate (7 mg) in dimethylformamide (4.8 mL) were heated at 130-140°C. After 14 h, several drops of triethylamine were added followed by solvent evaporation *in vacuo*. The resulting yellowish oil was chromatographed on a column of silica gel (940 g) using *n*-hexane-ethyl acetate-isopropanol (80:20:1) as eluent. The main fractions were concentrated to afford a mixture (0.528 g) of methyl 2,3-O-cyclohexylidene- $\alpha$ -D-xylopyranoside (9) and of its 8,4 isomer (in a ratio of 9:1 respectively) that could not be separated by column chromatography.<sup>109</sup>

<sup>1</sup>H-n.m.r. (200 MHz,  $CDCl_3$ ):  $\delta$  5.01 (d,  $J_{1,2} = 3.0$  Hz, 1 H, H-1), 3.99 (m, 1 H, H-4), 3.90 (dd,  $J_{2,3} = J_{3,4} = 9.0$  Hz, 1 H, H-3), 3.75 (dd,  $J_{4,5eq} = 5.0$  Hz,  $J_{5eq,5ax} = 11.0$  Hz, 1 H, H-5eq), 3.46 (s, 3 H,  $OCH_3$ ), 3.44 (dd,  $J_{1,2} = 3.0$  Hz,  $J_{2,3} = 9.0$  Hz, 1 H, H-2), 3.32 (dd,  $J_{4,5ax} = 9.5$  Hz,  $J_{5ax,5eq} = 11.0$  Hz, 1 H, H-5ax), 1.65 - 1.42 (10 H, cyclohexylidene).

The mixture of cyclohexylidenes (0.51 g, 2.09 mmol) was dissolved in dichloromethane (5 mL) and transferred to a flask containing powdered 4Å molecular sieves (6 g), tetraethylammonium bromide (0.44 g, 2.10 mmol) and dimethylformamide (1.7 mL) under nitrogen and stirred.<sup>110</sup> After 2 h, 2,3,4,6-tetra-*O*-benzyl- $\alpha$ -D-glucopyranosyl bromide (2.63 mmol) dissolved in dichloromethane was added by syringe and the solution was concentrated by flushing with nitrogen. After 22 h of stirring at room temperature methanol (3 mL) was added and the stirring continued for another 4 h. Then, the mixture was filtered through a pad of Celite and the filtrate was washed with water and saturated sodium bicarbonate. After drying, the solution was concentrated to an oil that was chromatographed using 80 g of silica gel with *n*-hexane - ethyl acetate - isopropanol (90:9:1) as eluent. The main fraction afforded the title compound as a thick syrup (0.786 g, 1.03 mmol, 23%). The <sup>1</sup>H-n.m.r. spectrum is reproduced in Figure 9.

<sup>1</sup>H-n.m.r. (200 MHz, CDCl<sub>3</sub>):  $\delta$  7.40 - 7.10 (20 H, aromatic), 5.52 (d,  $J_{1,2}$  = 3.5 Hz, 1 H, H-1'), 5.02 (d,  $J_{1,2}$  = 4.0 Hz, 1 H, H-1), 5.02 - 3.62 (15 H), 3.62 (dd,  $J_{1,2}$  = 3.5 Hz,  $J_{2,3}$  = 9.5 Hz, 1 H, H-2'), 3.62 - 3.45 (2 H), 3.45 (1 H, H-2), 3.43 (s, 3H, OCH<sub>3</sub>), 1.8 - 1.30 (10 H, cyclohexylidene).

*Methyl 4-O-(2,3,4,6-tetra-O-benzyl- $\alpha$ -D-glucopyranosyl)- $\alpha$ -D-xylopyranoside (11).* — Methyl 2,3-*O*-cyclohexylidene-4-*O*-(2,3,4,6-tetra-*O*-benzyl- $\alpha$ -D-glucopyranosyl)- $\alpha$ -D-xylopyranoside (10) (786 mg, 1.03 mmol) was dissolved in 90% trifluoroacetic acid (10 mL) and stirred for 10 min at room temperature.<sup>111</sup> Then it was rapidly concentrated *in vacuo* at 40°C and coevaporated 3 times with toluene. The resulting white solid (700 mg, 1.02 mmol) was recrystallized from ethanol to afford 365 mg (52%) of the title compound, m.p. 149-150°C.

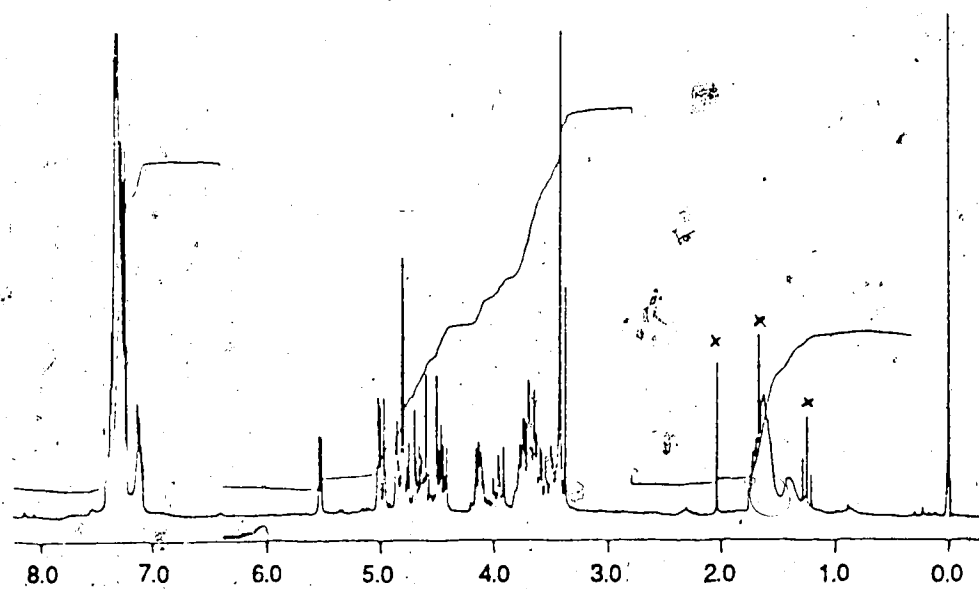


Figure 9. The <sup>1</sup>H-n.m.r. spectrum of compound 10 in CDCl<sub>3</sub> at 200 MHz.

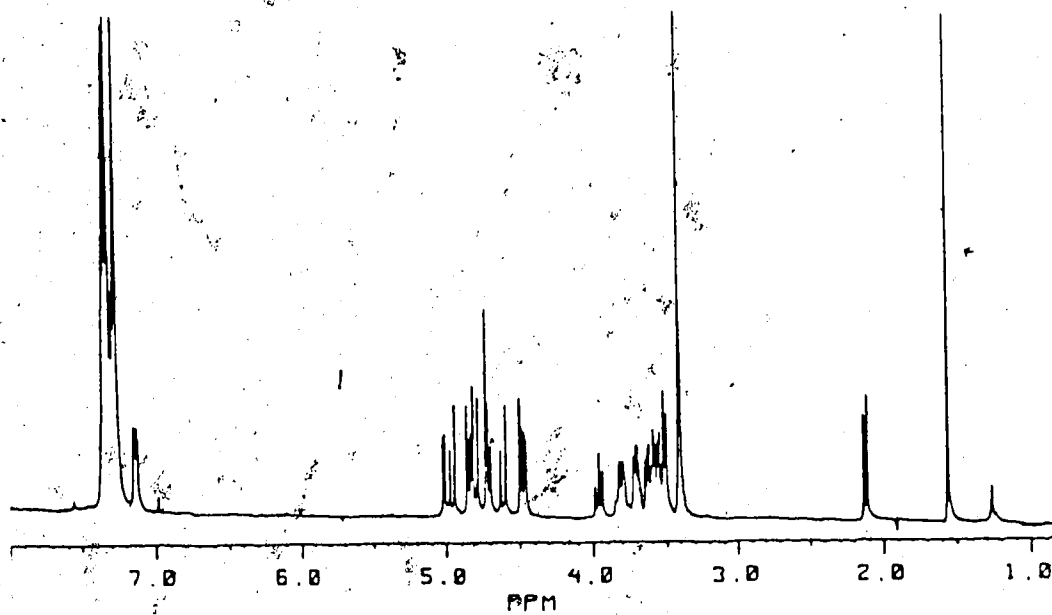


Figure 10. The <sup>1</sup>H-n.m.r. spectrum of compound 11 in CDCl<sub>3</sub>.

$[\alpha]_D^{24} +100^\circ$  (c 0.37,  $\text{CHCl}_3$ ). The  $^1\text{H}$ -n.m.r. spectrum is shown in Figure 10.

Anal. Calc. for  $\text{C}_{40}\text{H}_{46}\text{O}_{10}$ : C 69.95, H 6.75; found: C 69.97, H 6.77.

$^1\text{H}$ -n.m.r. ( $\text{CDCl}_3$ ):  $\delta$  7.40-7.10 (20 H,  $\text{C}_6\text{H}_5$ ), 5.00 (d,  $J_{1,2} = 3.5$  Hz, 1 H, H-1'), 4.94 (d,  $J = 11.0$  Hz, 1 H, Ph- $\text{CH}_2$ ), 4.83 (d,  $J = 11.0$  Hz, 1 H, Ph- $\text{CH}_2$ ), 4.81 (d,  $J = 11.0$  Hz, 1 H, Ph- $\text{CH}_2$ ), 4.78 (d,  $J = 11.5$  Hz, 1 H, Ph- $\text{CH}_2$ ), 4.71 (d,  $J_{1,2} = 4.0$  Hz, 1 H, H-1), 4.69 (d,  $J = 11.5$  Hz, 1 H, Ph- $\text{CH}_2$ ), 4.60 (d,  $J = 12.0$  Hz, 1 H, Ph- $\text{CH}_2$ ), 4.47 (d,  $J = 12.0$  Hz, 1 H, Ph- $\text{CH}_2$ ), 4.45 (d,  $J = 11.0$  Hz, 1 H, Ph- $\text{CH}_2$ ), 3.95 (dd,  $J = 9.0$  Hz, 1 H), 3.85-3.45 (10 H, ring protons), 3.40 (s, 3 H,  $\text{OCH}_3$ ).

*Methyl 4-O-( $\alpha$ -D-glucopyranosyl)- $\alpha$ -D-xylopyranoside (12).* — Methyl 4-O-(2,3,4,6-tetra-O-benzyl- $\alpha$ -D-glucopyranosyl)- $\alpha$ -D-xylopyranoside (11) (350 mg, 0.51 mmol) was dissolved in ethanol containing 10% palladium on charcoal (70 mg) and the mixture was stirred under hydrogen at 120 psi for 4 days. After removal of the catalyst the solution was evaporated to dryness to afford the title compound as a white solid, m.p.  $138^\circ$ - $141^\circ$  (135 mg, 0.41 mmol, 81%).  $[\alpha]_D^{23} +163.5^\circ$  (c 2.76,  $\text{H}_2\text{O}$ ). The  $^1\text{H}$ -n.m.r. spectrum is reproduced in Figure 15c.

$^1\text{H}$ -n.m.r. ( $\text{D}_2\text{O}$ ):  $\delta$  5.14 (d,  $J_{1,2} = 4.0$  Hz, 1 H, H-1'), 4.78 (d,  $J_{1,2} = 4.0$  Hz, 1 H, H-1), 3.91 (dd,  $J_{4,5ax} = 10.0$  Hz,  $J_{5ax,5eq} = 10.0$  Hz, 1 H, H-5ax), 3.85 (dd,  $J_{5,6b'} = 2.2$  Hz,  $J_{6a',6b'} = 12.0$  Hz, 1 H, H-6b'), 3.80 (dd,  $J_{2,3} = 9.8$  Hz,  $J_{3,4} = 9.2$ , 1 H, H-3), 3.75 (dd,  $J_{5,6a'} = 5.5$  Hz,  $J_{6a',6b'} = 12.0$  Hz, 1 H, H-6a'), 3.68 (dd,  $J_{2,3} = 10.0$  Hz,  $J_{3,4} = 9.0$  Hz, 1 H, H-3'), 3.64 (ddd,  $J_{3,4} = 9.2$  Hz,  $J_{4,5ax} = 10.0$  Hz,  $J_{4,5eq} = 4.0$ , 1 H, H-4), 3.64 (ddd,  $J_{4,5} = 9.8$  Hz,  $J_{5,6a'} = 5.5$  Hz,  $J_{5,6b'} = 2.2$  Hz, 1 H, H-5'), 3.61 (dd,  $J_{4,5eq} = 4.0$  Hz,  $J_{5ax,5eq} = 10.0$  Hz, 1 H, H-5eq), 3.60 (dd,  $J_{1,2} = 4.0$  Hz,  $J_{2,3} = 9.8$  Hz, 1 H, H-2), 3.54 (dd,  $J_{1,2} = 4.0$  Hz,  $J_{2,3} = 10.0$

Hz, 1 H, H-2'), 3.41 (s, 3 H, OCH<sub>3</sub>), 3.39 (dd,  $J_{3,4} = 9.0$  Hz,  $J_{4,5} = 9.8$  Hz, 1 H, H-4').

*Methyl 2,3-di-O-acetyl-6-bromo-6-deoxy-4-O-(2,3,4-tri-O-acetyl-6-bromo-6-deoxy- $\alpha$ -D-glucopyranosyl)- $\alpha$ -D-glucopyranoside (14).* — Methyl  $\alpha$ -maltoside (13) (1.00 g, 2.81 mmol), previously dried under vacuum at 110°C for several hours, was dissolved in dimethylformamide (15 mL) and heated to 65°C. Then, oxalyl bromide (6 mL, ca. 12 g, 55.6 mmol) was slowly added by syringe with stirring. After the addition of more dimethylformamide (10 mL), the mixture was kept at 65°C under nitrogen for 17 h. The dark solution was then concentrated at 50°C *in vacuo* and co-evaporated *in vacuo* once with toluene. The residue was taken up in methanol (15 mL) and methanolic sodium methoxide 3 M was added until the pH was 9. The resulting solution was stirred for 1 h, neutralized with Amberlite IRC-50(H<sup>+</sup>), and filtered. After evaporation of the solvent and co-evaporation with pyridine, the resulting syrup was acetylated with 40% acetic anhydride in pyridine. After 2 days at room temperature, the dark solution was poured into water-ice, and extracted 4 times with chloroform. The chloroform solution was washed with 10% sulfuric acid, saturated aqueous sodium bicarbonate and then with water and evaporated to afford 1.99 g of a yellow solid.<sup>112</sup> Column chromatography of the solid on 75 g of silica gel using *n*-hexane-ethyl acetate-isopropanol 80:20:1 as eluent and evaporation of the main fractions afforded the title compound as a white solid (0.70 g, 1.01 mmol, 36% yield),  $[\alpha]_D^{24} +138^\circ$  (c 0.24, CHCl<sub>3</sub>). The <sup>1</sup>H-n.m.r. spectrum is reproduced in Figure 11.

<sup>1</sup>H-n.m.r. (CDCl<sub>3</sub>):  $\delta$  5.56 (dd,  $J_{2,3} = 10.0$  Hz,  $J_{3,4} = 8.5$  Hz, 1 H, H-3), 5.50 (d,  $J_{1,2} = 4.0$  Hz, 1 H, H-1'), 5.38 (dd,  $J_{2,3} = 11.0$  Hz,  $J_{3,4} = 9.5$  Hz, 1 H, H-3'), 5.06 (dd,  $J_{3,4} = J_{4,5} = 9.5$  Hz, 1 H, H-4'), 4.90 (d,  $J_{1,2} = 3.5$  Hz, 1 H, H-1),

4.85 (dd,  $J_{1,2'} = 4.0$  Hz,  $J_{2,3'} = 10.5$  Hz, 1 H, H-2'), 4.78 (dd,  $J_{1,2} = 4.0$  Hz,  $J_{2,3} = 10.5$  Hz, 1 H, H-2), 4.03 (dd,  $J_{3,4} = J_{4,5} = 9$  Hz, 1 H, H-4), 4.01 (m, 2 H, H-5 and H-5'), 3.78 (dd,  $J_{5,6} = 2.0$  Hz,  $J_{6,6} = 11.5$  Hz, 1 H, H-6a), 3.72 (dd,  $J_{5,6} = 4.0$  Hz,  $J_{6,6} = 12.0$  Hz, 1 H, H-6a'), 3.64 (dd,  $J_{5,6} = 3.0$  Hz,  $J_{6,6} = 11.5$  Hz, 1 H, H-6b'), 3.45 (s, 3 H, OCH<sub>3</sub>), 3.44 (dd,  $J_{5,6} = 5.0$  Hz,  $J_{6,6} = 12.0$  Hz, 1 H, H-6b), 2.07, 2.06, 2.05, 2.03, 2.02 (s each, 3 H each, 5 acetyl).

*Methyl 2,3-di-O-acetyl-6-deoxy-4-O-(2,3,4-tri-O-acetyl-6-deoxy- $\alpha$ -D-glucopyranosyl)- $\alpha$ -D-glucopyranoside (15).* — *Methyl 2,3-di-O-acetyl-6-bromo-6-deoxy-4-O-(2,3,4-tri-O-acetyl-6-bromo-6-deoxy- $\alpha$ -D-glucopyranosyl)- $\alpha$ -D-glucopyranoside (14)* (0.70 g, 1.01 mmol) was dissolved in dimethylsulfoxide (20 mL). Sodium borohydride (0.4 g, 10.6 mmol) was added and the temperature was raised to 70°C under nitrogen. After 3.5 h, glacial acetic acid was added dropwise to the solution until effervescence ceased, then the solvent was evaporated at 60°C under vacuum and the residue was co-evaporated several times with methanol. The residue (0.432 g) was treated with acetic anhydride-pyridine overnight. The dark yellow solution was then poured into ice-water and the mixture was extracted with chloroform several times. After washing the chloroform solution with 10% H<sub>2</sub>SO<sub>4</sub>, saturated NaHCO<sub>3</sub> and water, it was dried and the solvent was removed.<sup>112</sup> The product, which consisted of a dark oil (0.393 g) was chromatographed over silica gel using *n*-hexane - ethyl acetate - isopropanol (70:30:1). The fraction containing the major compound was concentrated and filtered through a small plug of charcoal to afford 0.334 g of an almost white solid. This material was again chromatographed over silica gel (15 g) using *n*-hexane - ethyl acetate - isopropanol (90:10:1) to provide the title compound as a white solid (172 mg, 0.322 mmol, 32% overall) which showed only one spot on t.l.c. This spot developed an intense yellow color when charring the plate with 10% H<sub>2</sub>SO<sub>4</sub> in



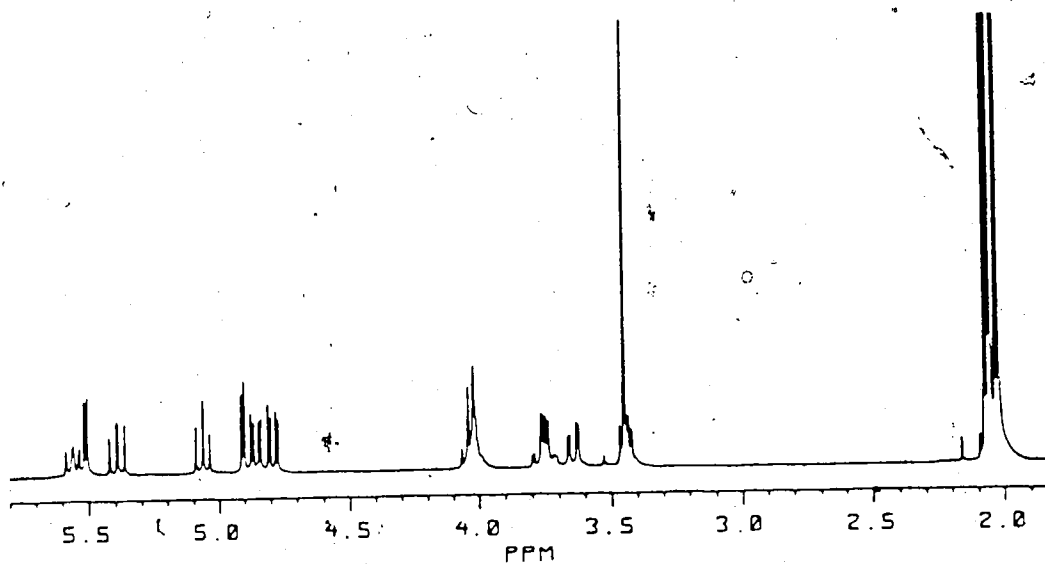


Figure 11. The  $^1\text{H}$ -n.m.r. spectrum of compound 14 in  $\text{CDCl}_3$ .

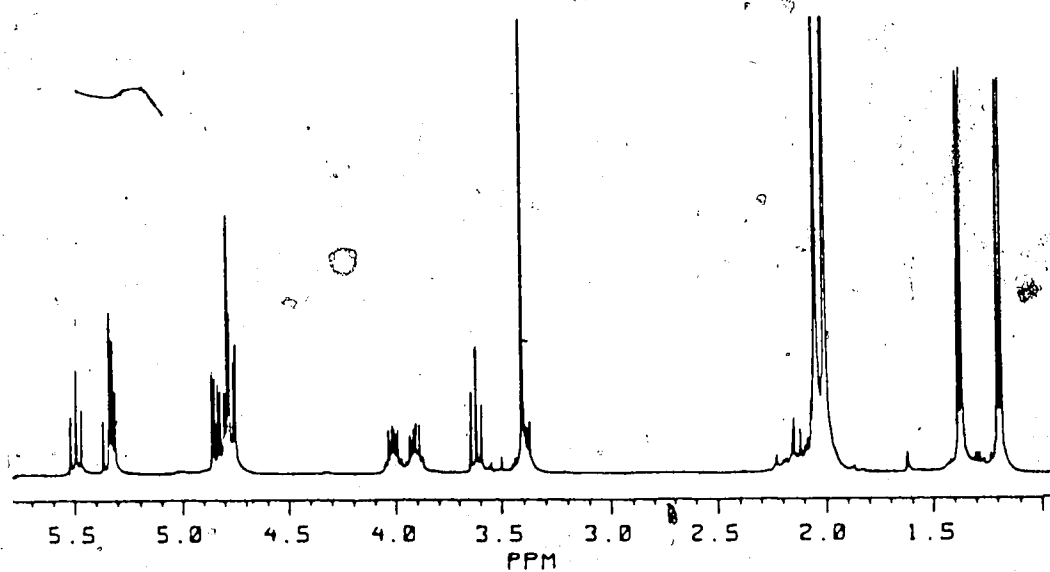


Figure 12. The  $^1\text{H}$ -n.m.r. spectrum of compound 15 in  $\text{CDCl}_3$ .

ethanol,  $[\alpha]_D^{24} +147^\circ$  (c 1.80,  $\text{CHCl}_3$ ). The  $^1\text{H}$ -n.m.r. spectrum is shown in Figure 12.

$^1\text{H}$ -n.m.r. ( $\text{CDCl}_3$ ):  $\delta$  3.40 (dd,  $J_{2,3} = J_{3,4} = 9.0$  Hz, 1 H, H-3), 5.33 (dd,  $J_{2,3} = J_{3,4} = 10.0$  Hz, 1 H, H-3'), 5.32 (d,  $J_{1,2} = 4.0$  Hz, 1 H, H-1'), 4.84 (dd,  $J_{1,2} = 4.0$  Hz,  $J_{2,3} = 11.0$  Hz, 1 H, H-2'), 4.79 (d,  $J_{1,2} = 4.0$  Hz, 1 H, H-1), 4.77 (dd,  $J_{4,3} = J_{4,5} = 10.0$  Hz, 1 H, H-4'), 4.76 (dd,  $J_{1,2} = 3.5$  Hz,  $J_{2,3} = 10.0$  Hz, 1 H, H-2), 4.00 (dq,  $J_{4,5} = 10.0$  Hz,  $J_{5,6} = 6.5$  Hz, 1 H, H-5'), 3.90 (dq,  $J_{4,5} = 9.5$  Hz,  $J_{5,6} = 6.0$  Hz, 1 H, H-5), 3.61 (dd,  $J_{3,4} = J_{4,5} = 9.0$  Hz, 1 H, H-4), 3.40 (s, 3 H,  $\text{OCH}_3$ ), 2.05 (s, 3 H,  $\text{OAc}$ ), 2.04 (s, 6 H,  $\text{OAc}$ ), 2.00, 1.99 (s each, 3 H each,  $\text{OAc}$ ), 1.37 (d,  $J_{5,6} = 6.0$  Hz, 3 H, H<sub>3</sub>-6), 1.18 (d,  $J_{5,6} = 6.5$  Hz, 3 H, H<sub>3</sub>-6').

$^{13}\text{C}$ -n.m.r. ( $\text{CDCl}_3$ ):  $\delta$  170.69, 170.31, 169.94, 169.89, 169.71 (carbonyl carbons), 96.53, 95.32 (C-1, C-1'), 77.69, 73.47, 72.76, 71.87, 70.48, 69.61, 66.05, 65.40 (ring carbons), 55.14 ( $\text{OCH}_3$ ), 20.96, 20.69, 20.66, 20.63, 20.59 (acetyl carbons), 18.53, 16.95 (C-6, C-6').

*Methyl 6-deoxy-4-O-(6-deoxy- $\alpha$ -D-glucopyranosyl)- $\alpha$ -D-glucopyranoside (16).* — Methyl 2,3-di-O-acetyl-6-deoxy-4-O-(2,3,4-tri-O-acetyl-6-deoxy- $\alpha$ -D-glucopyranosyl)- $\alpha$ -D-glucopyranoside (15) (80 mg, 0.150 mmol) was deacetylated according to Zemplén's method<sup>107</sup> to afford a yellow solid (45 mg, 0.140 mmol, 93% yield) that was passed through a Biogel column (Bio-Rad Laboratories) and eluted with 10% ethanol producing a white solid,  $[\alpha]_D^{24} +192^\circ$  (c 0.66,  $\text{H}_2\text{O}$ ),  $[\alpha]_D^{24} +180^\circ$  (c 0.22, DMSO). The  $^1\text{H}$ -n.m.r. spectrum is reproduced in Figure 20c.

$^1\text{H}$ -n.m.r. ( $\text{D}_2\text{O}$ ):  $\delta$  5.32 (d,  $J_{1,2} = 3.5$  Hz, 1 H, H-1'), 4.75 (d,  $J_{1,2} = 4.0$  Hz, 1 H, H-1), 3.85 (dd,  $J_{2,3} = 9.0$  Hz,  $J_{3,4} = 9.5$  Hz, 1 H, H-3), 3.85 (dq,  $J_{4,5} = 9.5$  Hz,  $J_{5,6} = 6.3$  Hz, 1 H, H-5), 3.85 (dq,  $J_{4,5} = 9.2$  Hz,  $J_{5,6} = 6.3$  Hz, 1 H,

H-5'), 3.60 (dd,  $J_{1,2} = 4.0$  Hz,  $J_{2,3} = 9.0$  Hz, 1 H, H-2), 3.60 (dd,  $J_{1,2} = 3.5$  Hz, 1 H, H-2), 3.60 (dd,  $J_{3,4} = 9.2$  Hz, 1 H, H-3'), 3.41 (s, 3 H, OCH<sub>3</sub>), 3.31 (dd,  $J_{3,4} = J_{4,5} = 9.5$  Hz, 1 H, H-4), 3.16 (dd,  $J_{3,4} = J_{4,5} = 9.2$  Hz, 1 H, H-4'), 1.32 (d,  $J_{5,6} = 6.3$  Hz, 3 H, H-6 or H-6'), 1.27 (d,  $J_{5,6} = 6.3$  Hz, 3 H, H-6' or H-6).

*Methyl β-maltoside (18)*. — The title compound was prepared according to published procedures<sup>113,114</sup>, m.p. 111-3 °C,  $[\alpha]_D +79.0$  (c 1.9, H<sub>2</sub>O); lit.<sup>115</sup> m.p. 108-9 °C,  $[\alpha]_D^{23} +78$  (c 2, H<sub>2</sub>O). The <sup>1</sup>H-n.m.r. spectrum is reproduced in Figure 13a.

*Methyl α-maltoside (13)*. — The title compound was synthesized by anomerization of methyl β-maltoside heptaacetate (17) with TiCl<sub>4</sub> in CHCl<sub>3</sub> as previously described<sup>116-118</sup> followed by selective removal of the remaining β-anomer with CrO<sub>3</sub> in acetic acid<sup>119,120</sup>. After deacetylation, the material was purified<sup>121,122</sup> by passing it through a column containing Amberlite IRA-400(OH<sup>-</sup>),  $[\alpha]_D +182.1$  (c 3.7, H<sub>2</sub>O); lit.<sup>130</sup>  $[\alpha]_D +183$ . The <sup>1</sup>H-n.m.r. spectrum is reported in Figure 13b.

### III. DISCUSSION

#### 1. Synthesis

A review on the chemistry of maltose and derivatives was recently published by Khan.<sup>123</sup>

Methyl  $\beta$ -maltoside heptaacetate (**17**) was prepared by way of Koenigs-Knorr reaction according to published procedures.<sup>113,114</sup> Deacetylation provided crystalline methyl  $\beta$ -maltoside (**18**) with the <sup>1</sup>H-n.m.r. spectrum shown in Figure 13a. The synthesis of methyl  $\alpha$ -maltoside (**13**) was carried out as follows. The acetate **17** was converted to a mixture with its  $\alpha$ -anomer (about 80%) using titanium tetrachloride in chloroform<sup>116-118</sup> from which compound **13** was isolated following the procedure of Angyal and James<sup>124</sup> as applied by Dick and coworkers<sup>119-120</sup>. The process is outlined in Scheme 1. The selective removal of the remaining  $\beta$ -anomer depends on a much more rapid oxidation of the acetylated methyl  $\beta$ -maltoside (**17**) by chromium trioxide to form the esterified ulonic acid. The crude product was deacetylated, dissolved in water and the solution passed through a column containing Amberlite IRA-400(OH<sup>-</sup>). This treatment is to decompose the methyl ester either through  $\beta$ -elimination on the  $\alpha$ -D-glucopyranosyl unit which then undergoes degradation to saccharinic-type products or by saponification of the methyl ester. Thus, all the products are carboxylic acids which are retained by the column. The desired methyl  $\alpha$ -maltoside (**13**) in the eluate was essentially pure as seen from its <sup>1</sup>H-n.m.r. spectrum presented in Figure 13b.

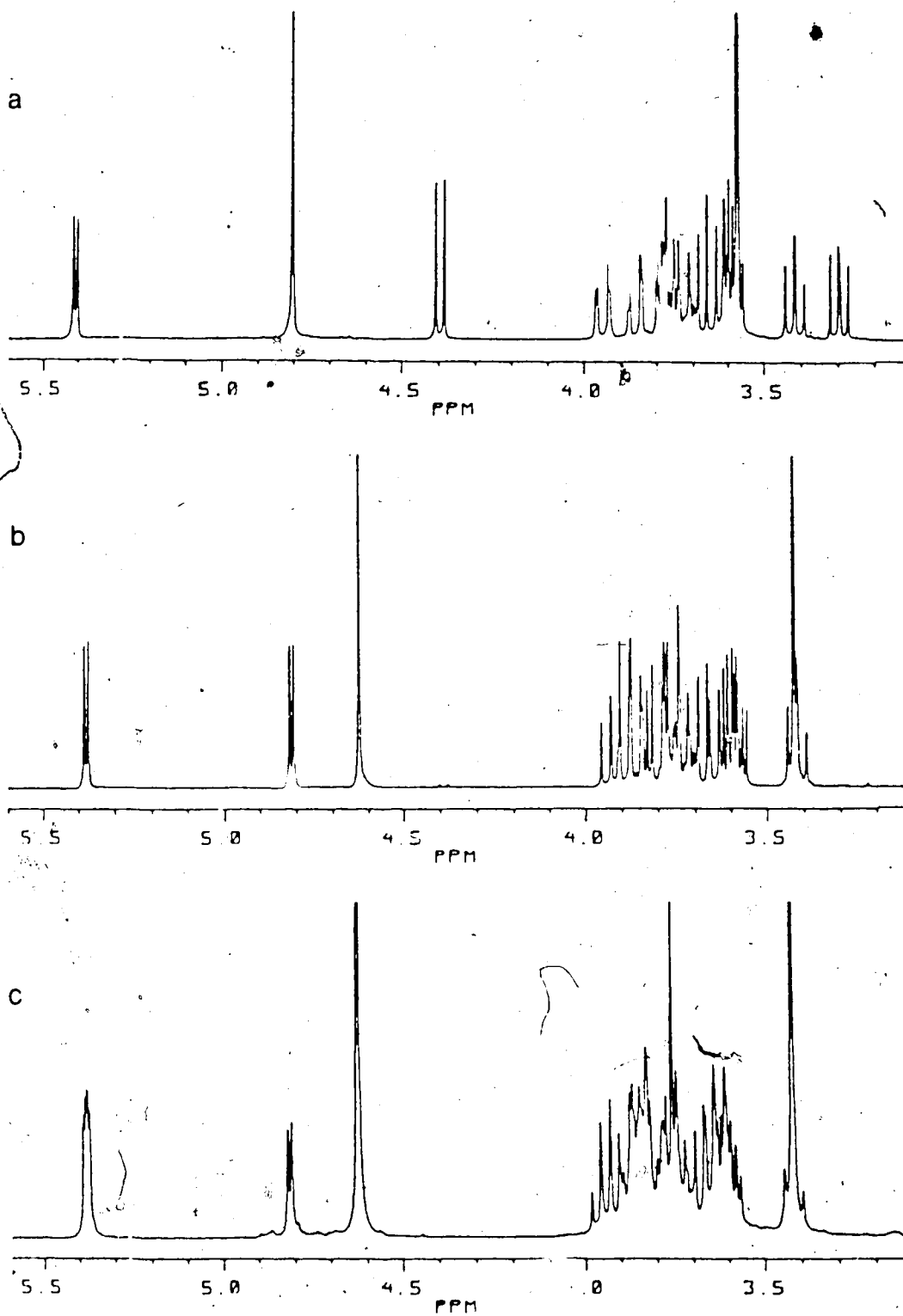
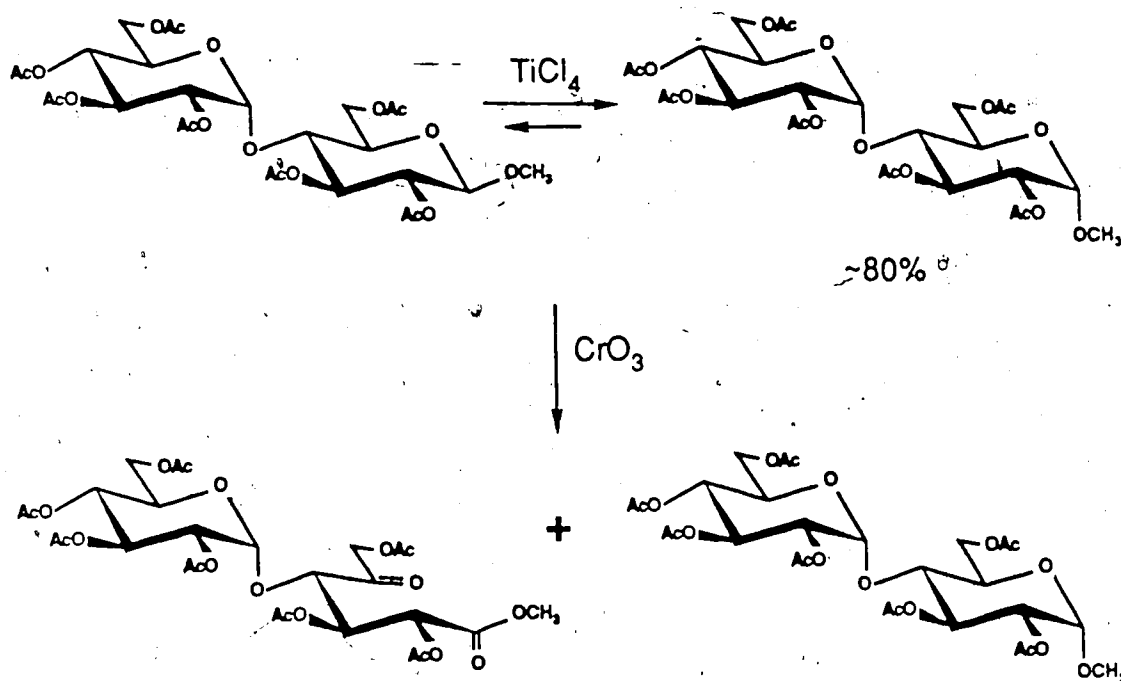


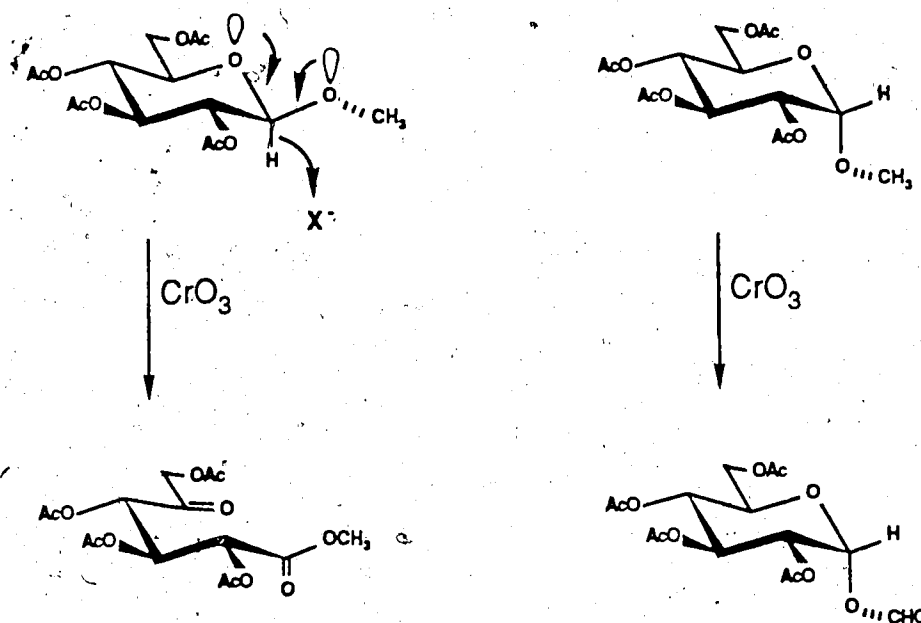
**Figure 13.** The <sup>1</sup>H-n.m.r. spectrum in D<sub>2</sub>O of a) methyl β-maltoside (18) at 295 °K, b) methyl α-maltoside (13) at 310 °K and c) methyl α-maltotrioside (4) at 310 °K.



Scheme 1

Chromium trioxide in acetic acid was shown by Angyal and James<sup>124</sup> to oxidize acetals of aldehydes,  $R_1CH(OR_2)OR_3$ , to esters,  $R_1COOR_2$ , in which one of the alcohols of the acetal is retained while the other is oxidized to a ketone. Glycopyranosides are oxidized to the esters of 5-hexulosonic acids, in which the aglycon is retained and the ring is ruptured. Although the selectivity of the reaction to oxidize only  $\beta$ -anomers was first rationalized<sup>125</sup> in terms of the relative steric accessibility of H-1 in the  $\alpha$ - and  $\beta$ -conformers, it is, in all probability, a consequence of a stereoelectronic effect which requires both oxygen atoms of the acetal system to have a lone pair orbital oriented antiperiplanar to the C—H bond of the acetal as shown by Deslongchamps<sup>126</sup> for the ozonolysis of acetals. As seen in Scheme 2, the lone pair orbitals of the

ring oxygen of an  $\alpha$ -glycoside are never antiperiplanar to the C—H bond while in the  $\beta$ -anomer, in the most stable orientation of the aglycon<sup>127</sup>, both oxygen atoms have lone pair orbitals oriented antiperiplanar to the C—H bond. This arrangement would facilitate the initial electrophilic attack on the C—H bond<sup>128</sup> as displayed in Scheme 2. The  $\alpha$ -anomer, on the other hand, only undergoes a slow oxidation of the methoxy group<sup>129</sup>.



Scheme 2

The synthesis of "1,2-dideoxymaltose" (7) started from maltal hexaacetate (5) which was prepared by reduction of peracetylated maltosyl bromide with zinc and acetic acid according to the procedure of Haworth and coworkers<sup>106</sup>. Deacetylation and hydrogenation provided the desired 1,2-dideoxymaltose. Its <sup>1</sup>H-n.m.r. spectrum is reproduced in Figure 14a. The acetate (6) of compound 7 crystallized readily from ethanol and was purified by recrystallization from the same solvent. Deacetylation of pure 6 then afforded pure 7.

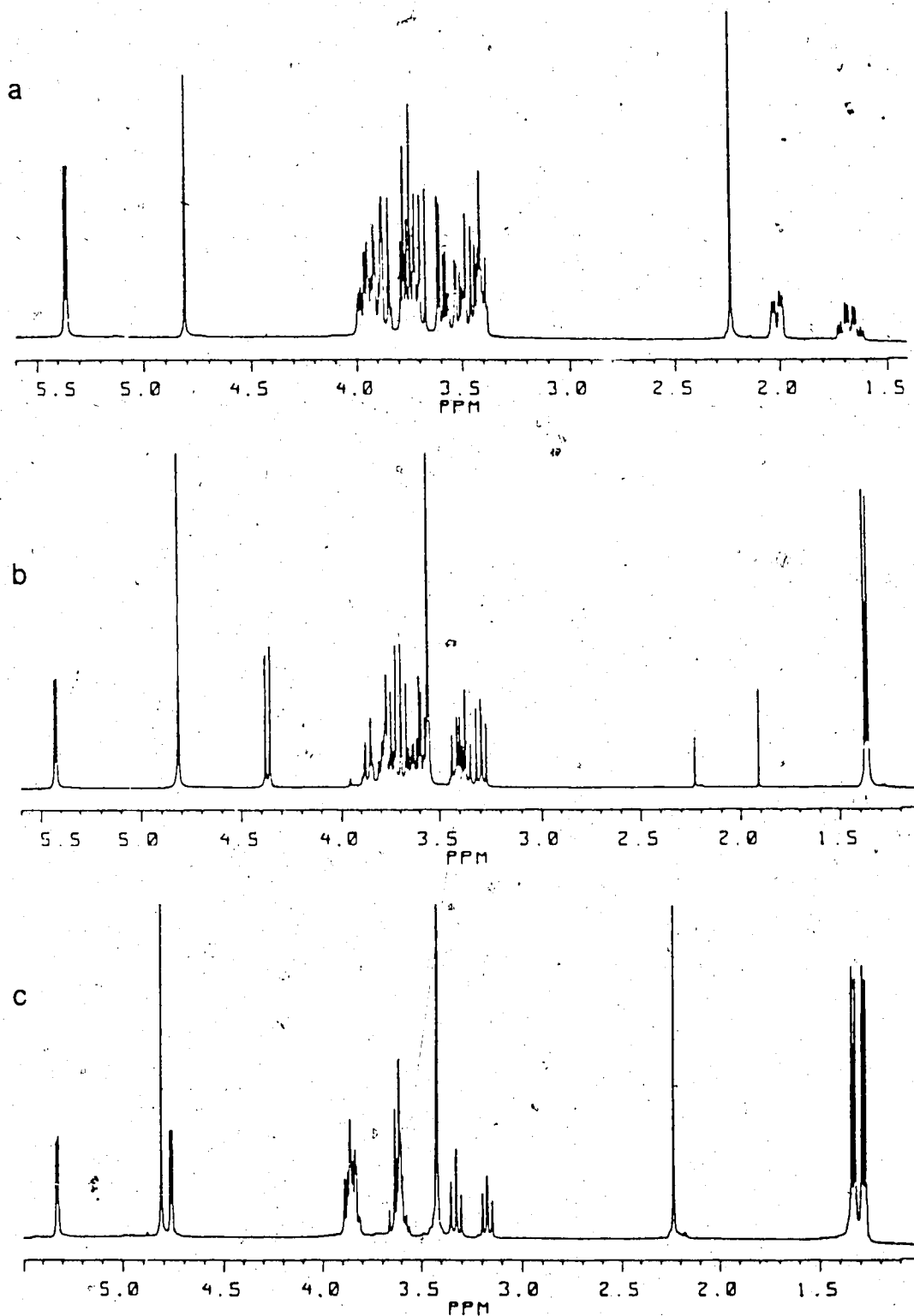
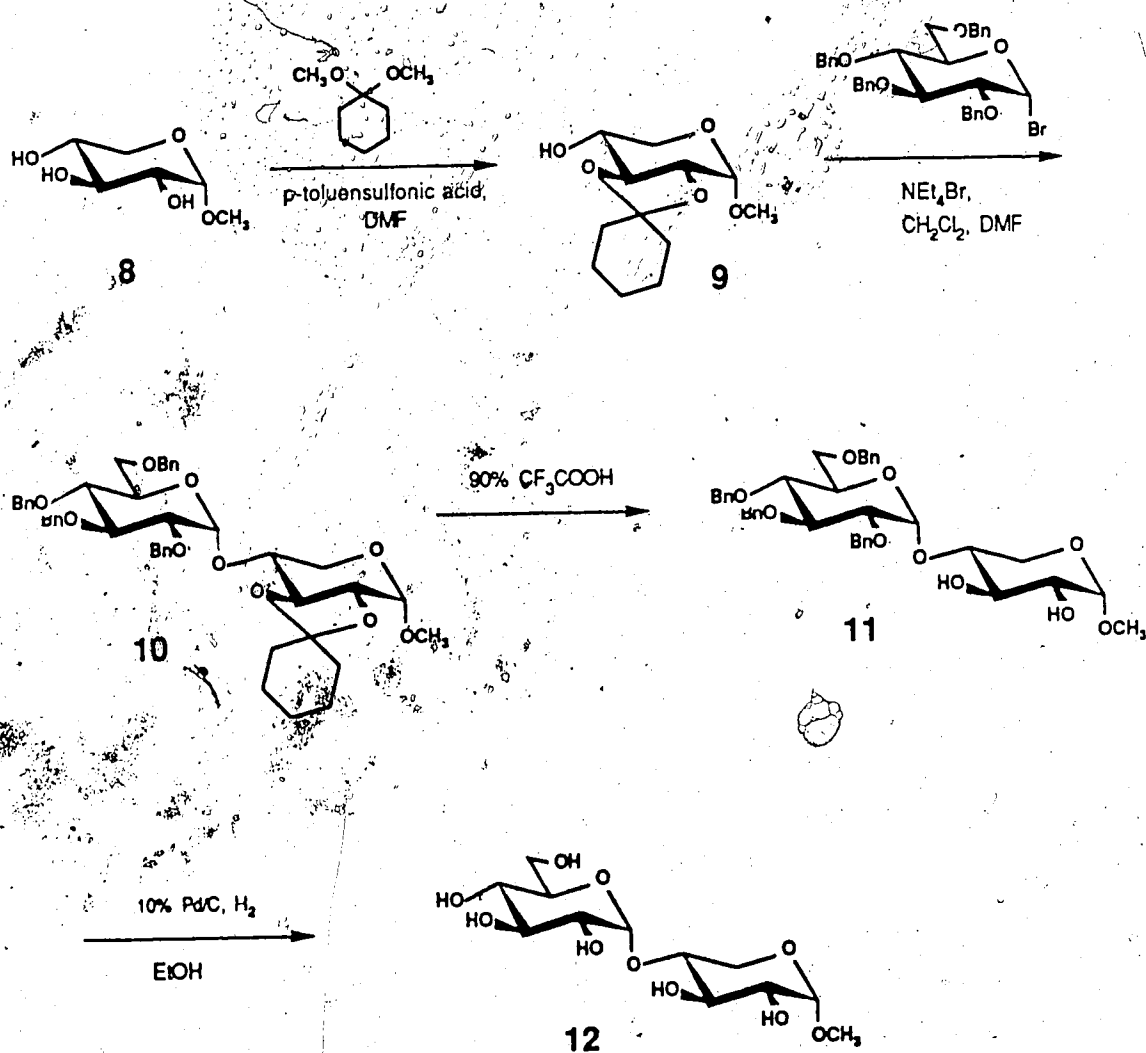


Figure 14. The  $^1\text{H-n.m.r.}$  spectrum in  $\text{D}_2\text{O}$  at 295 °K of a) 1,2-dideoxymaltose (7), b) methyl 6-deoxy- $\beta$ -maltoside (2) and c) methyl 6,6'-dideoxy- $\alpha$ -maltoside (16).



A derivative of methyl  $\alpha$ -D-xylopyranoside (8), protected at the 2 and 3 positions, was required for the synthesis of compound 12. The compound selected was methyl 2,3-O-cyclohexylidene- $\alpha$ -D-xylopyranoside (9) which had been prepared by Koto and coworkers<sup>109</sup> in 63% yield. The synthesis, according to the published method proceeded as reported but the product, which consisted of a mixture of the 2,3 and 3,4-cyclohexylidenes, could not be purified by column chromatography. Nevertheless, purification was achieved at a later stage in the synthesis using the procedure outlined in Scheme 3.



Scheme 3

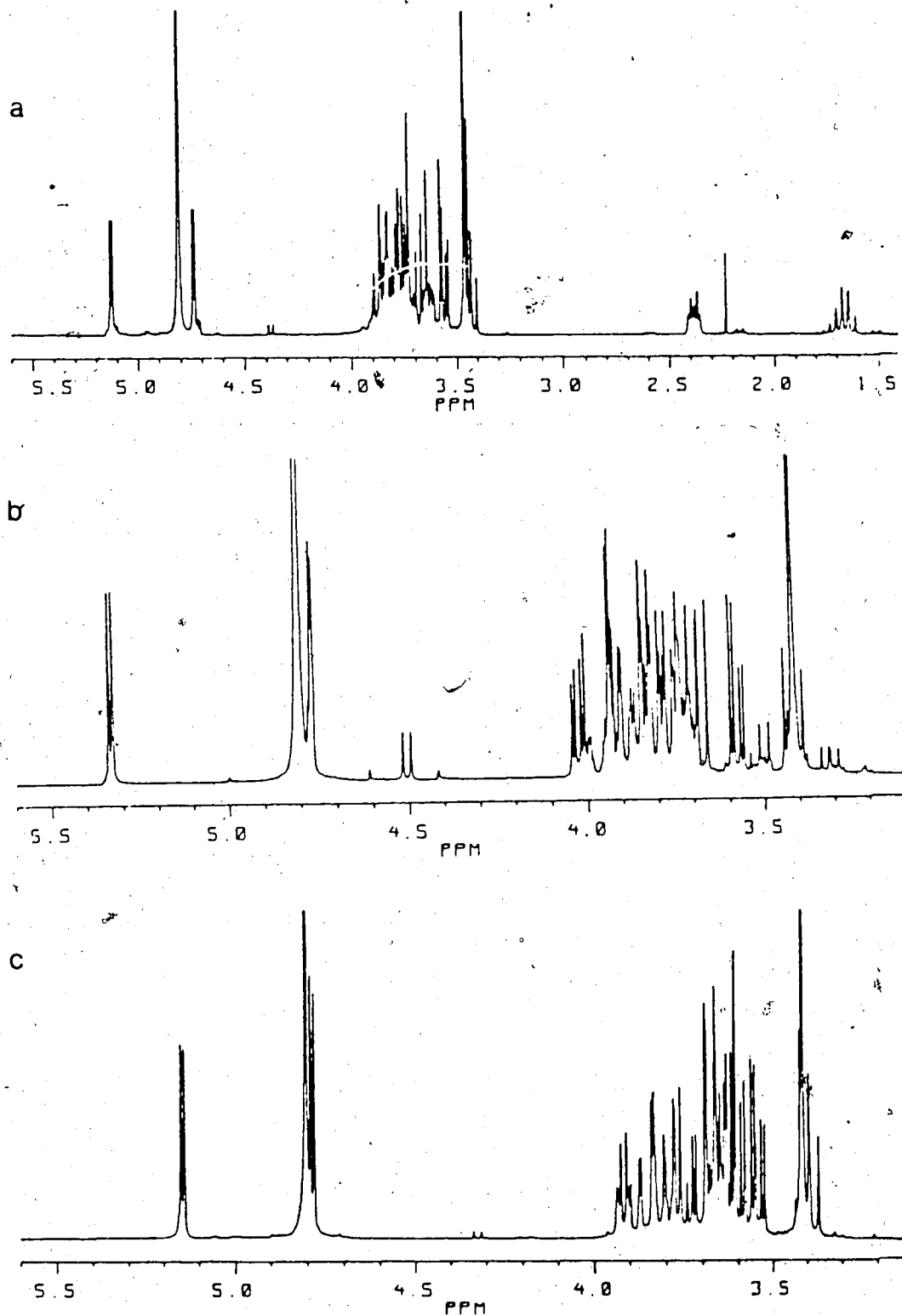
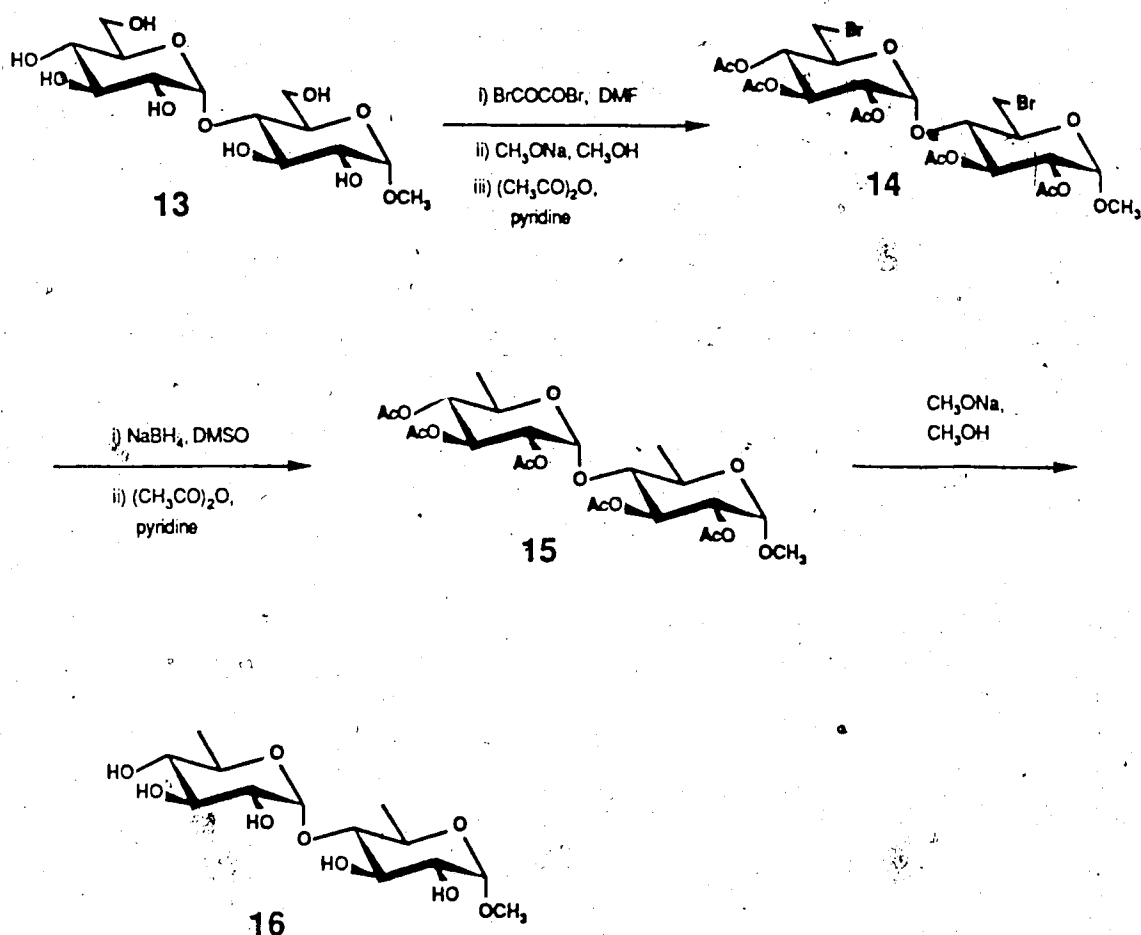


Figure 15. The <sup>1</sup>H-n.m.r. spectrum in D<sub>2</sub>O at 295 °K of a) methyl 3-deoxy- $\alpha$ -maltoside (1), b) methyl 4-O-( $\alpha$ -D-glucopyranosyl)- $\alpha$ -D-mannopyranoside (3) and c) methyl 4-O-( $\alpha$ -D-glucopyranosyl)- $\alpha$ -D-xylopyranoside (12).

The halide ion glycosidation<sup>110</sup> of 2,3,4,6-tetra-*O*-benzyl- $\alpha$ -D-glucopyranosyl bromide with compound 9 was as expected to give the disaccharide 10. The <sup>1</sup>H-n.m.r. spectrum is shown in Figure 9. The  $\alpha$  configuration of the glucosyl unit is clearly established by the coupling constant (3.5 Hz) of its anomeric proton ( $\delta = 5.52$  ppm). The integration of the signals between 1.6 and 1.4 ppm require the presence of one cyclohexylidene group. The selective removal of the cyclohexylidene group was accomplished with 90% trifluoroacetic acid<sup>111</sup> to give compound 11 which was easily recrystallized from ethanol. The high purity of compound 11 can be appreciated in its <sup>1</sup>H-n.m.r. spectrum which is reproduced in Figure 10. The absence of signals in the region between 1.7 and 1.5 ppm indicated the complete removal of the cyclohexylidene group. The last step was the removal of the benzyl groups by hydrogenolysis with 10% palladium on charcoal as the catalyst. The <sup>1</sup>H-n.m.r. spectrum of the deprotected disaccharide (12) is shown in Figure 15c. The 1 $\rightarrow$ 4 linkage was established by the n.O.e. experiments to be discussed in section 5.

The first step in the synthesis of methyl 6,6'-dideoxy- $\alpha$ -maltoside (16), which was patterned after the method described by Takeo and coworkers<sup>112</sup> for the preparation of 6-bromo derivatives of cyclodextrins and amylose, involved the preparation of the dibromo compound 14 by treating methyl  $\alpha$ -maltoside (13) with oxalyl bromide in dry N,N-dimethylformamide (Scheme 4). This bromination procedure presumably involves the *in situ* formation of bromomethylenedimethyliminium bromide (Vilsmeier bromide). The formate esters formed in the reaction were then hydrolyzed with 3M sodium methoxide in methanol. Since attempts to purify the compound by crystallization of the resulting syrup failed, its purification was accomplished by acetylation with 40% acetic anhydride in pyridine followed by column chromatography. The



Scheme 4

<sup>1</sup>H-n.m.r. spectrum (Figure 11) indicated that the acetate was essentially pure. As expected, the spectrum exhibited five singlets between 2.1 and 2.0 ppm and the chemical shift of the C-5-bromomethylene hydrogens ( $\delta = 3.78, 3.72, 3.64$  and  $3.44$  ppm) appeared at the appropriate field. The second step in the synthesis consisted of the reductive debromination of compound 14 with sodium borohydride in DMSO according to the procedure of Takeo and

coworkers.<sup>112</sup> Since it is known that the conditions of the reaction also cause partial removal of acetyl groups, the resulting product was re-acetylated. The dark oil produced by this process was purified by column chromatography to yield the disaccharide **15** as a white solid in 32% yield. The <sup>1</sup>H-n.m.r. spectrum, reproduced in Figure 12, exhibits two doublets at 1.37 and 1.18 ppm which correspond to the protons of the methyl groups and four singlets between 2.05 and 1.99 ppm which integrate to five acetyl groups. Finally, deacetylation with sodium methoxide in methanol afforded the deprotected disaccharide **16** whose <sup>1</sup>H-n.m.r. spectrum is presented in Figure 14c.

As previously mentioned, compounds **1**, **2** and **3** were provided by Professor Bock. The coupling constant exhibited by the anomeric proton for the non-reducing units of these compounds (4.0 Hz) and the nuclear Overhauser enhancements on H-4 that these compounds showed when H-1' was saturated clearly established that the linkages are  $\alpha 1 \rightarrow 4$ . These enhancements will be discussed in detail in section 5. The <sup>1</sup>H-n.m.r. spectrum of the 3-deoxy compound (**1**), which is reproduced in Figure 15a, shows two signals at 1.65 and 2.38 ppm which, on the basis of decoupling experiments, are coupled to both H-2 and H-4 and thereby establish unambiguously the deoxygenation at C-3. The chemical shift and the coupling constant of the anomeric proton of the reducing unit ( $\delta = 4.73$  ppm,  $J = 3.5$  Hz) are very similar to those of methyl  $\alpha$ -maltoside ( $\delta = 4.81$  ppm,  $J = 3.5$  Hz) indicating the  $\alpha$  configuration of this unit.

The <sup>1</sup>H-n.m.r. spectrum of the 6-deoxy compound (**2**) is displayed in Figure 14b. The  $\beta$  configuration for the reducing unit is firmly established by the large coupling constant (8.0 Hz) and the chemical shift (4.36 ppm) of the anomeric proton of this unit; for comparison, the parameters of methyl  $\beta$ -

maltoside are  $\delta = 4.39$  ppm and  $J = 8.0$  Hz. As expected<sup>131</sup>, the spectrum exhibited a doublet at high field (1.36 ppm) which is coupled to H-5 and gives an integral corresponding to three protons.

Although the <sup>1</sup>H-n.m.r. spectrum of the mannoside **3**, reproduced in Figure 15b, indicated that it is not pure, its condition proved to be adequate for the n.O.e. and hydrogen bonding studies to be discussed later on. The doublet at 4.76 ppm for H-1 ( $J = 2.0$  Hz) and the coupling constants for H-2 ( $J_{1,2} = 2.0$  Hz,  $J_{2,3} = 3.5$  Hz) are typical<sup>131</sup> of methyl  $\alpha$ -D-mannopyranosides.

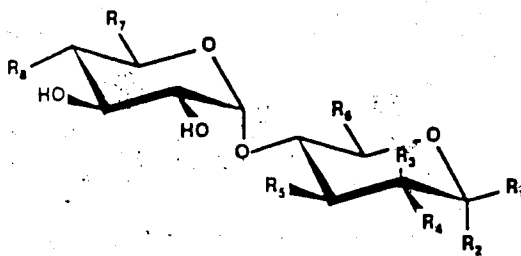
The sample of methyl  $\alpha$ -maltotrioside (**4**), provided by Dr. Ragauskas was pure as evidenced by its <sup>1</sup>H-n.m.r. spectrum reproduced in Figure 13c which was in agreement with the data reported by Takeo and coworkers<sup>132</sup>.

## 2. The model compounds

The compounds selected for this investigation are listed in Table 5. These were chosen because of structural features that could be expected to provide information on the interactions that dictate the conformation of the parent compound, maltose. It was clear from molecular modelling studies<sup>51</sup> that important non-bonded interactions exist between the hydroxymethyl group of the reducing end and H-5' of the non-reducing unit and between O-3 and H-1' (Figure 16). Furthermore, an important contribution by the *exo*-anomeric effect was to be expected especially in the solvent water<sup>24</sup>. Compounds **16** and **2** were studied in order to establish whether or not a preferred orientation of the hydroxymethyl group has any influence on the conformation. It was expected that, in the absence of this group, a  $\phi$  angle close to  $-60^\circ$  would be

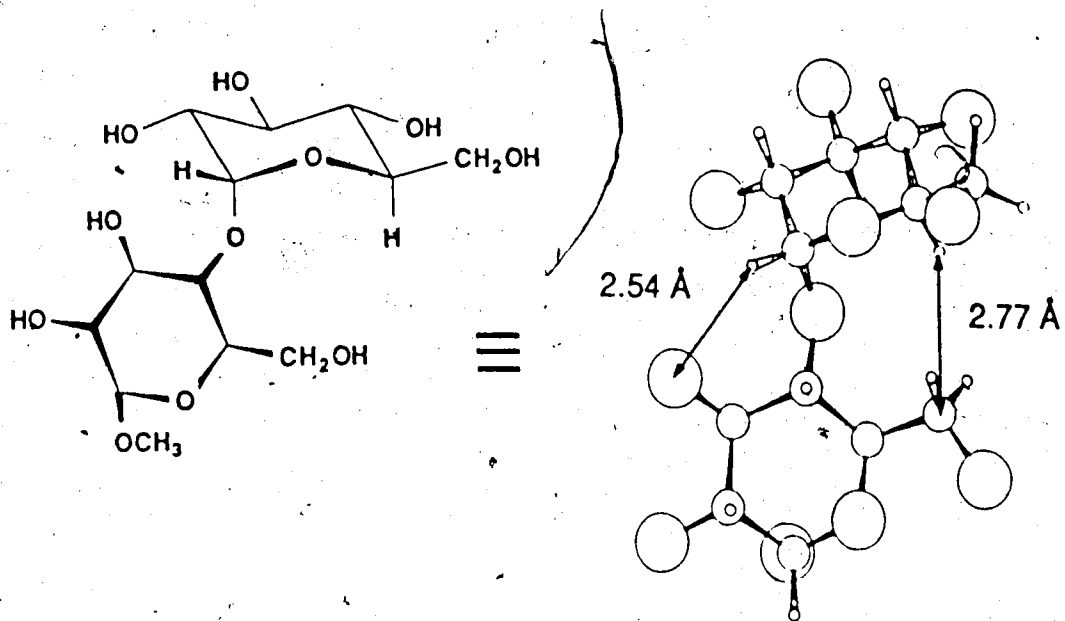
achieved since this would be more favorable in terms of the *exo*-anomeric effect. With this idea in mind, the xyloside **12** was synthesized and examined.

**Table 5.** Structures of the model compounds that were used in the development of this thesis.

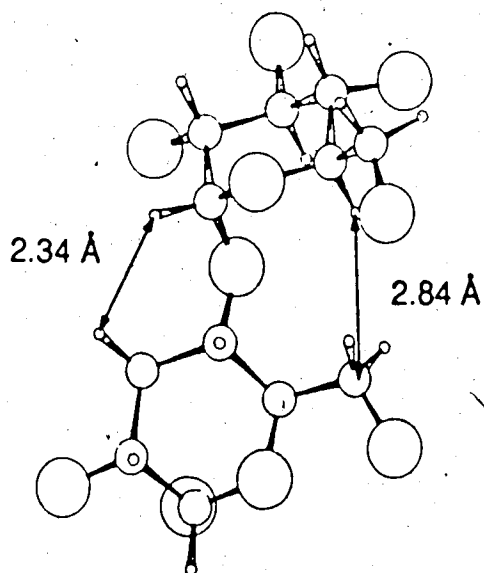


	R1	R2	R3	R4	R5	R6	R7	R8
methyl $\beta$ -maltoside ( <b>18</b> )	OMe	H	H	OH	OH	CH <sub>2</sub> OH	CH <sub>2</sub> OH	OH
methyl $\alpha$ -maltoside ( <b>13</b> )	H	OMe	H	OH	OH	CH <sub>2</sub> OH	CH <sub>2</sub> OH	OH
1,2-dideoxymaltose ( <b>7</b> )	H	H	H	H	OH	CH <sub>2</sub> OH	CH <sub>2</sub> OH	OH
methyl 3-deoxy- $\alpha$ -maltoside ( <b>1</b> )	H	OMe	H	OH	H	CH <sub>2</sub> OH	CH <sub>2</sub> OH	OH
methyl 6,6'-dideoxy- $\alpha$ -maltoside ( <b>16</b> )	H	OMe	H	OH	OH	CH <sub>3</sub>	CH <sub>3</sub>	OH
methyl 6-deoxy- $\beta$ -maltoside ( <b>2</b> )	OMe	H	H	OH	OH	CH <sub>3</sub>	CH <sub>2</sub> OH	OH
$\alpha$ DGlc $\beta$ (1 $\rightarrow$ 4) $\alpha$ DMan $\rho$ -OMe ( <b>3</b> )	H	OMe	OH	H	OH	CH <sub>2</sub> OH	CH <sub>2</sub> OH	OH
$\alpha$ DGlc $\rho$ (1 $\rightarrow$ 4) $\alpha$ DXyl $\rho$ -OMe ( <b>12</b> )	H	OMe	H	OH	OH	H	CH <sub>2</sub> OH	OH
methyl $\alpha$ maltotrioside ( <b>4</b> )	H	OMe	H	OH	OH	CH <sub>2</sub> OH	CH <sub>2</sub> OH	$\alpha$ DGlcO

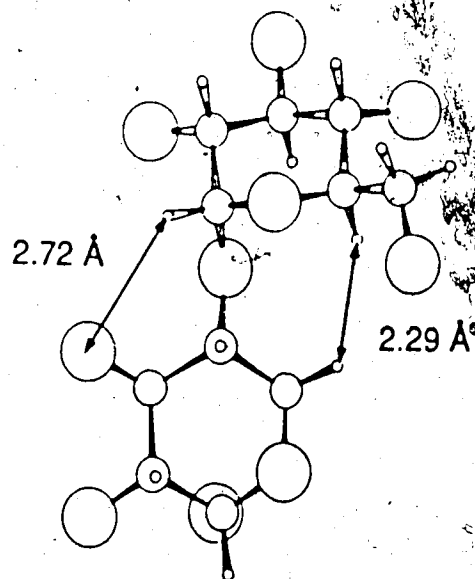
Another force that may play a role in the establishment of the preferred conformation for maltose is an interaction between H-1' and O-3 (see Figure 16). It was also desired to evaluate how the formation of an intramolecular hydrogen bond affects the conformation of maltose. For these reasons, the conformational preference for the 3-deoxy derivative (**1**) was studied.

methyl  $\alpha$ -maltoside (13)

$$\phi / \psi = -30^\circ / -25^\circ$$

methyl 3-deoxy- $\alpha$ -maltoside (1)

$$\phi / \psi = -35^\circ / -35^\circ$$

methyl 4-O-( $\alpha$ -D-glucopyranosyl) $\alpha$ -D-xylopyranoside (12)

$$\phi / \psi = -50^\circ / -10^\circ$$

**Figure 16.** Computer drawn structures for methyl  $\alpha$ -maltoside (13) and the derivatives 1 and 12. The formula for compound 13 is reproduced in the more usual form to assist in the interpretation of the molecular models.



Compounds **3** and **7** were selected in order to test whether or not solvation effects arising from interactions with and between solute molecules participate in the establishment of the conformation in solution. Finally, the trioside **4** was examined to determine whether the information gained from the studies of the simpler model compounds (Table 5) could be applied to higher oligomers of glucose with the  $\alpha(1\rightarrow4)$  linkage. In this regard, it should be kept in mind that the interunit torsion angles are very different in the crystalline state for the maltoside **18** and the maltotrioside **4**; namely,  $\phi/\psi = 4.8^\circ/13.3^\circ$  and  $-38.0^\circ/-29.0^\circ$ , respectively (see Table 1).

### 3. HSEA calculations

Lemieux and Bock<sup>51</sup> published a detailed study of the problems arising from the use of atomic coordinates from different sources to build the coordinates of maltose by the HSEA program. The problems arise primarily from differences in the  $\omega$  angle present in the crystal structures of the carbohydrates used in the calculations. Since a very important part of the conformational energy comes from Van der Waal's interactions between the hydrogen atoms, it was decided to use only coordinates from neutron diffraction determinations where the positions of the hydrogen atoms are well defined. HSEA calculations change the angles  $\phi$  and  $\psi$  of the disaccharide in steps within user-defined limits but the program does not simultaneously inspect the values for the changes in  $\omega$  angles as does the more recent version termed GESA calculations<sup>133</sup>. In order to obtain a favorable orientation for the hydroxymethyl group, since the GESA program was not available, the following procedure was used. First of all, HSEA calculations were performed for both the 6-deoxy and 6,6'-dideoxy derivatives of methyl  $\alpha$ -maltoside; namely,

**Table 6.** Conformational preferences and energies as indicated by HSEA calculations setting  $\omega = -90^\circ$  and  $\tau = 117^\circ$ .

Compound <sup>a</sup>	$\phi/\psi$	E(kcal/mol)
7, 13, 18	-30°/-25°	-1.4
1	-35°/-35°	-1.8
16, 2,	-30°/-25°	-1.4
3	-35°/-25°	-1.5
12	-50°/-10°	-1.7

<sup>a</sup>See Table 5.

compounds 2 and 16. As seen in Table 6, both the compounds are expected to possess the same  $\phi/\psi = -30^\circ/-25^\circ$  orientations for the nonreducing unit. Therefore, it is apparent that the orientation of the hydroxymethyl group at C-5' has no influence on the conformational preference about the interunit glycosidic bond. In order to estimate the most favorable orientation about the C-5 — CH<sub>2</sub>OH-6 bond, methyl  $\alpha$ -maltoside was set in the conformation  $\phi/\psi = -30^\circ/-25^\circ$  and the value of  $\omega$  was changed in 5° steps to cover the whole 0° to 360° range. As seen in Figure 17, three energy wells are encountered,  $\omega = -90^\circ$ , E = -0.3,  $\omega = 15^\circ$ , E = 0.3 and  $\omega = 160^\circ$ , E = 0.1 kcal/mole. In accord with this calculation, the preferred conformer predicted by GESA calculations has  $\omega = -89^\circ$ .<sup>134</sup> On this basis, the angle  $\omega = -90^\circ$  was used for all calculations wherein this hydroxymethyl had to be accommodated. Not surprisingly, HSEA calculations for methyl  $\beta$ -maltoside (18), its  $\alpha$ -anomer (13) and 1,2-dideoxymaltose (7) all showed the same conformational preference with equal conformational energies (see Table 6). The shape of the energy well produced

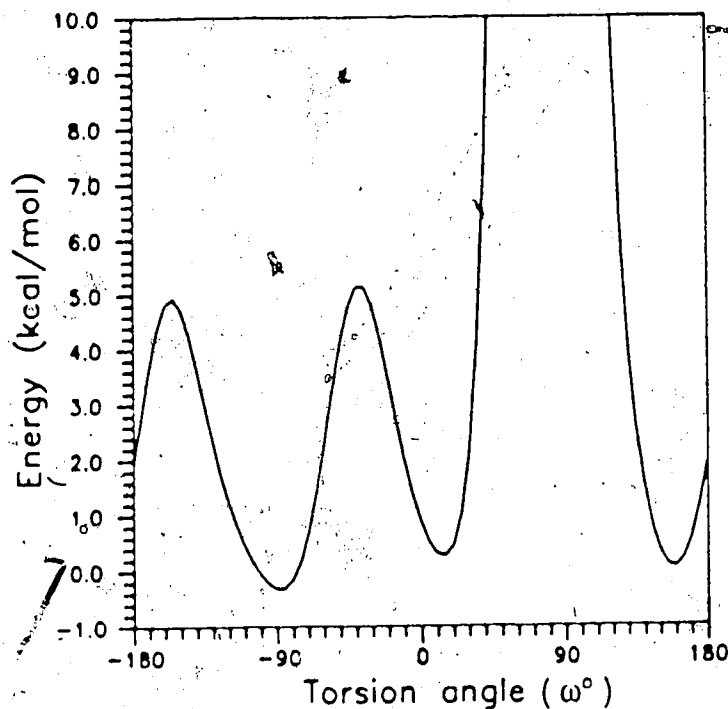


**Figure 17.** Variation in conformational energy with rotation about the C-5 — C-6 bond of methyl  $\alpha$ -maltoside in the conformation  $-30^\circ/-25^\circ$ .

by the calculation for methyl  $\alpha$ -maltoside (13) can be appreciated in Figure 18. It is seen that the calculation produces two conformers with torsion angles  $\phi/\psi = -65^\circ/-55^\circ$  ( $E = 0.4$  kcal/mol) and  $-30^\circ/-25^\circ$  ( $E = -1.4$  kcal/mol). The higher energy conformation roughly corresponds to the lowest energy conformers calculated by Kochetkov *et al*<sup>56</sup> (Table 2), Melberg and Rasmussen<sup>90</sup> (Table 3) and Tvaroska and Pérez<sup>92</sup> (Table 4) but in contrast to these, the population of this conformer as predicted by HSEA calculation is negligible. That the conformer with torsion angles  $-65^\circ/-55^\circ$  in fact does not appreciably contribute to the conformational preferences of maltosides in solution will be

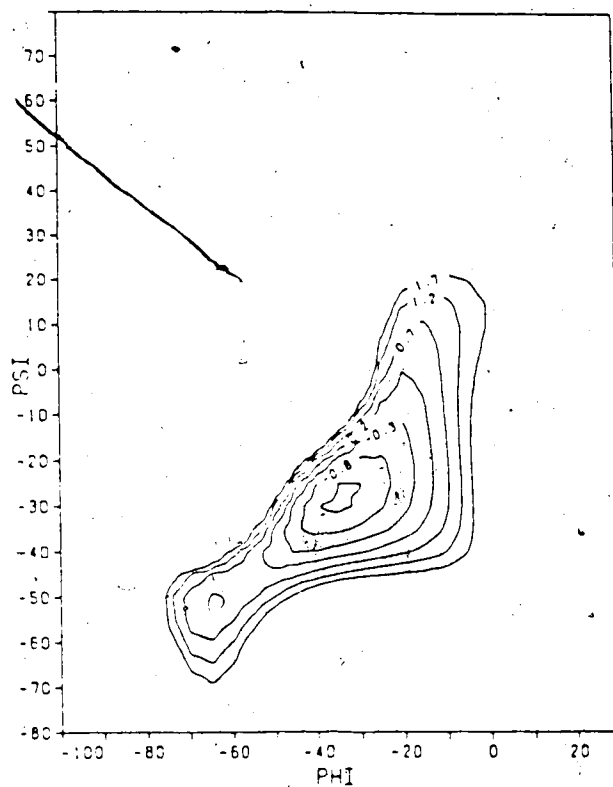


Figure 18. HSEA calculated energy contour map of methyl  $\alpha$ -maltoside (13) with  $\omega = -90^\circ$  and  $\psi = 117^\circ$ . Each contour represents 0.5 kcal/mol.

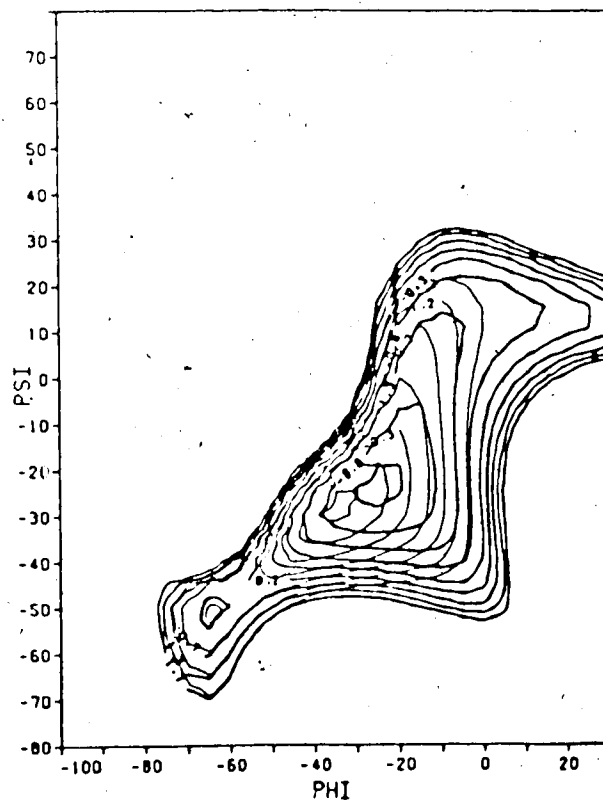
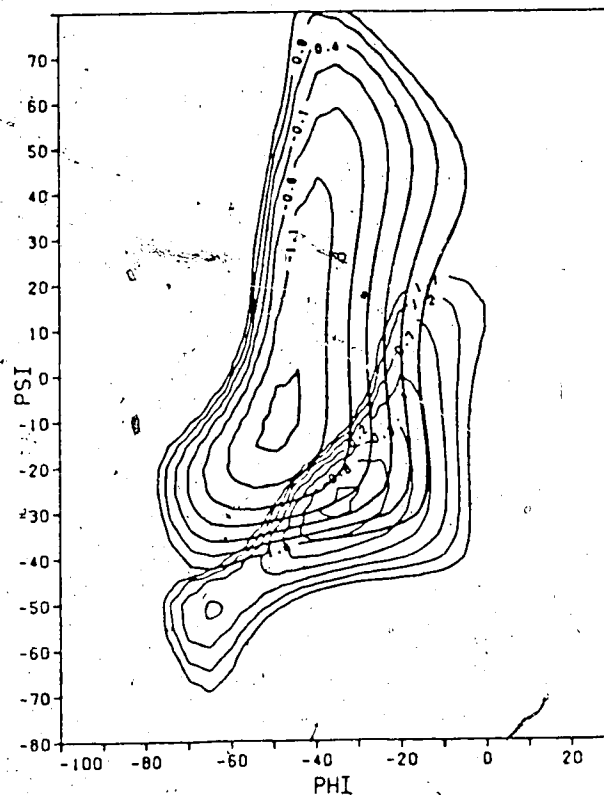
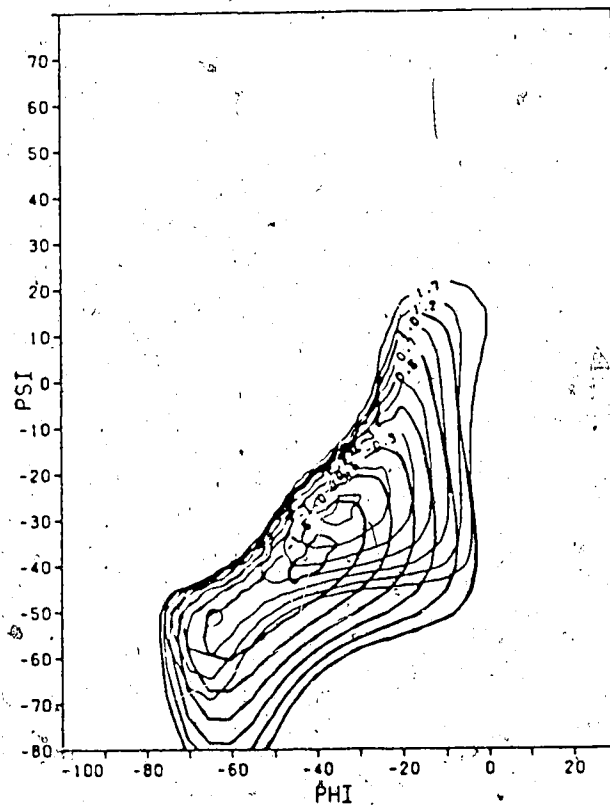


Figure 19. Overlap of the HSEA and HS calculated energy contour maps of methyl  $\alpha$ -maltoside (13) to display the influence of the *exo*-anomeric effect on the conformational preference.



**Figure 20.** Overlap of the HSEA calculated energy contour maps of methyl  $\alpha$ -maltoside (13) and methyl 4-O-( $\alpha$ -D-glucopyranosyl)- $\alpha$ -D-xylopyranoside (12) to display the effect of replacing the hydroxymethyl group of the reducing unit on the conformational preference of 13.



**Figure 21.** Overlap of the HSEA calculated energy contour maps of methyl  $\alpha$ -maltoside (13) and methyl 3-deoxy- $\alpha$ -maltoside (1) to display the effect of deoxygenation at C-3 on the conformational preference of 13.

demonstrated in the following sections of this thesis. The influence of the *exo*-anomeric effect on the calculations is displayed in Figure 19. It is seen that the *exo*-anomeric effect provides a well-defined, narrower energy well. The positions of the two conformers in the map and the shape of the energy well do not change significantly when the *exo*-anomeric effect is not taken into account in the calculation, the only difference in energy of the conformers being 1.8 kcal/mol (HSEA) and 2.7 kcal/mol (HS). That a proper orientation of the C-5 hydroxymethyl group is needed can be appreciated from the major change in conformational equilibrium which is indicated by HSEA calculations when the group is replaced by hydrogen to provide the xyloside **12** (see Table 6). The conformational map provided by HSEA calculation (Figure 20) exhibits a broader energy well with only one conformer. The position and shape of the well are different from those of maltosides in which the C-5 hydroxymethyl group deeply influences the conformational characteristics of the molecule. Finally, the data calculated for methyl 3-deoxy- $\alpha$ -maltoside (**1**) are noteworthy. It is apparent that, in the maltoside **13**, O-3 is in close nonbonded interaction with the anomeric hydrogen of the non-reducing unit since its replacement by hydrogen leads to a slight change in the conformational preference with a slight (0.4 kcal/mole) decrease in the conformational energy. In fact, inspection of the molecular models indicates an only 2.54 Å distance between the nuclei of H-1' and O-3 and the sum of the Van der Waal radii is 2.5 Å (see Figure 16). The conformational map, reproduced in Figure 21, shows that the replacement of O-3 by a hydrogen in methyl  $\alpha$ -maltoside produces an energy well that extends more towards more negative  $\psi$  angles and provides more flexibility around the O-1 — C-4 bond. Before closing the section on HSEA calculations, it is to be noted<sup>19</sup> that HSEA calculations were not designed to provide the conformational preferences about glycosidic bonds. Instead, these

were formulated in the first instance to provide molecular models in the computer memory for assessment of n.m.r. data.<sup>74</sup> As it turned out, the simple HSEA-type calculation is not only the cheapest procedure for the estimation of these conformational preferences but, indeed, provides models which are normally in accord, within the limits of interpretation, with the n.m.r. parameters for the oligosaccharide dissolved in water.

#### 4. Chemical shifts

The <sup>1</sup>H-n.m.r. parameters of the simpler model compounds in aqueous solution are presented in Tables 7 and 8 and the spectra are reproduced in Figures 13 to 15. The <sup>1</sup>H-n.m.r. parameters for these compounds, dissolved in DMSO-d<sub>6</sub>, are reported in Tables 9 and 10. These spectra are in general accord with expectation.<sup>131</sup> A brief assessment of this claim follows. The coupling constants are typical for pyranoid rings in the <sup>4</sup>C<sub>1</sub> conformation, also, the positions of the chemical shifts of the anomeric protons are in the spectral regions expected; namely, H-1 $\alpha$   $\approx$  4.8 ppm and H-1 $\beta$   $\approx$  4.4 ppm for the reducing units and H-1'  $\approx$  5.4 ppm for the non-reducing units. The signals for H-1' of the 3-deoxy compound **1** and the xyloside **12** are shifted 0.28 and 0.26 ppm, respectively, to higher field than in methyl  $\alpha$ -maltoside (**13**). As pointed out by Lemieux and Bock<sup>51</sup> this is because of a specific interunit deshielding of the anomeric hydrogen caused by a non-bonded interaction with an oxygen atom. That H-1' of methyl  $\alpha$ -maltoside (**13**) is in fact deshielded by O-3 can be appreciated from the data presented in Table 11. For  $\alpha$ -kojibiose [ $\alpha$ DGlc(1 $\rightarrow$ 2) $\alpha$ DGlc] and the 3-deoxy compound **1**, HSEA calculations<sup>51</sup> indicate that H-1' is in non-bonded interaction with H-1 and H-3<sub>eq</sub>, respectively. These interactions are not expected to have a deshielding effect on H-1'. As

**Table 7.** The  $^1\text{H}$ -n.m.r. chemical shifts ( $\delta$ , ppm)<sup>a</sup> for the compounds listed in Table 5.

Proton	18	13	7 <sup>b</sup>	1 <sup>c</sup>	16	2	3	12 <sup>e</sup>
H-1	4.393	4.813	3.964	4.729	4.750	4.360	4.765	4.781
H-2	3.293	3.596	1.664	3.820	3.60	3.287	3.929	3.596
H-3	3.775	3.928	3.91	1.651	3.85	3.715	4.023	3.799
H-4	3.63	3.640	3.475	3.74	3.314	3.365	3.820	3.64
H-5	3.60	3.76	3.40	3.72	3.85	3.629	3.74	3.61
H-6a	3.775 <sup>*</sup>	3.87	3.75	3.74	1.319 <sup>d</sup>	1.360	3.83	N/A
H-6b	3.947	3.85	3.75	3.74	N/A	N/A	3.82	N/A
H-1'	5.406	5.007	5.355	5.120	5.315	5.417	5.331	5.140
H-2'	3.578	3.569	3.589	3.552	3.60	3.577	3.575	3.538
H-3'	3.682	3.684	3.689	3.660	3.60	3.690	3.685	3.685
H-4'	3.414	3.412	3.406	3.425	3.160	3.405	3.412	3.388
H-5'	3.70	3.70	3.90	3.630	3.85	3.77	3.73	3.640
H-6a'	3.761	3.85	3.75	3.758	1.267 <sup>d</sup>	3.76	3.918	3.748
H-6b'	3.858	3.76	3.75	3.840	N/A	3.86	3.806	3.846
-OCH <sub>3</sub>	3.573	3.418	N/A	3.450	3.409	3.549	3.411	3.407

<sup>a</sup>Dissolved in D<sub>2</sub>O at 295 °K.<sup>b</sup>H-1<sub>ax</sub>, 3.521 and H-2<sub>eq</sub>, 2.008 ppm.<sup>c</sup>H-3<sub>eq</sub>, 2.378 ppm<sup>d</sup>Assignments may be reversed.<sup>e</sup>H-5<sub>eq</sub>, 3.913 ppm.

was mentioned in the previous section, it was expected that the xyloside **12** would exhibit a conformation different from that of the maltoside **13**. Indeed, in its minimum energy HSEA conformer, H-1' of the compound **12** is not in close contact with O-3 (see Figure 16) and the chemical shift of the anomeric proton is similar to those of  $\alpha$ -kojibiose and the 3-deoxy compound **1**. On the other hand,  $\beta$ -kojibiose [ $\alpha$ DGlc(1 $\rightarrow$ 2) $\beta$ DGlc],  $\alpha$ -nigerose [ $\alpha$ DGlc(1 $\rightarrow$ 3) $\alpha$ DGlc],



**Table 8.** The  $^1\text{H}$ -n.m.r. coupling constants ( $^3J$ , Hz)<sup>a</sup> for the compounds listed in Table 5.

Protons	18	13	7 <sup>b</sup>	1 <sup>c</sup>	16	2	3	12 <sup>d</sup>
1,2	8.0	3.5	5.0	3.5	4.0	8.0	2.0	4.0
2,3	9.5	9.0	9.0	12.0	9.0	9.5	3.5	9.8
3,4	9.0	10.0	9.0	11.0	9.5	9.0	9.0	9.2
4,5	-	9.0	9.0	10.0	9.5	9.0	9.0	10.0
5,6a	4.0	1.5	-	-	6.3	6.5	-	N/A
5,6b	1.9	-	-	-	N/A	N/A	-	N/A
6a,6b	12.0	11.5	-	-	N/A	N/A	-	N/A
1',2'	3.8	4.0	4.0	4.0	3.5	4.0	4.0	4.0
2',3'	10.0	9.5	10.0	9.5	-	10.0	10.0	10.0
3',4'	9.0	9.0	9.5	8.5	9.2	10.0	9.5	9.0
4',5'	9.5	9.5	9.5	9.5	9.2	9.0	9.5	9.8
5',6a'	4.0	-	-	2.0	6.3	-	2.0	5.5
5',6b'	1.9	-	-	5.0	N/A	-	6.0	2.2
6a',6b'	12.0	-	-	11.5	N/A	11.5	12.0	12.0

<sup>a</sup>Dissolved in D<sub>2</sub>O at 295 °K.

<sup>b</sup> $J_{1ax,1eq}$ , 12.0;  $J_{1eq,2eq}$ , 1.5;  $J_{1ax,2ax}$ , 12.0;  $J_{1ax,2eq}$ , 2.0;  $J_{2ax,2eq}$ , 13.0;  $J_{2eq,3}$ , 2.0 Hz.

<sup>c</sup> $J_{2,3eq}$ , 4.5;  $J_{3ax,3eq}$ , 11.0;  $J_{3eq,4}$ , 4.5 Hz.

<sup>d</sup> $J_{4,5eq}$ , 4.0 Hz;  $J_{5ax,5eq}$ , 10.0 Hz.

and methyl  $\alpha$ -maltoside (13) are expected to have H-1' in strong non-bonded interaction with an oxygen atom of the reducing unit, and, as seen in Table 11, these three disaccharides produce their signal for H-1' at 0.3 ppm to lower field than do  $\alpha$ -kojibiose and compounds 1 and 12.

Comparison of the chemical shifts of the signal for H-4 of the 6,6'-dideoxy maltoside 16 and the 6-deoxy  $\beta$ -maltoside 2 with that for H-4 of methyl  $\alpha$ -maltoside (13) show, that these are to higher field by about 0.3 ppm. Proton

**Table 9.** The  $^1\text{H}$ -n.m.r. chemical shifts ( $\delta$ , ppm) for the compounds listed in Table 5.<sup>a</sup>

Proton	18	13	7 <sup>b</sup>	1 <sup>c</sup>	16	2	3	12 <sup>d</sup>
H-1	4.218	4.662	3.915	4.609	4.616	4.214	4.633	4.645
H-2	3.131	3.381	1.570	3.570	3.40	3.14	3.78	3.375
H-3	3.545	3.767	3.728	1.650	3.688	3.49	3.76	3.660
H-4	3.445	3.443	3.310	3.641	3.108	3.49	3.71	3.46
H-5	3.35	3.53	3.18	3.53	3.644	3.49	3.49	3.46
H-6a	3.695	3.792	3.810	3.777	1.321	1.376	3.69	N/A
H-6b	3.840	3.718	3.680	3.56	N/A	N/A	3.828	N/A
H-1'	5.147	5.118	5.100	4.930	5.053	5.143	5.061	5.010
H-2'	3.360	3.353	3.380	3.306	3.386	3.368	3.355	3.255
H-3'	3.503	3.508	3.528	3.483	3.453	3.50	3.516	3.476
H-4'	3.196	3.194	3.210	3.184	2.917	3.196	3.205	3.118
H-5'	3.61	3.62	3.62	3.50	3.705	3.63	3.60	3.50
H-6a'	3.58	3.75	3.73	3.760	1.238	3.59	3.73	3.755
H-6b'	3.74	3.580	3.60	3.56	N/A	3.730	3.60	3.53
-OCH <sub>3</sub>	3.531	3.404	N/A	3.451	3.398	3.496	3.388	3.401
OH-2	5.21	4.90	N/A	4.82	4.86	5.18	4.93	4.87
OH-3	5.57	5.43	5.59	N/A	5.41	5.57	5.38	5.11
OH-6	4.58	4.56 <sup>e</sup>	4.60	4.55	N/A	N/A	4.51	N/A
OH-2'	5.47	5.46	5.79	4.63	5.50	5.53	5.54	4.44
OH-3'	4.78	4.92	5.04	4.76	4.92	4.93	4.93	4.82
OH-4'	4.96	4.95	5.01	4.92	4.99	4.95	4.95	4.93
OH-6'	4.57	4.54 <sup>e</sup>	4.50	4.50	N/A	4.53	4.54	4.57

<sup>a</sup>In DMSO-*d*<sub>6</sub> at 310 °K.

<sup>b</sup>H-1ax, 8.445; H-2eq, 1.932 ppm.

<sup>c</sup>H-3eq, 2.220 ppm.

<sup>d</sup>H-5eq, 3.870 ppm.

<sup>e</sup>Assignments may be reversed.

Table 10. The  $^1\text{H}$ -n.m.r. coupling constants ( $^3J$ , Hz) for the compounds listed in Table 5.<sup>a</sup>

Protons	18	13	7 <sup>b</sup>	1 <sup>c</sup>	16	2	3	12 <sup>d</sup>
1,2	7.8	3.7	5.0	3.5	4.0	7.8	1.5	3.6
2,3	8.5	10.0	12.0	11.0	9.0	-	-	9.5
3,4	9.0	8.5	9.0	10.0	9.5	-	-	8.5
4,5	9.0	10.0	9.0	10.0	9.0	-	9.0	-
5,6a	2.0	2.0	2.0	1.5	6.0	6.1	-	N/A
5,6b	5.5	5.0	6.5	-	N/A	N/A	2.0	N/A
6a,6b	12.0	12.0	12.0	10.5	N/A	N/A	12.0	N/A
1',2'	3.8	3.8	4.0	3.5	4.0	3.9	4.0	3.8
2',3'	9.5	9.5	10.0	9.5	9.0	9.5	9.5	10.0
3',4'	9.0	9.0	9.5	9.0	9.5	9.5	9.0	9.5
4',5'	9.0	9.5	9.0	10.0	9.0	9.5	9.0	9.0
5',6a'	-	4.0	-	2.0	6.0	-	-	-
5',6b'	-	5.5	-	-	N/A	-	-	6.5
6a',6b'	-	10.5	-	11.0	N/A	10.5	-	13.0
OH-2,H-2	5.0	6.6	N/A	7.0	7.0	5.0	4.0	6.6
OH-3,H-3	3.0	3.3	3.0	N/A	3.0	3.0	3.5	3.8
OH-6,H-6	6.0	6.3	6.0	6.0	N/A	N/A	6.0	N/A
OH-2',H-2'	6.5	6.2	5.5	6.5	5.5	5.5	6.0	9.1
OH-3',H-3'	4.5	4.9	4.0	5.0	4.5	5.0	4.0	4.8
OH-4',H-4'	5.5	5.6	5.5	6.0	5.5	5.0	5.5	5.7
OH-6',H-6'	6.0	5.9	6.0	6.0	N/A	6.0	6.0	5.8

<sup>a</sup>In DMSO- $d_6$  at 310 °K.

<sup>b</sup> $J_{1ax,1eq}$ , 12.0;  $J_{1eq,2eq}$ , 1.5;  $J_{1ax,2ax}$ , 12.0;  $J_{1ax,2eq}$ , 2.0;  $J_{2ax,2eq}$ , 12.0;  $J_{2eq,3}$ , 2.0 Hz.

<sup>c</sup> $J_{2,3eq}$ , 4.5;  $J_{3ax,3eq}$ , 11.0;  $J_{3eq,4}$ , 4.0 Hz.

<sup>d</sup> $J_{4,5eq}$ , 1.5;  $J_{5ax,5eq}$ , 17.0 Hz.

H-4' of compound **16** is also shielded by about 0.25 ppm as compared with H-4' of compound **13**. These increased shieldings may result in part from a deshielding effect from a contribution to the conformational equilibrium by the conformer with  $\omega = 180^\circ$  which brings O-6 into near *syn*-axial like relationship with H-4. The  $^1\text{H-n.m.r.}$  data for methyl  $\alpha$ -maltotrioside (**4**) in  $\text{D}_2\text{O}$  are presented in Table 12 and the spectrum is reproduced in Figure 13c. The close similarity between this spectrum and that for **13** (Figure 13b) suggests that their conformations in  $\text{D}_2\text{O}$  are very similar. This indication was supported by the nuclear Overhauser enhancement studies, the results of which are presented in the following section.

**Table 11.** Specific interunit deshielding of the anomeric hydrogen of  $\alpha$ -linked disaccharides because of non-bonded interaction with an oxygen atom.

Compound	Chemical shift, H-1', ppm	Distance from H-1', Å
$\alpha\text{DGlc}\rho(1\rightarrow2)\alpha\text{DGlc}\rho$	5.10 <sup>a</sup>	2.30(H-1)
methyl 3-deoxy- $\alpha$ -maltoside ( <b>1</b> )	5.12	2.34(H-3 <sub>eq</sub> )
$\alpha\text{DGlc}\rho(1\rightarrow4)\alpha\text{DXyl}\rho\text{OMe}$ ( <b>12</b> )	5.14	2.72(O-3)
$\alpha\text{DGlc}\rho(1\rightarrow2)\beta\text{DGlc}\rho$	5.41 <sup>a</sup>	2.45(O-1)
$\alpha\text{DGlc}\rho(1\rightarrow3)\alpha\text{DGlc}\rho$	5.38 <sup>a</sup>	2.54(O-4)
methyl $\alpha$ -maltoside ( <b>13</b> )	5.40	2.54(O-3)

<sup>a</sup>Data from reference 135.

The  $^{13}\text{C-n.m.r.}$  chemical shifts of the simpler model compounds are presented in tables 13 and 14. In the 3-deoxy compound **1**, the carbons C-1',

C-2' and C-5' resonate at higher fields than the corresponding carbons in methyl  $\alpha$ -maltoside **13**. Similarly, C-5' in the xyloside **12** resonates at higher field than C-5' in **13**. These observations may find explanation in the different conformations adopted by these compounds as indicated by HSEA calculations (Figure 16) and supported by n.O.e. studies.

**Table 12.**  $^1\text{H}$ -n.m.r. chemical shifts and vicinal coupling constants for methyl  $\alpha$ -maltoside (**13**) and methyl  $\alpha$ -maltotrioside (**4**) in  $\text{D}_2\text{O}$  at 295 °K.

Proton	$\delta(\text{ppm})$		$^3J(\text{Hz})$	
	<b>13</b>	<b>4</b>	<b>13</b>	<b>4</b>
H-1	4.813	4.805	3.5	4.0
H-2	3.596	3.595	9.0	9.5
H-3	3.928	3.929	10.0	9.5
H-4	3.640	3.646	9.0	9.5
H-1'		5.391		3.0
H-2'		3.611		9.5
H-3'		3.955		9.0
H-4'		3.646		9.5
H-1''	5.397	5.402	4.0	3.0
H-2''	3.569	3.581	9.5	9.5
H-3''	3.684	3.686	9.0	9.0
H-4''	3.412	3.417	9.5	9.0
H-5''	3.70	3.74		
-OCH <sub>3</sub>	3.418	3.419		

**Table 13.** The  $^{13}\text{C}$ -n.m.r. chemical shifts (ppm) in  $\text{D}_2\text{O}$  at 305 °K for the compounds listed in Table 5.<sup>a</sup>

Carbon	18	13	7	1	16	2	3	12
C-1	103.91	99.94	66.08	99.13	100.80	103.90	101.59	100.86
C-2	73.79	71.93	33.62	67.01	72.11	74.08	70.83	71.78
C-3	77.04	74.35	79.69	31.20	74.29	76.98	71.86	73.64
C-4	77.70	78.12	80.78	68.71	84.22	83.12	76.43	79.05
C-5	75.39	71.02	73.41	73.30	66.88	71.46	72.11	60.80
C-6	61.58	61.49	62.05	61.54	17.92	18.21	61.91	N/A
C-1'	100.42	100.58	100.96	95.06	99.88	100.36	100.77	100.03
C-2'	72.49	72.64	72.74	71.46	72.91	72.55	72.74	72.42
C-3'	73.68	73.79	73.85	73.79	73.64	73.74	73.91	73.13
C-4'	70.18	70.30	70.30	70.36	75.69	70.33	70.43	70.39
C-5'	73.53	73.55	73.56	71.80	69.30	73.44	73.60	72.92
C-6'	61.35	61.46	61.46	61.37	17.24	61.46	61.58	61.43
-OCH <sub>3</sub>	58.00	55.95	N/A	55.74	55.94	57.98	55.67	56.01

<sup>a</sup>All assignments are tentative (except those for compounds **18** and **13**) and were made by comparison with model compounds.

In order to gain information about the role that the solvent may play in the conformation of maltose, the  $^{13}\text{C}$ -n.m.r. spectra of methyl  $\alpha$ -maltoside (**13**) in mixtures of  $\text{H}_2\text{O}$  and  $\text{DMSO-}d_6$  were recorded.<sup>136</sup> The differences of chemical shift are plotted in Figure 22 as a function of the solvent composition (molar percent of  $\text{DMSO-}d_6$  in  $\text{H}_2\text{O}$ ). It is seen that the variation in chemical shift is not linear, that, except for C-3 and for the methoxy carbon, the signals move downfield when going from  $\text{H}_2\text{O}$  to  $\text{DMSO-}d_6$  and that the largest variations in chemical shift are experienced by C-4 and C-1'; namely, those

**Table 14.** The  $^{13}\text{C}$ -n.m.r. chemical shifts (ppm) in  $\text{DMSO}-d_6$  at 305 °K for the compounds listed in Table 5.<sup>a</sup>

Carbon	18	13	7	1	16	2	3	12
C-1	104.81	100.56	65.63	99.55	100.70	104.54	101.84	100.89
C-2	74.43	72.56	34.55	67.44	72.52	74.00	70.71	72.39
C-3	77.43	74.39	80.90	32.48	74.07	77.16	72.10	74.46
C-4	80.54	81.05	83.47	68.94	87.74	86.42	78.43	80.67
C-5	76.25	71.89	73.23	74.03	66.48	70.82	73.15	60.95
C-6	62.01	61.90	62.19	61.79	18.84	18.78	61.84	N/A
C-1'	101.73	101.84	102.23	95.52	102.69	102.06	101.84	101.82
C-2'	73.51	73.61	73.66	72.45	73.82	73.45	73.56	72.95
C-3'	74.39	74.49	74.44	74.21	74.14	74.35	74.33	74.36
C-4'	71.14	71.01	71.06	71.10	76.42	71.02	70.97	71.45
C-5'	74.04	74.22	74.33	72.28	69.12	74.24	74.28	73.36
C-6'	61.72	61.44	61.94	61.71	18.64	61.87	61.79	62.20
-OCH <sub>3</sub>	56.98	55.44	N/A	55.10	55.65	56.76	54.96	55.72

<sup>a</sup>All assignments are tentative (except those for compound 13) and were made by comparison with model compounds.

atoms which are directly involved in the glycosidic linkage. These observations may be related to a modification of the conformational preferences or to simple general solvent effect or both.<sup>136</sup> However, the fact that the largest variations in chemical shift were measured for C-4 and C-1' suggests that a solvent-induced conformational change is important. Further information can be obtained by comparing the chemical shifts of C-4 of the compounds dissolved in  $\text{D}_2\text{O}$  and  $\text{DMSO}-d_6$  (Tables 13 and 14). The differences are 2.84 (18), 2.93 (13), 2.69 (7), 0.23 (1), 3.52 (16), 3.30 (2), 2.00

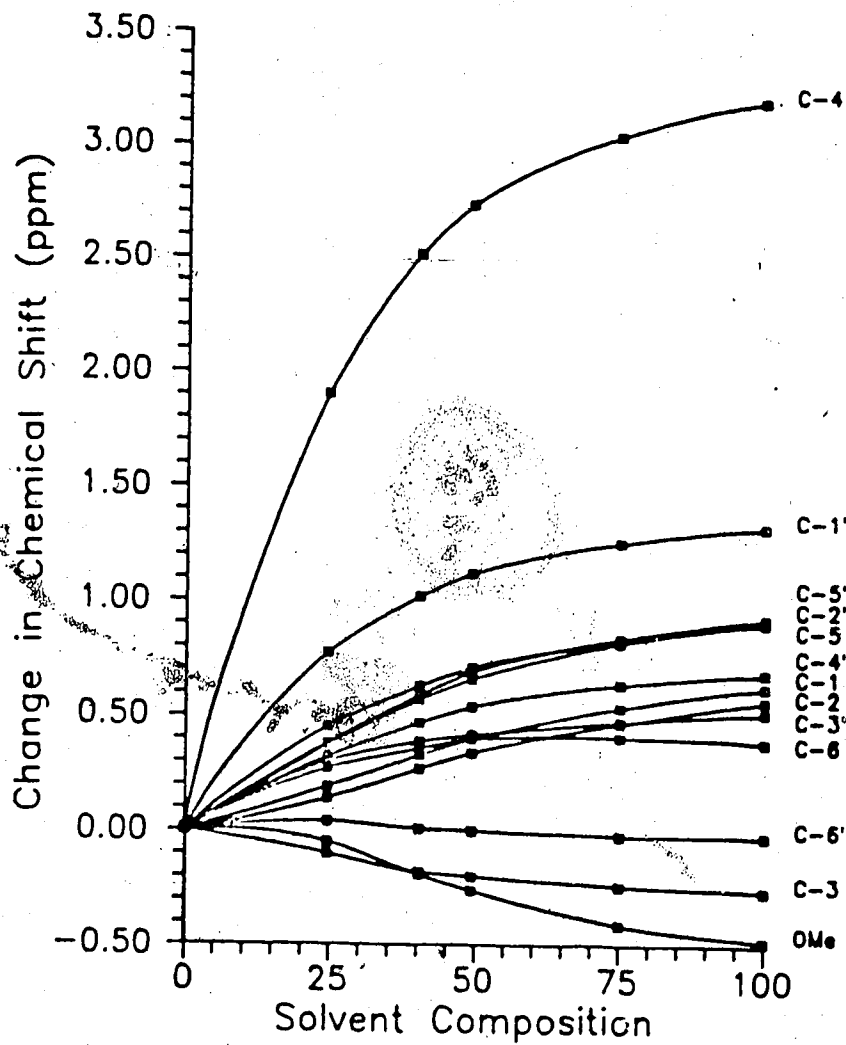
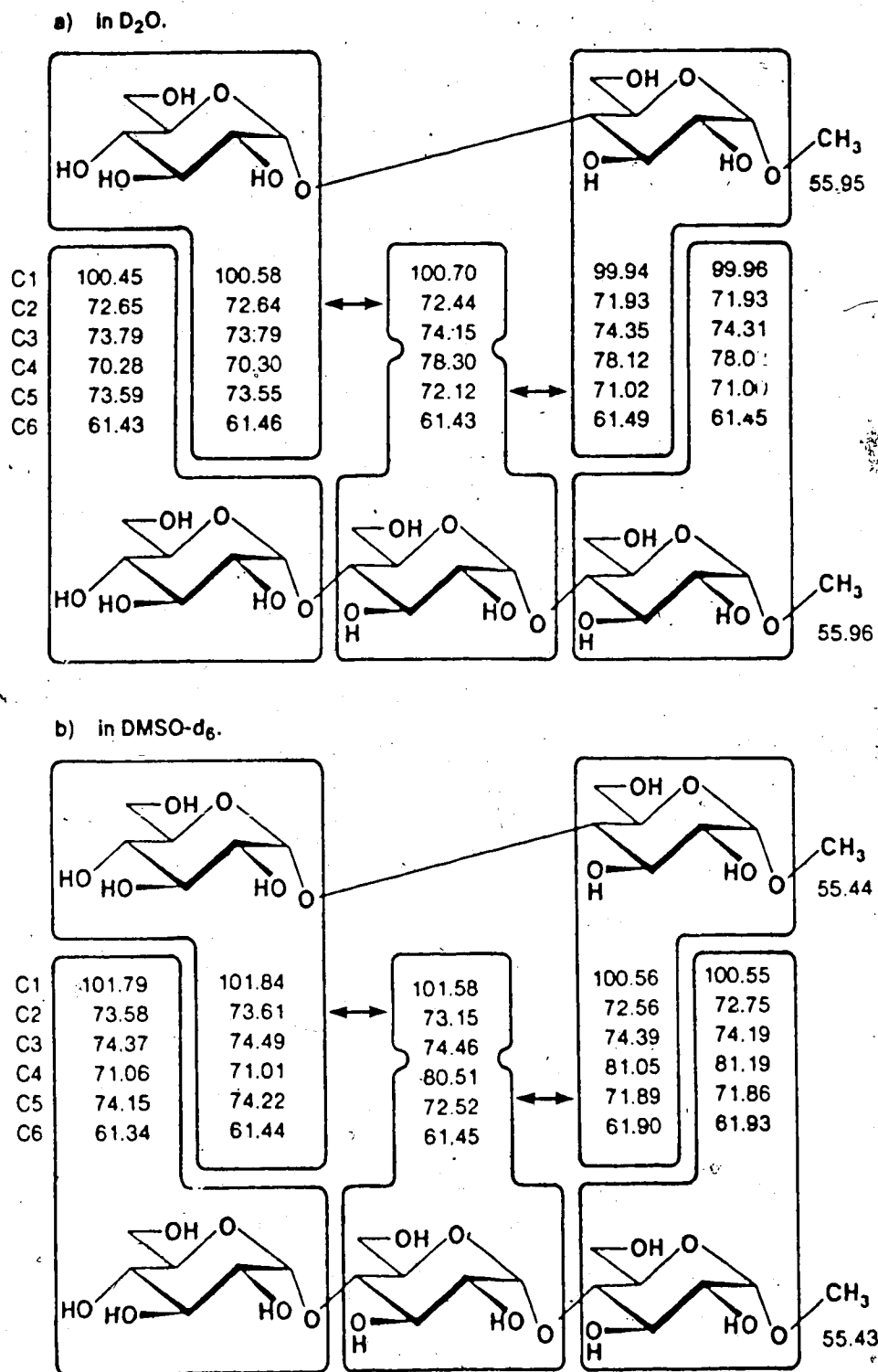


Figure 22. Change of the  $^{13}\text{C}$ -n.m.r. chemical shifts of methyl  $\alpha$ -maltoside (13) with change in the molar percent of  $\text{DMSO-}d_6$  in  $\text{H}_2\text{O}$ .





a) At 90.5 MHz, internal standard dioxane (67.4 ppm). The assignments of methyl  $\alpha$ -maltoside are tentative.

Figure 23. Comparison of the  $^{13}C$ -n.m.r. chemical shifts of methyl  $\alpha$ -maltoside (13) and methyl  $\alpha$ -maltotriose (4) a) in  $D_2O$  and b) in  $DMSO-d_6$  at 305 °K.

(3) and 1.62 (12) ppm, respectively. The smaller changes that occur for compounds **1**, **3** and **12**, suggest that the conformational preferences for these compounds are less sensitive to the changes in solvent. The  $^{13}\text{C}$ -n.m.r. chemical shifts of methyl  $\alpha$ -maltoside (**13**) and methyl  $\alpha$ -maltotrioside (**4**) in  $\text{D}_2\text{O}$  and  $\text{DMSO}-d_6$  solutions are compared in Figure 23. The close similarity of these shifts strongly suggests that, for both solvents, the conformation of **13** is well maintained by **4**. This observation is of major importance in view of the major difference between the conformations of these compounds in the crystalline state (see Table 1). The conclusion that methyl  $\alpha$ -maltoside (**13**) and methyl  $\alpha$ -maltotrioside (**4**) have similar conformations was also indicated by the similarities on their  $^1\text{H}$ -n.m.r. parameters (Table 12). It is well established<sup>24</sup> that solvents have a more direct influence on  $^1\text{H}$ -chemical shifts than on  $^{13}\text{C}$ -shifts since the latter atoms are better shielded by the substituent atoms from anisotropic solvent effects.

## 5. Nuclear Overhauser enhancements

### 5.1. Theoretical relative nuclear Overhauser enhancements

As previously mentioned, the theoretical nuclear Overhauser enhancements were calculated using a computer program developed by Dr. H. Beierbeck.<sup>104</sup> For the case of isotropic motion and dipole-dipole relaxation the enhancement  $f_d(s)$  at nucleus  $d$  on saturation of signal  $s$  is given by:<sup>71</sup>

$$f_d(s) = A [ \sum g_d(s) - \sum f_i(s) g_d(i) ], \quad (17)$$

where,

$g_d(i)$  = the geometric term,

$$= N_i r_{di}^{-6} / \sum N_j r_{dj}^{-6} ,$$

- $N_j$  = number of magnetically equivalent nuclei  $j$ ,  
 $r_{dj}$  = distance between protons  $d$  and  $j$ ,  
 $A$  = the correlation term,  

$$= [6\tau_c/(1+4\omega^2\tau_c^2) - \tau_c] / [\tau_c + 3\tau_c/(1+\omega^2\tau_c^2) + 6\tau_c/(1+4\omega^2\tau_c^2)],$$
 $\tau_c$  = correlation time,  
 $\omega$  = spectrometer frequency.

The proton-proton distances were derived from the atomic coordinates of the conformers provided by HSEA calculations. Using an assumed correlation time; namely,  $\tau_c = 0.1$  ns, the program evaluates the enhancements on selected protons by way of Equation 17. The theoretical n.O.e.'s for the model compounds upon saturation of H-1' calculated for the minimum energy conformations provided by HSEA calculations are reported in Table 15.

**Table 15.** Theoretical relative nuclear Overhauser enhancements.

Compound	$\phi^\circ/\psi^\circ$	H-4/H-2'	H-3/H-2'
13, 16, 2	-30°/-25°	0.76	0.11
7	-30°/-25°	0.73	0.04
1	-35°/-35°	0.41	-0.07 <sup>a</sup>
3	-35°/-25°	0.84	0.07
12	-50°/-10°	0.73	0.06

<sup>a</sup>H-3ax/H-2' = -0.07; H-3eq/H-2' = 0.31.

As previously mentioned, the goal was to measure the n.O.e. of a signal relative to that for H-2' which could be used as a "reference" since the H-1' to H-2' distance is known with sufficient accuracy. These theoretical values will be shown to be in good agreement with the experimental values. It may be

noticed at this point that the n.O.e. ratio H-4/H-2' for the 3-deoxy derivative **1** is smaller than for methyl  $\alpha$ -maltoside (**13**) even for similar conformations mainly because  $3e_q$  in compound **1** provides H-4 with a new relaxation pathway. The enhancement on H-3 $a_x$ , as can be appreciated from Table 15, is small and negative<sup>137</sup> for the same reason. In this case (compound **1**), the relative n.O.e. calculated for H-3 $e_q$  ( $H-3e_q/H-2' = 0.31$ ) should provide valuable information and, in fact, an important experimental n.O.e. was found. That the n.O.e. ratio calculated for the mannoside **3** is larger, as compared to the situation for the glucoside **13**, is not surprising since the configuration at C-2 is inverted and H-4 cannot relax through interaction with H-2.

## 5.2. Experimental nuclear Overhauser enhancements

Before the experimental n.O.e.'s reported in Table 17 (Figures 24 - 32) can be interpreted, it is necessary to test the validity of the assumptions made when the theoretical values were calculated. The anisotropy of molecular tumbling can be judged from a consideration of the  $T_1$  relaxation times of the  $^{13}\text{C}$  atoms. Thus, the  $^{13}\text{C}$  relaxation times of methyl  $\beta$ -maltoside (**18**) in  $\text{D}_2\text{O}$  and  $\text{DMSO-}d_6$  were measured as reported in Table 16. Assuming dipole-dipole relaxation only, the relaxation times should depend almost exclusively on the number of hydrogen atoms directly attached to the  $^{13}\text{C}$  carbon (see section 1.3.3.3.). In fact, the observed values are relatively constant, showing only some dispersion for the reducing units in  $\text{DMSO-}d_6$ . Therefore, the molecule is tumbling very nearly isotropically in both solutions and sufficiently so for the present purpose.

**Table 16.** Carbon-13 spin-lattice relaxation times (s) of methyl  $\beta$ -maltoside (18) in D<sub>2</sub>O and in DMSO-*d*<sub>6</sub>.<sup>a</sup>

Carbon	D <sub>2</sub> O	DMSO- <i>d</i> <sub>6</sub>
C-1	0.64	0.51
C-2	0.62	0.39
C-3	0.59	0.46
C-4	0.61	0.43
C-5	0.60	0.48 <sup>p</sup>
C-6	0.29	0.27
C-1'	0.52	0.40
C-2'	0.50	0.39
C-3'	0.51	0.39
C-4'	0.51	0.42
C-5'	0.41	0.46
C-6'	0.31	0.26

<sup>a</sup>Measured by the non-selective inversion recovery method. Values in D<sub>2</sub>O are  $\pm 0.02$  s and in DMSO-*d*<sub>6</sub>  $\pm 0.05$  s.

The experimental relative n.O.e.'s are presented in Table 17. These data are those derived from selective saturation of H-1' which as seen in Figures 13 - 15 produces a signal which is well separated from the other signals in the spectra. Compound 18 was not included since at 360 MHz (the frequency of the spectrometer available) the signals of H-4 and H-2' partially overlap precluding the measurement of their individual enhancements. Also, the signals for H-1' and H-1'' of the maltotrioside 4 overlap with each other in the <sup>1</sup>H-n.m.r. spectrum (see Figure 13c) making impossible the selective saturation of either one of these protons. Each value reported is the average

of 2 to 5 independent measurements. The reproducibility is indicated by the standard deviations. It is seen that the relative n.O.e.'s on H-4, H-4/H-2', could be reproduced well to within  $\pm 15\%$ . On the other hand, the relative n.O.e.'s on H-3, H-3/H-2', could not be reproduced well. This is because the enhancements observed on H-3 are small (between 1.0 and 3.0% as compared to between 12.0 and 18.0% for H-4 and H-2') and in consequence the relative uncertainty in its measurement is large. For this reason, the relative enhancements H-3/H-2' can only be used qualitatively for the assessment of conformational preference.

**Table 17.** Experimental average relative nuclear Overhauser enhancements with the standard deviations in parenthesis.

Compound	n <sup>a</sup>	D <sub>2</sub> O		n <sup>a</sup>	DMSO-d <sub>6</sub>	
		H-4/H-2'	H-3/H-2' <sup>c</sup>		H-4/H-2'	H-3/H-2'
13	4	0.98(0.07)	0.17(0.05)	2	1.26(0)	0.36(0.11)
7	2	0.91(0.04)	0(-)	4	1.28(0.15)	0(-)
1	3	0.41(0.03)	0.38 <sup>b</sup> (0.04)	2	0.47(0.13)	0.35 <sup>b</sup> (0.05)
16	2	0.68 <sup>c</sup> (0.07)	0(-)	2	1.55(0.14)	0(-)
2	4	0.91(0.04)	0.14(0.04)	-	<sup>d</sup>	<sup>d</sup>
3	5	0.91(0.15)	0.11(0.05)	1	1.17(N/A)	0.33(N/A)
12	4	0.79 <sup>e</sup> (0.08)	0(-)	2	0.82 <sup>e</sup> (0.01)	0.11(0)

<sup>a</sup>Number of independent measurements.

<sup>b</sup>This is the ratio H-3<sub>eq</sub>/H-2', no enhancement was detected for H-3<sub>ax</sub>.

<sup>c</sup>Second order system (H-2', H-3').

<sup>d</sup>Second order system (H-3, H-4, H-5).

<sup>e</sup>Second order system (H-4, H-5).

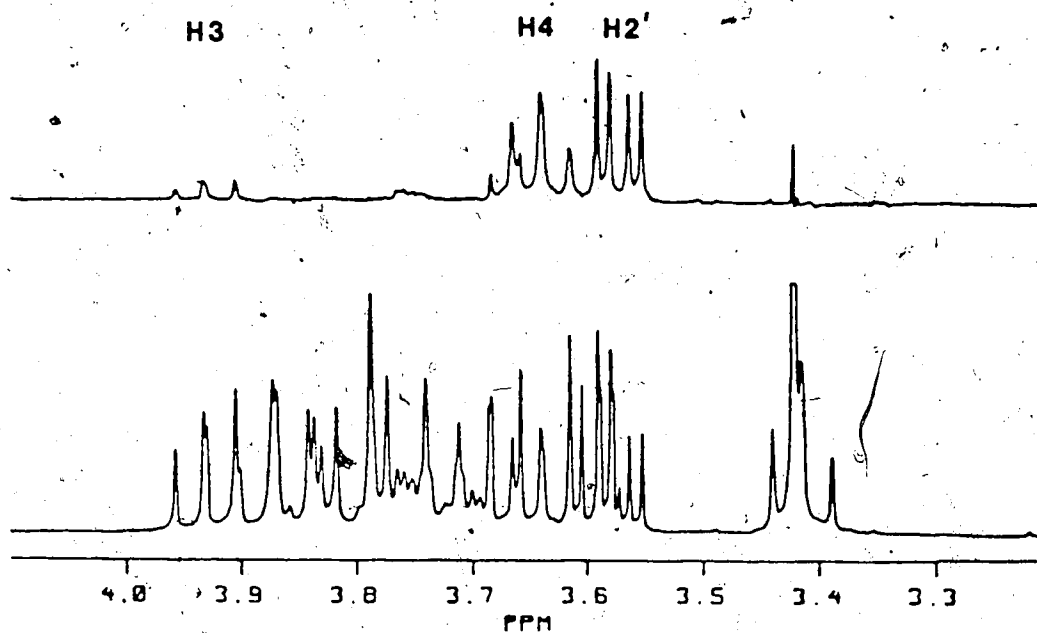


Figure 24. Partial  $^1H$ -n.m.r. spectrum of methyl  $\alpha$ -maltoside (13) in  $D_2O$  (lower trace) and n.O.e. difference spectrum (top trace) obtained upon saturation of  $H-1'$ .

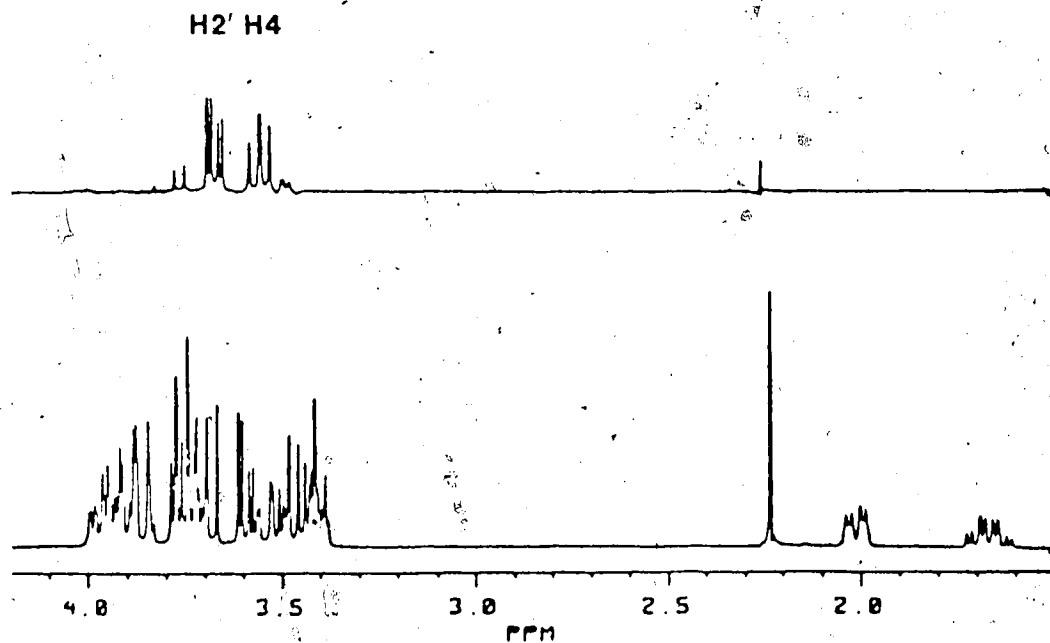


Figure 25. Partial  $^1H$ -n.m.r. spectrum of 1,2-dideoxymaltose (7) in  $D_2O$  (lower trace) and n.O.e. difference spectrum (top trace) obtained upon saturation of  $H-1'$ .

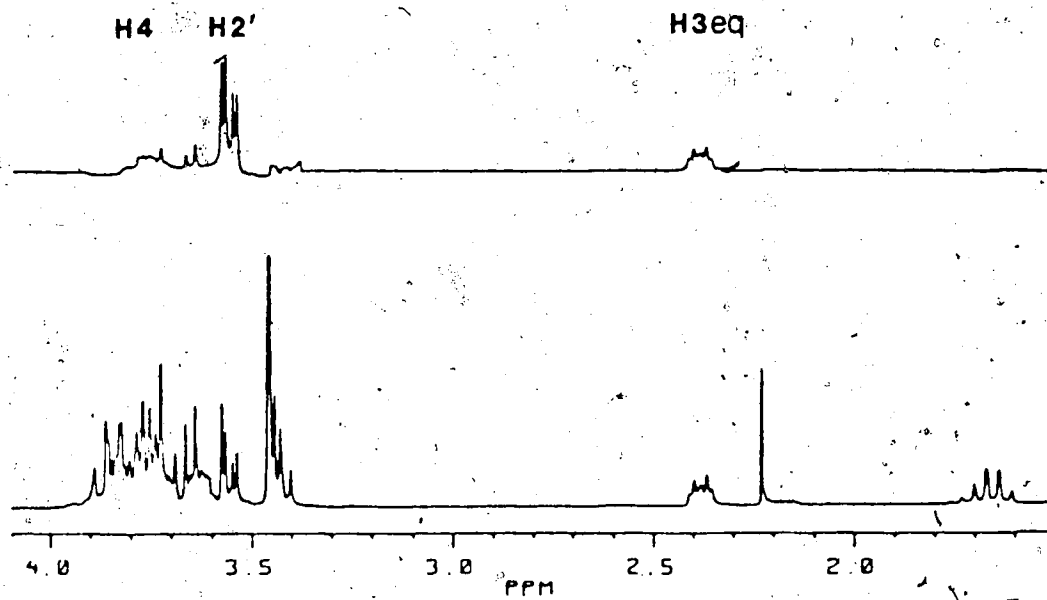


Figure 26. Partial <sup>1</sup>H-n.m.r. spectrum of methyl 3-deoxy- $\alpha$ -maltoside (1) in D<sub>2</sub>O (lower trace) and n.O.e. difference spectrum (top trace) obtained upon saturation of H-1'.

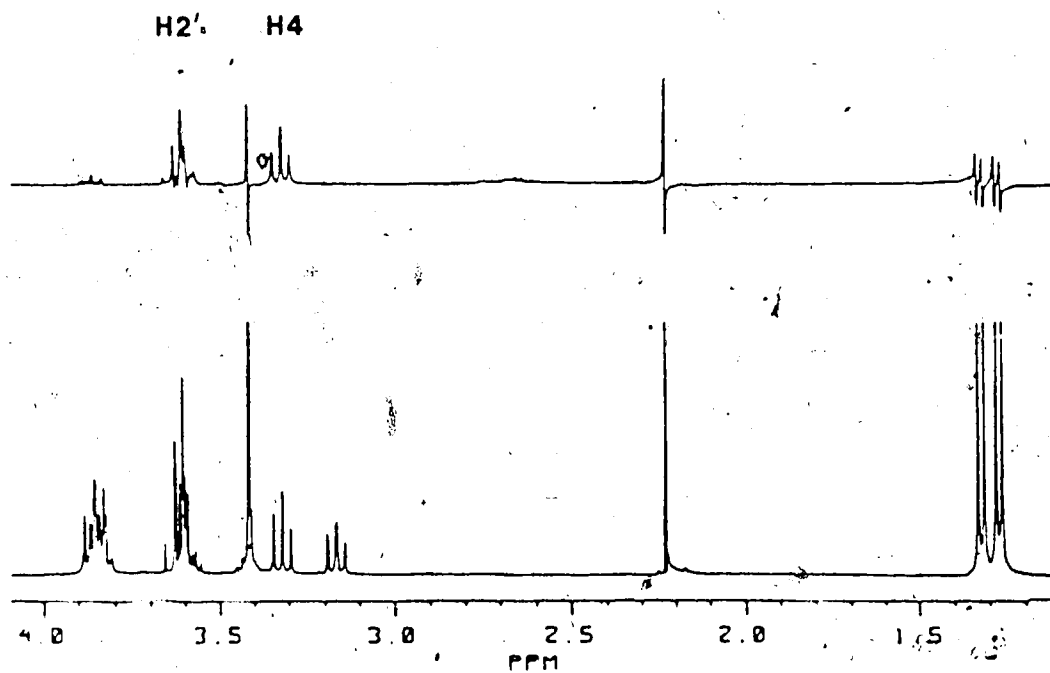


Figure 27. Partial <sup>1</sup>H-n.m.r. spectrum of methyl 6,6'-dideoxy- $\alpha$ -maltoside (16) in D<sub>2</sub>O (lower trace) and n.O.e. difference spectrum (top trace) obtained upon saturation of H-1'.



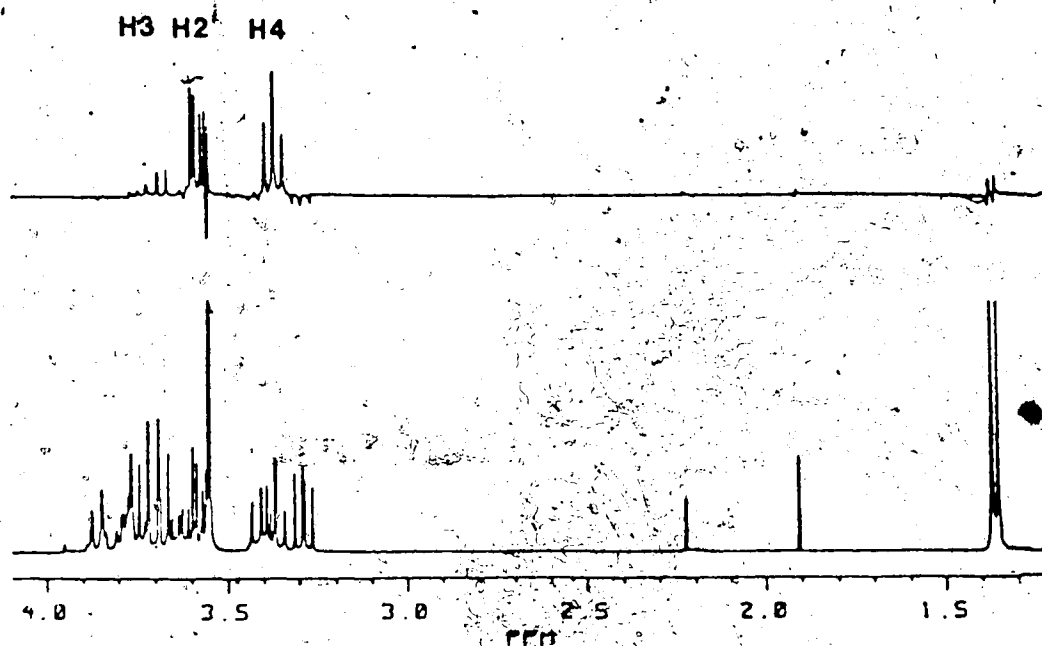


Figure 28. Partial  $^1\text{H}$ -n.m.r. spectrum of methyl 6-deoxy- $\beta$ -maltoside (2) in  $\text{D}_2\text{O}$  (lower trace) and n.O.e. difference spectrum (top trace) obtained upon saturation of  $\text{H}-1'$ .

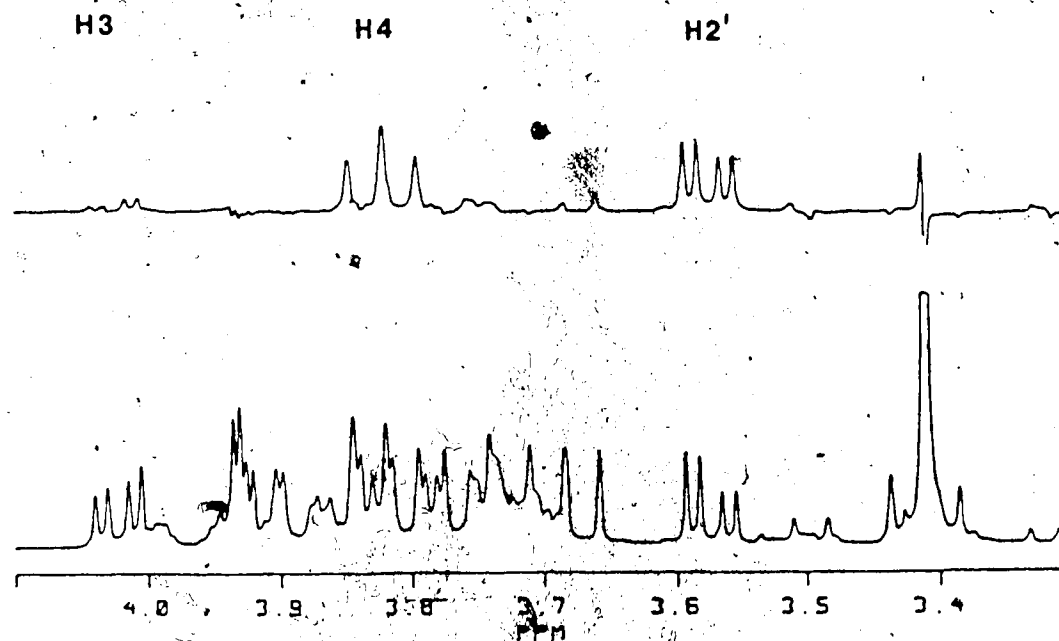


Figure 29. Partial  $^1\text{H}$ -n.m.r. spectrum of methyl 4- $O$ -( $\alpha$ -D-glucopyranosyl)- $\alpha$ -D-mannopyranoside (3) in  $\text{D}_2\text{O}$  (lower trace) and n.O.e. difference spectrum (top trace) obtained upon saturation of  $\text{H}-1'$ .

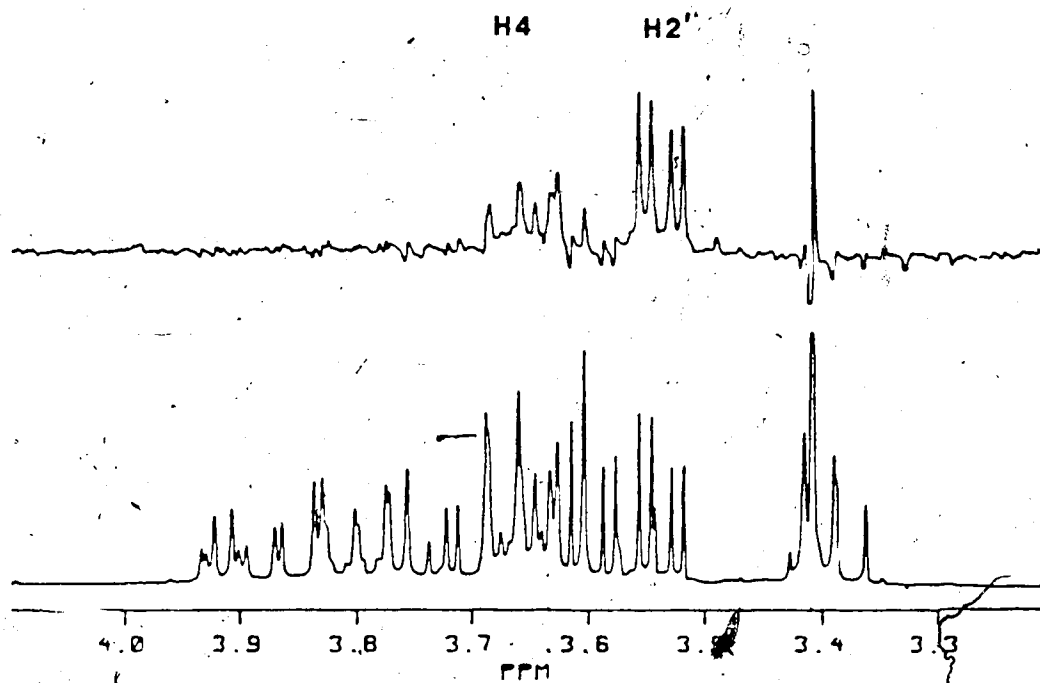


Figure 30. Partial <sup>1</sup>H-n.m.r. spectrum of methyl 4- $\text{O}$ -( $\alpha$ -D-glucopyranosyl)- $\alpha$ -D-xylopyranoside (12) in D<sub>2</sub>O (lower trace) and n.O.e. difference spectrum (top trace) obtained upon saturation of H-1'.

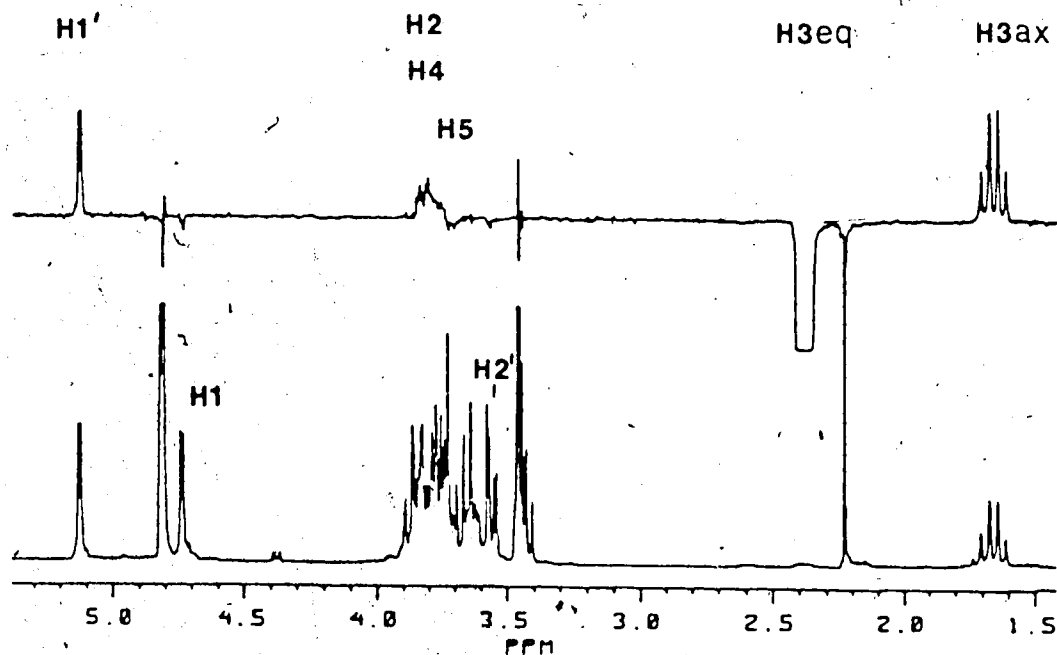
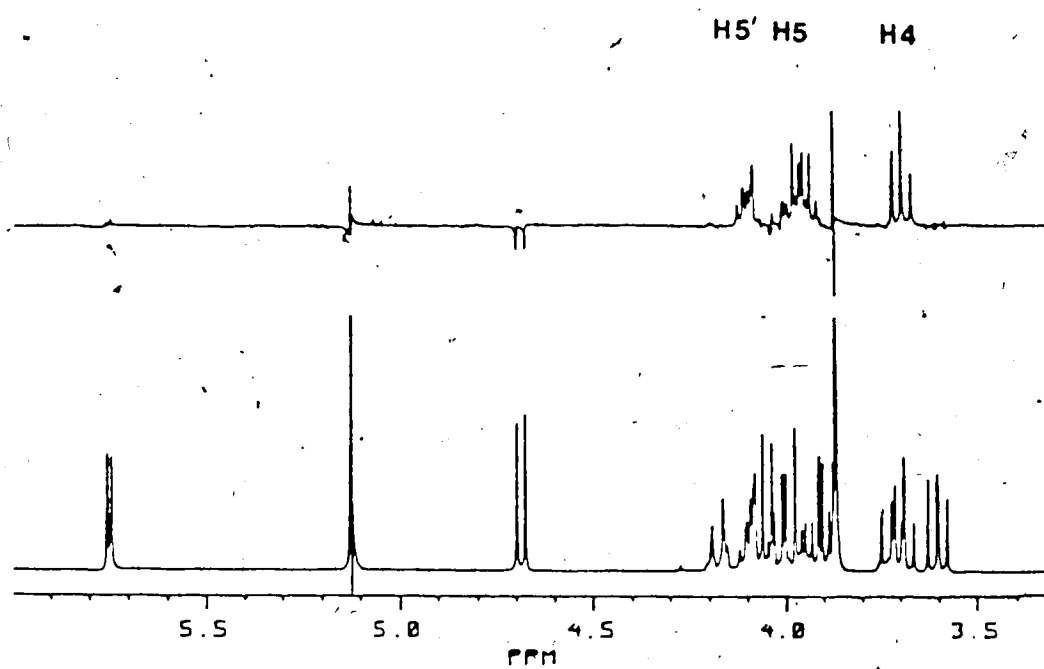


Figure 31. Partial <sup>1</sup>H-n.m.r. spectrum of methyl 3-deoxy- $\alpha$ -maltoside (1) in D<sub>2</sub>O (lower trace) and n.O.e. difference spectrum (top trace) obtained upon saturation of H-3<sub>eq</sub>.



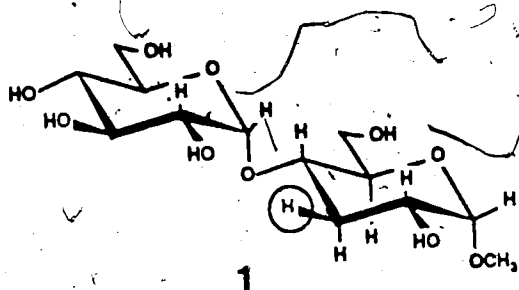
**Figure 32.** Partial <sup>1</sup>H-n.m.r. spectrum of methyl 6-deoxy-β-maltoside (2) in D<sub>2</sub>O (lower trace) and n.O.e. difference spectrum (top trace) obtained upon saturation of the methyl group.

All the relative n.O.e.'s presented in Table 17 are seen to be larger than those predicted on the basis of HSEA conformers except for the 6,6'-dideoxy compound 16 (see Table 16). This exception may result from the fact that H-2' and H-3' form a second order system in the n.m.r. spectrum (see Table 7). The n.O.e.'s are also consistently larger in DMSO- $d_6$  suggesting a change of the conformation in agreement with the  $^{13}C$  data.

The quality of the n.O.e. data can be judged from the appearance of the n.O.e. difference spectra registered in Figures 24 - 32. The n.O.e. difference spectra of methyl  $\alpha$ -maltoside (13) and 1,2-dideoxymaltose (7) are reproduced in Figures 24 and 25. The data indicate similar conformations for these compounds. It is not surprising that no enhancement is detected on H-3 of 1,2-dideoxymaltose (7) since H-2 $_{eq}$  can provide an alternative relaxation path for H-3. It was expected that the 6-deoxy compounds 16 and 2 would be in conformations similar to methyl  $\alpha$ -maltoside (13) and in fact compound 2 shows similar enhancements. The 6,6'-dideoxy derivative 16 has a different enhancement ratio on H-4/H-2', however H-2' is involved in a second order system with H-3' and under these circumstances the n.O.e.'s can provide only qualitative information.<sup>71,138</sup> In agreement with the calculations reported in Table 15, an important relative n.O.e. was found for H-3 $_{eq}$  of the 3-deoxy compound 1 which requires that hydrogen atom to be located in time close to H-1' as was illustrated in Figure 16.

The conformation of the xyloside compound 1 and the xyloside 12, as indicated by the almost constant relative n.O.e.'s in D<sub>2</sub>O and DMSO- $d_6$ , do not change much when the solvent is changed and are already in good agreement with the HSEA calculations. In the xyloside 12, H-4 and H-5 are strongly coupled and therefore the n.O.e.'s should be interpreted with caution.<sup>71,138</sup>

**Table 18.** Comparison of theoretical and experimental n.O.e.'s when H-3<sub>eq</sub> of methyl 3-deoxy- $\alpha$ -maltoside (1) was saturated.



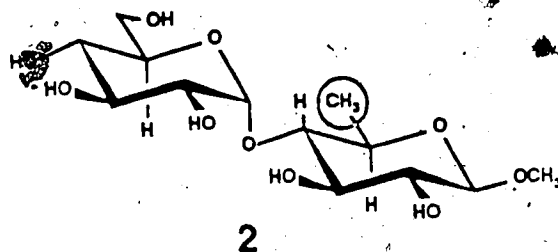
	Enhancement (%) on protons,						
	H-1	H-2	H-4	H-3 <sub>ax</sub>	H-5	H-1'	H-2'
theoretical	-2.9	9.0	4.5	26.1	-1.8	10.6	-1.6
experimental	-0.8	(11.5)		27.7	-1.0	11.1	-1.4

Alternative n.O.e. experiments are provided by the 3-deoxy compound 1 and the 6-deoxy compound 2 since these provide signals that are well separated from the other signals in the  $^1\text{H-n.m.r.}$  spectra. Saturation of H-3<sub>eq</sub> of 1 was expected, on the basis of the HSEA conformers to produce enhancements of H-3<sub>ax</sub>, H-2, H-4 and H-1'. The experimental and calculated (at  $-35^\circ/-35^\circ$ ) n.O.e.'s when H-3<sub>eq</sub> was saturated are presented in Table 18 where it is seen that the theoretical and experimental values are in very good agreement. The negative enhancements arise from third spin, indirect n.O.e.'s.<sup>71,137</sup>

The  $^1\text{H-n.m.r.}$  spectrum for the 6-deoxy compound (2) also provided an opportunity for an n.O.e. study since the signal for CH<sub>3</sub>-6 is well resolved from other signals ( $\delta = 1.36$  ppm, see Figure 14b). Saturation of the methyl group at C-5 of this compound produced the enhancements reported in Table 19, and the n.O.e. difference spectrum is reproduced in Figure 32. Calculation of the

theoretical n.O.e.'s is difficult because the three hydrogen atoms of the methyl group are saturated simultaneously and provide varying n.O.e. contributions. Nevertheless, the data require the methyl group to be located in time close to H-5' (2.77 Å) as expected from HSEA calculations (see Figure 16).

**Table 19.** Experimental n.O.e.'s obtained when CH<sub>3</sub>-6 of methyl 6-deoxy-β-maltoside (2) was saturated.



	Enhancement (%) on protons,		
	H-4	H-5	H-5'
observed	2.2	3.6	1.7

## 6. Hydrogen bonding studies

The study of the properties of exchangeable protons by n.m.r. is conveniently performed in aprotic solvents in which the protons exchange slowly on the n.m.r. timescale. For this purpose DMSO-*d*<sub>6</sub> is frequently used. Indeed, the early studies by Casu *et al.*<sup>38</sup> used this solvent and arrived at a detailed appreciation of the association of carbohydrates with DMSO including intramolecular hydrogen bonding in maltose, amylose and cyclodextrins.

Limbach<sup>139</sup> recently published a review on the use of n.m.r. spectroscopy in the study of hydrogen bonding in solution.

St.-Jacques and coworkers<sup>140</sup> studied intramolecular hydrogen bonds in maltose, cyclohexaamylose and amylose by measuring the temperature dependence of the chemical shifts of the hydroxyls' protons in DMSO- $d_6$ . The large chemical shifts of exchangeable protons usually decrease with increasing temperature because of the disruption of hydrogen bonding with the solvent. A large dependence with temperature indicates that the proton is exposed to and interacting (hydrogen bonding) with the solvent. On the other hand, a small dependence is considered to correspond to a proton shielded from the solvent or intramolecular hydrogen bonding. On this basis, St.-Jacques and coworkers<sup>140</sup> provided evidence for the existence of intramolecular hydrogen bonds in which OH-3 is the proton donor in the compounds that he studied.

A powerful technique for the study of intramolecular hydrogen bonds for carbohydrates dissolved in DMSO- $d_6$  was discovered by Bock and Lemieux.<sup>141,142</sup> The method, first applied to sucrose, consists of measuring isotope shifts<sup>143-145</sup> induced for the signals for OH-protons when these are half-exchanged with deuterium as displayed in the following formulations; DMSO→H-O→D-O or DMSO→D-O→H-O, as compared to the chemical shifts for the undeuterated system DMSO→H-O→H-O. This property is displayed by the spectra shown in Figure 33. Thus, when two hydroxyl groups in DMSO- $d_6$  are hydrogen bonded and enough D<sub>2</sub>O has been added to the solution to half-exchange the protons by deuterium, an isotope shift is transmitted through the hydrogen bond from one deuteroyl group to the neighbouring hydroxyl group. Using this technique Christofides and Davies<sup>146</sup> found direct evidence for a hydrogen bond in cyclohexaamylose. It was found that, after partial

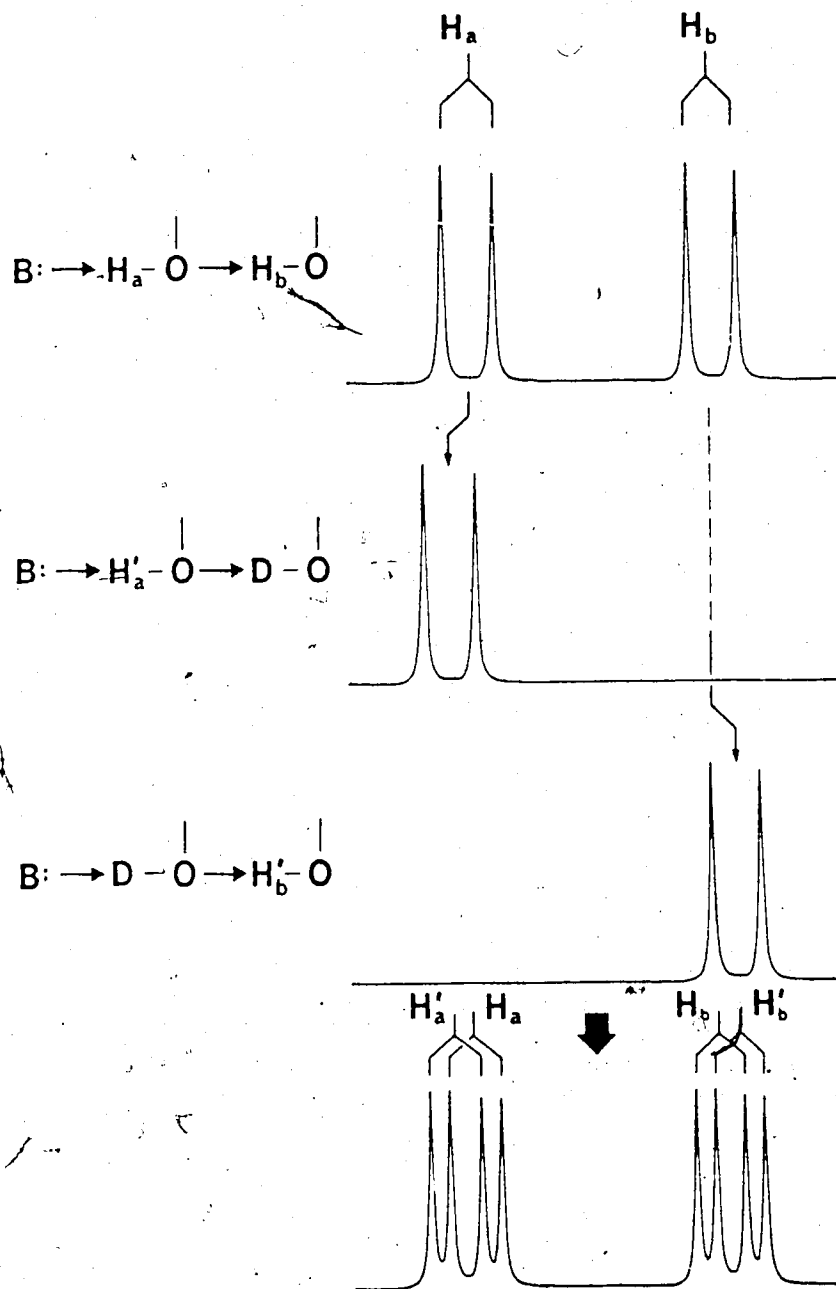


**Figure 33.** Deuterium-induced isotope shifts in the  $^1\text{H}$ -n.m.r. spectrum in  $\text{DMSO}-d_6$  of systems containing hydroxyl groups that form intramolecular hydrogen bonds.



deuteration of the hydroxyl groups, the signal of OH-3 exhibits a negative (to high field) isotope shift of 0.01 ppm while that for H-2' exhibits a positive or downfield shift of the same magnitude. These isotope shifts are similar in kind to those observed in  $^{13}\text{C}$ -n.m.r. spectra when a hydrogen of a hydroxyl group is replaced by deuterium.<sup>147-150</sup>

**Table 20.** Deuterium isotope shifts in  $\text{DMSO-}d_6$ , ppm.

Compound	OH-2'	OH-3	OH-3'
18	0.0126	-0.0093	-
13	0.0109	-0.0099	0.0030
7	0.0075	-0.0137	<sup>a</sup>
16	0.0094	-0.0096	<sup>a</sup>
2	0.0091	-0.0098	-
3	0.0075	-0.0139	-
12	0.0045	-	-
4	0.0092	-0.0097	-
	0.0109	-0.0095	-

<sup>a</sup>Broad signal.

In this investigation, the presence of intramolecular hydrogen bonds in  $\text{DMSO-}d_6$  were first probed by addition of  $\text{D}_2\text{O}$  to solutions of the compounds. The isotope shifts were clearly visible when the hydroxyl groups were half-exchanged with deuterium (see Figures 34 - 41). In each case, the spectrum

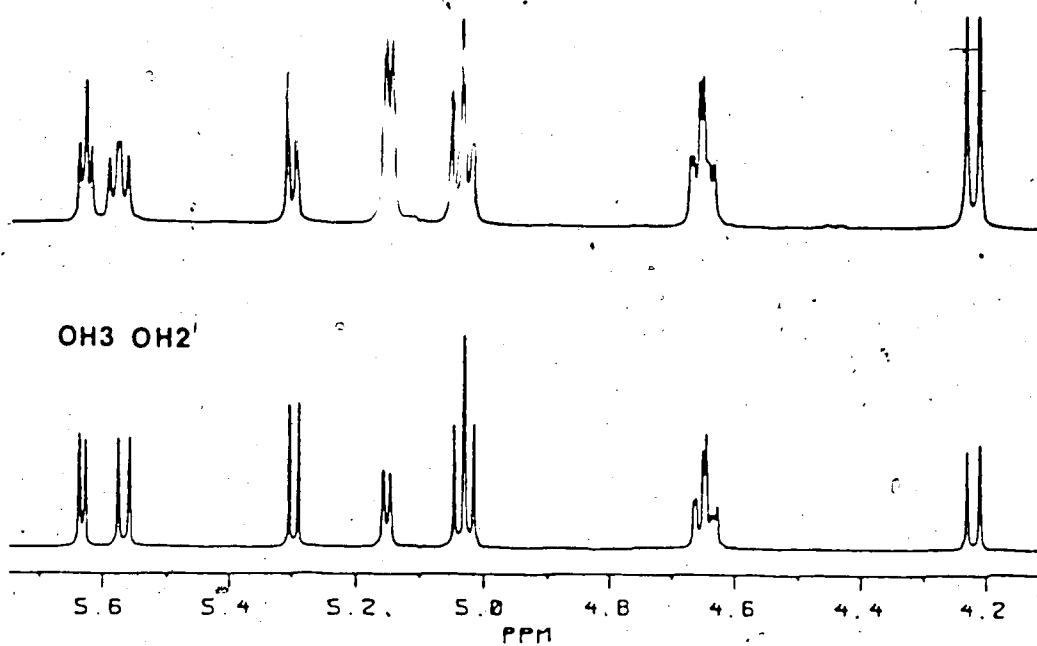


**Figure 34.** Partial <sup>1</sup>H-n.m.r. spectrum of methyl β-maltoside (18) in DMSO-*d*<sub>6</sub> at 295 °K before (lower trace) and after (top trace) the addition of enough D<sub>2</sub>O to half-exchange the hydroxyl protons with deuterium.

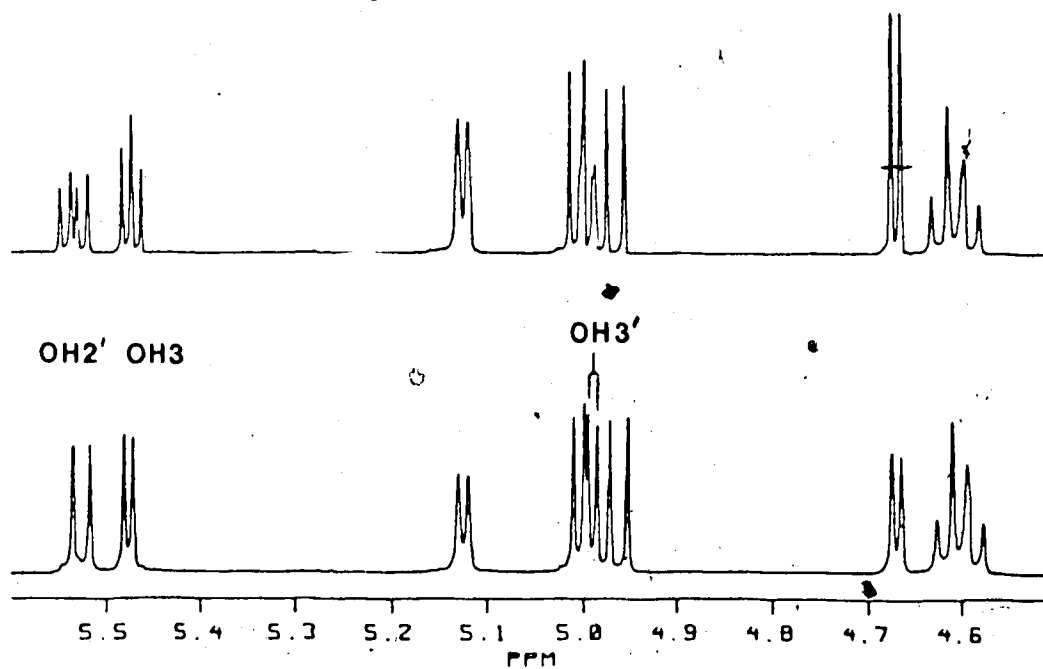


**Figure 35.** Partial <sup>1</sup>H-n.m.r. spectrum of methyl α-maltoside (13) in DMSO-*d*<sub>6</sub> at 301 °K before (lower trace) and after (top trace) the addition of enough D<sub>2</sub>O to half-exchange the hydroxyl protons with deuterium.

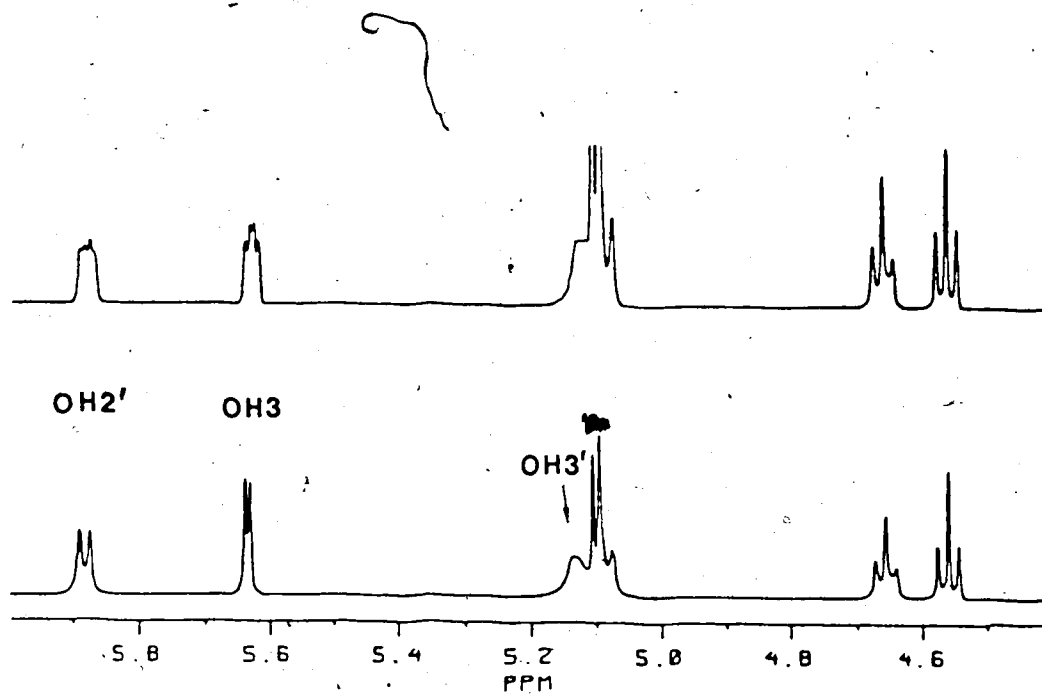


Figure 36. Partial  $^1\text{H}$ -n.m.r. spectrum of 1,2-dideoxymaltose (7) in  $\text{DMSO-}d_6$  at 293  $^\circ\text{K}$  before (lower trace) and after (top trace) the addition of enough  $\text{D}_2\text{O}$  to half-exchange the hydroxyl protons with deuterium.

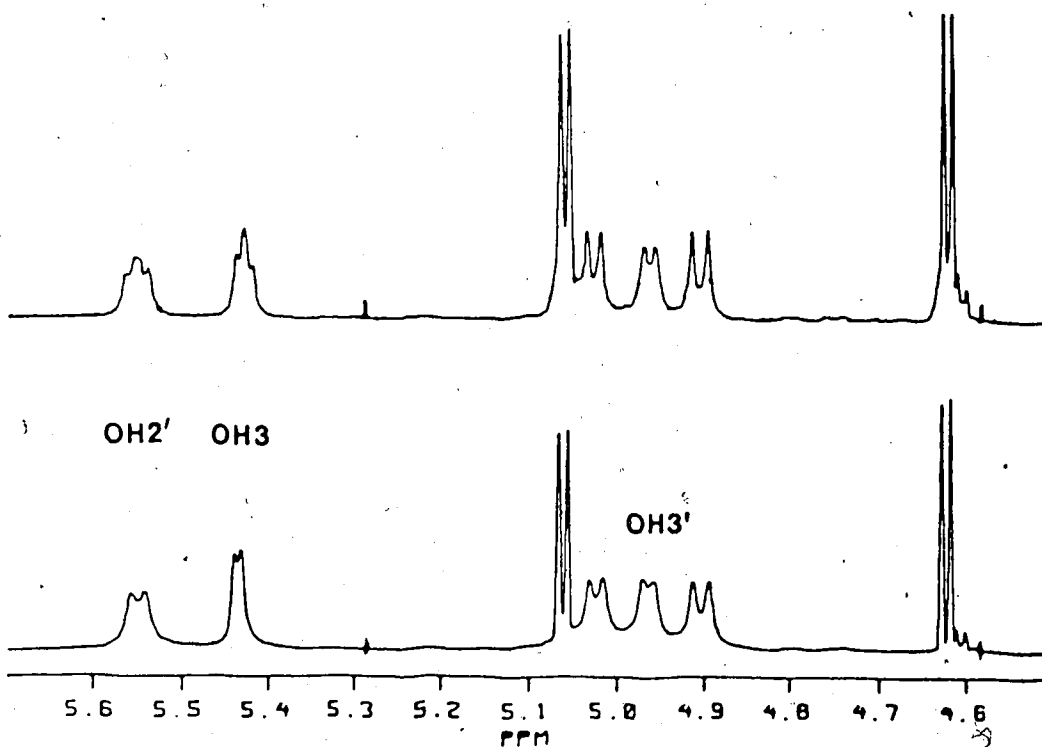


Figure 37. Partial  $^1\text{H}$ -n.m.r. spectrum of methyl 6,6'-dideoxy- $\alpha$ -maltoside (16) in  $\text{DMSO-}d_6$  at 305  $^\circ\text{K}$  before (lower trace) and after (top trace) the addition of enough  $\text{D}_2\text{O}$  to half-exchange the hydroxyl protons with deuterium.

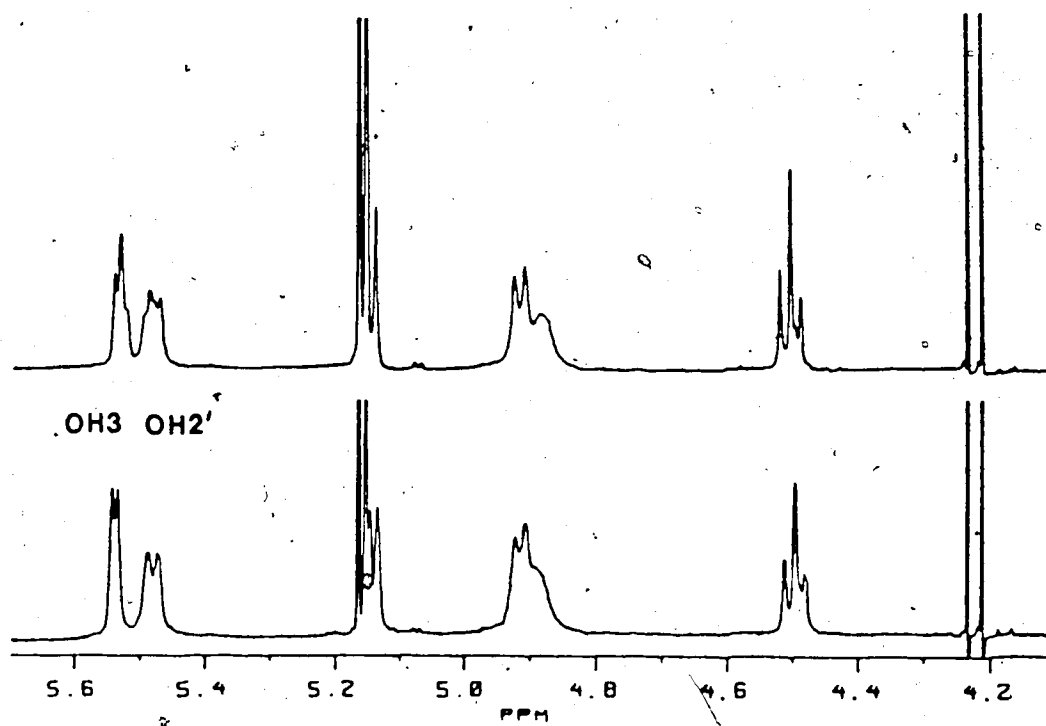


Figure 38. Partial  $^1\text{H}$ -n.m.r. spectrum of methyl 6-deoxy- $\beta$ -maltoside (2) in  $\text{DMSO}-d_6$  at 315  $^\circ\text{K}$  before (lower trace) and after (top trace) the addition of enough  $\text{D}_2\text{O}$  to half-exchange the hydroxyl protons with deuterium.

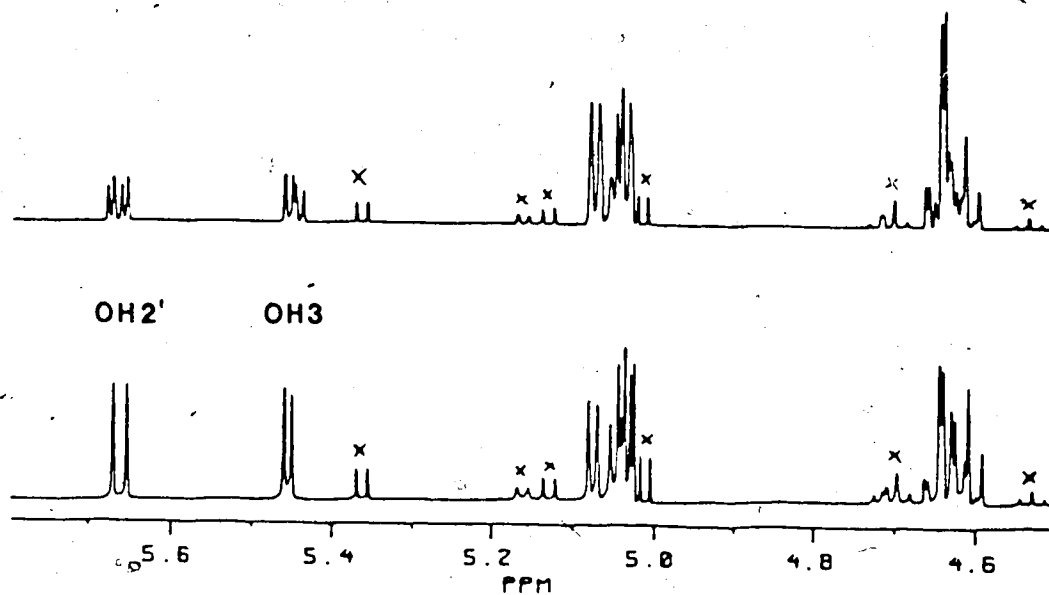


Figure 39. Partial  $^1\text{H}$ -n.m.r. spectrum of methyl 4- $O$ -( $\alpha$ -D-glucopyranosyl)- $\alpha$ -D-mannopyranoside (3) in  $\text{DMSO}-d_6$  at 297  $^\circ\text{K}$  before (lower trace) and after (top trace) the addition of enough  $\text{D}_2\text{O}$  to half-exchange the hydroxyl protons with deuterium.

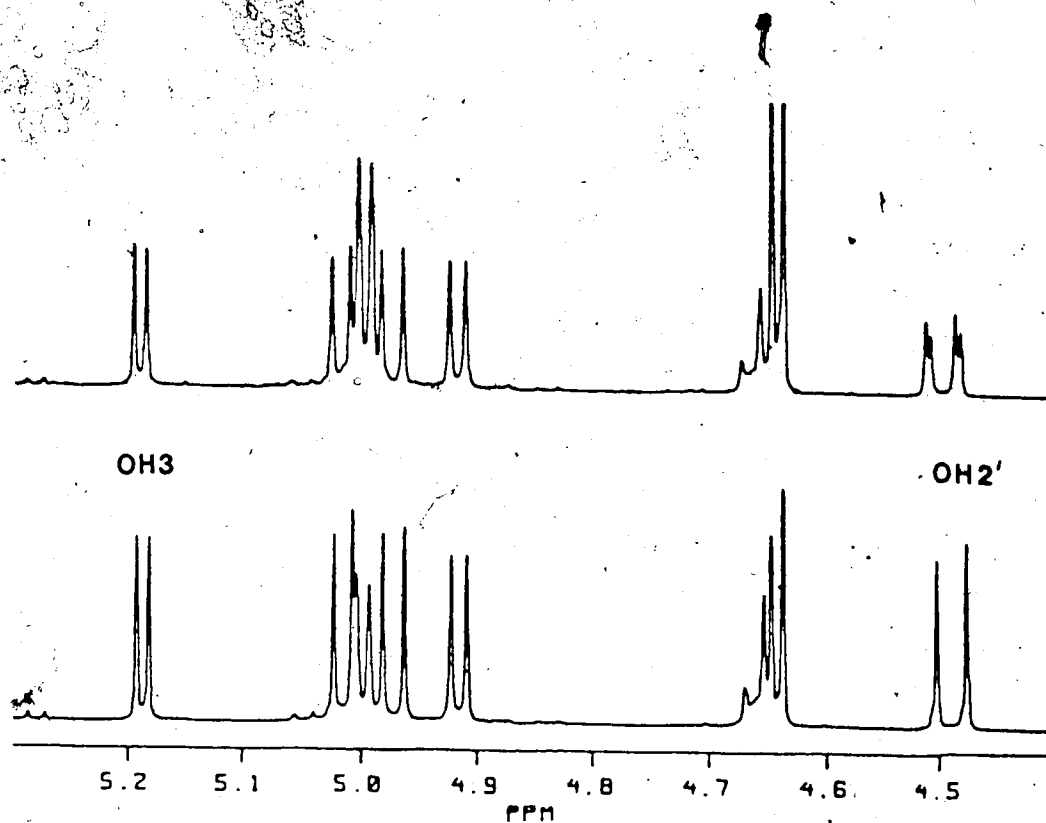


Figure 40. Partial  $^1\text{H}$ -n.m.r. spectrum of methyl 4- $O$ -( $\alpha$ -D-glucopyranosyl)- $\alpha$ -D-xylopyranoside (12) in  $\text{DMSO}-d_6$  at 295  $^\circ\text{K}$  before (lower trace) and after (top trace) the addition of enough  $\text{D}_2\text{O}$  to half-exchange the hydroxyl protons with deuterium.

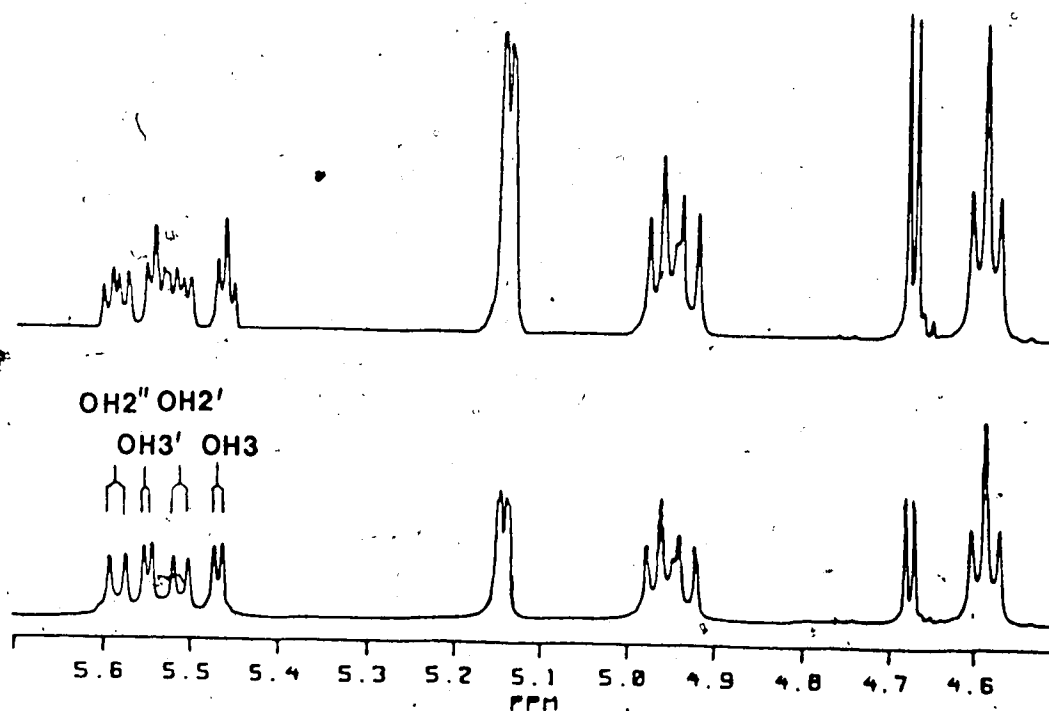


Figure 41. Partial  $^1\text{H}$ -n.m.r. spectrum of methyl  $\alpha$ -maltotriose (4) in  $\text{DMSO}-d_6$  at 307  $^\circ\text{K}$  before (lower trace) and after (top trace) the addition of enough  $\text{D}_2\text{O}$  to half-exchange the hydroxyl protons with deuterium.

consists of doublets corresponding to the coupling of the hydroxyl groups with the vicinal methine proton, or of pseudo-triplets corresponding to the coupling of the hydroxyl of the hydroxymethyl group with the methylene protons. The isotope shifts are reported in Table 20. Each compound, except the xyloside **12**, gives rise to a negative (upfield) isotope shift and an unusual positive (downfield) isotope shift, in agreement with previous observations on sucrose,<sup>141,142</sup> cyclohexaamylose,<sup>146</sup> and recently observed for derivatives of sucrose.<sup>151,152</sup>

Although the reason is not completely understood, the direction of the isotope shift can be interpreted in terms of the role of the hydroxyl group as proton donor or acceptor in the hydrogen bond.<sup>151,152</sup> Observations on different compounds indicate that the hydroxyl group which donates the proton (OH<sub>b</sub> in Figure 33) experiences an upfield (negative) shift when the neighbouring hydroxyl group is deuterated. On the other hand, a positive isotope shift is induced on the hydroxyl group that acts as acceptor on deuteration of its neighbour. Therefore, the signs of the isotope shifts reported in Table 20 suggest, with the exception of the xyloside **12**, that the proton donor in the hydrogen bond is OH-3. A small, 3 ppb, isotope shift is also observed in OH-3' of methyl  $\alpha$ -maltoside (**13**), suggesting an extended hydrogen bonding network as illustrated in Figure 42. A similar network may also be present in compounds **7**, **16** and **3** (see Figures 36, 37 and 39), but in these cases the isotope shifts on OH-3' were observed only as a broadening of the resonance for that proton. Interestingly, when methyl 4',6'-O-benzylidene- $\alpha$ -maltoside was subjected to the same technique, it also showed isotope shifts on OH-2', OH-3 and OH-3' (0.0116, -0.0097 and 0.0027 ppm, respectively).

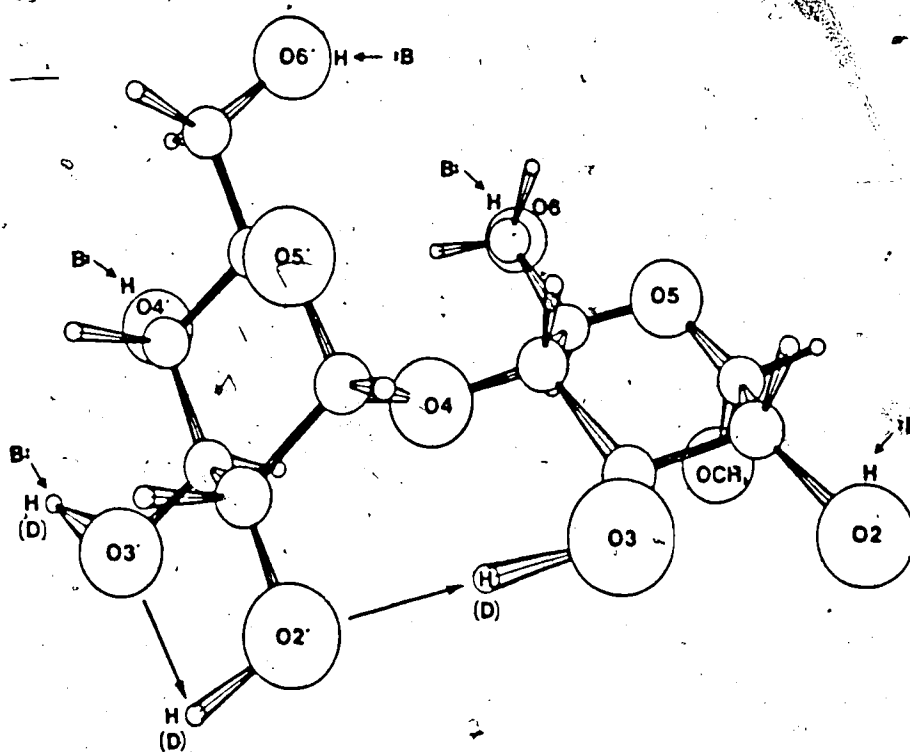


Figure 42. Computer drawn structure for methyl  $\alpha$ -maltoside (13) to display the hydrogen bond network  $\text{HO-3}' \rightarrow \text{HO-2}' \rightarrow \text{HO-3}$

The magnitudes of the isotope shifts can provide information about the relative strengths of hydrogen bonds for molecules in solution.<sup>151</sup> The magnitude of the isotope shift of OH-3' in the maltoside 13 is significantly smaller than on OH-2' or OH-3 suggesting a weaker hydrogen bond. Indeed, such hydrogen bond networks where hydrogen bonds debilitate as they move away from a central, strong hydrogen bond have been observed, using this method, for derivatives of sucrose<sup>151,152</sup> and first rationalized as hydrogen bond conjugation<sup>153</sup>. The term "cooperative effect" was later introduced.<sup>154</sup>

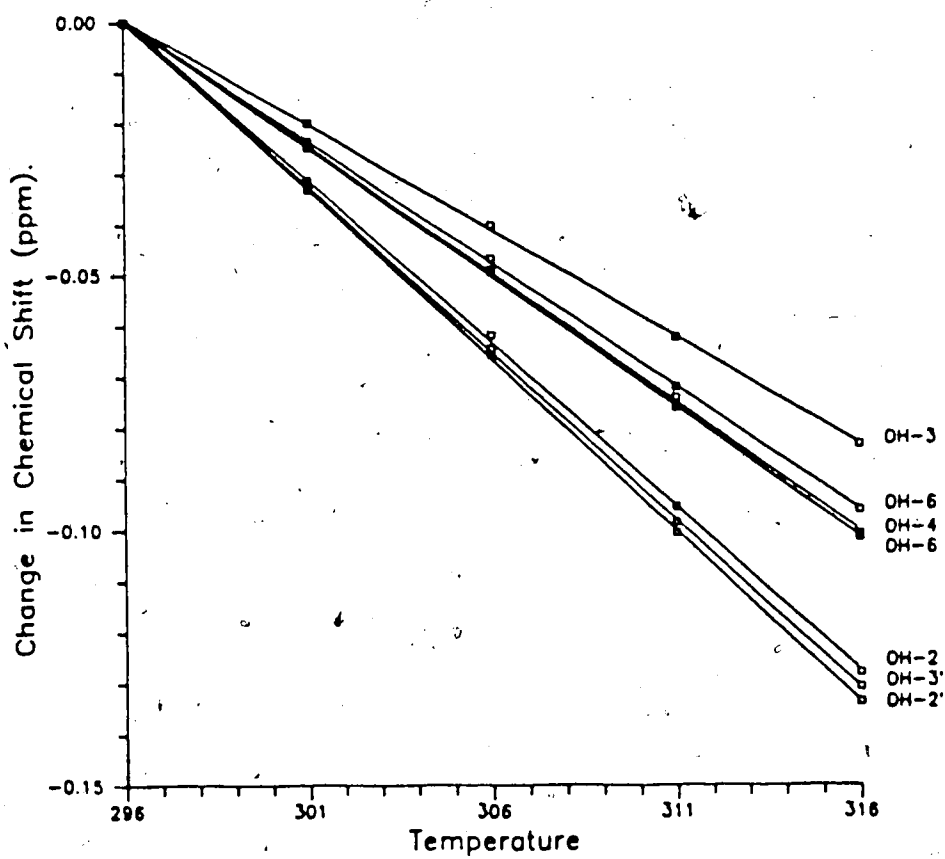


Figure 43. Dependence of the  $^1\text{H}$ -n.m.r. chemical shifts of methyl  $\alpha$ -maltoside (13) in  $\text{DMSO-}d_6$  with changes in temperature.



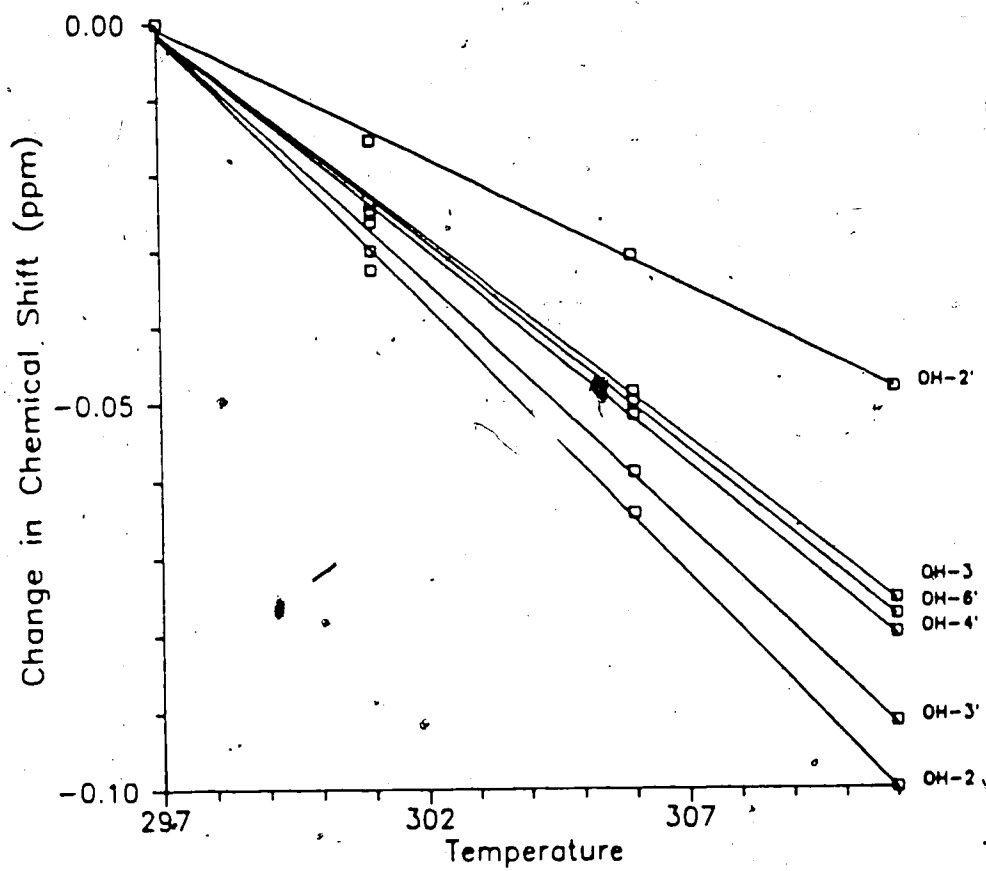


Figure 44. Dependence of the  $^1\text{H}$ -n.m.r. chemical shifts of methyl 4-O-( $\alpha$ -D-glucopyranosyl)- $\alpha$ -D-xylopyranoside (12) in DMSO- $d_6$  with changes in temperature.

That the donor in the hydrogen bond is OH-3 is also demonstrated by the dependence of the proton n.m.r. chemical shifts of the hydroxyl protons of methyl  $\alpha$ -maltoside (13) in DMSO- $d_6$  (Figure 43). It can be observed that the resonance of OH-3 is the least sensitive to a change of temperature, indicating that it is not predominantly hydrogen bonded to the solvent but, instead, to a neighbouring hydroxyl group (OH-2').<sup>140</sup>

The spectra of the xyloside 12 present an entirely different situation (Figure 40). It is first noticed that the resonance of OH-2' appears at very high field ( $\delta = 4.44$  ppm) as compared with the signals for the same proton of the other model compounds ( $\delta = 5.5$  ppm, see Table 9). Furthermore, its coupling constant with the vicinal H-2 is large (9.1 Hz) as compared to that for 13, namely; 6.2 Hz. This fact requires a predominant conformation in which the O-2'—H bond is *antiperiplanar* to the C-2'—H bond. After D<sub>2</sub>O was added to the DMSO- $d_6$  solution a small, positive isotope shift was detected for OH-2', but no other isotope shift could be observed for the remaining hydroxyl groups. The sign of the isotope shift indicated that OH-2' was the acceptor of a hydrogen bond, but the donor could not be a neighbouring hydroxyl group since no isotope shift was detected for them. The only plausible alternative is that the isotope shift is induced from a molecule of HDO which is weakly hydrogen bonded to OH-2'. Being in an *antiperiplanar* conformation to H-2', the O-2'—H bond projects in the appropriate direction for hydrogen bonding to O-1'. Its low chemical shift suggests<sup>38</sup> that OH-2' is not strongly hydrogen bonded to the solvent and additional evidence may be found in the plot of the change in <sup>1</sup>H chemical shift with changes of temperature (Figure 44). In sharp contrast with methyl  $\alpha$ -maltoside (13), the proton which is the least sensitive to a change in temperature is OH-2' instead of OH-3, suggesting that it is the donor in an intramolecular hydrogen bond (to O-1') as shown in Figure 45.

Even though a hydrogen bond of the type that forms in methyl  $\alpha$ -maltoside (13) cannot be established in the 3-deoxy derivative 1, this was subjected to the same examination with the purpose of determining whether or not the hydrogen bond that occurs in the xyloside 12 is formed whenever the bond between OH-2' and OH-3 is not possible. Interestingly, no isotope effect was detected for any hydroxyl group and the chemical shift and coupling constant of its OH-2' were rather average values (see Tables 9 and 10). Apparently, the intra- and intermolecular hydrogen bonding shown in Figure 45 for the xyloside (12) demand that a very specific environment be developed.

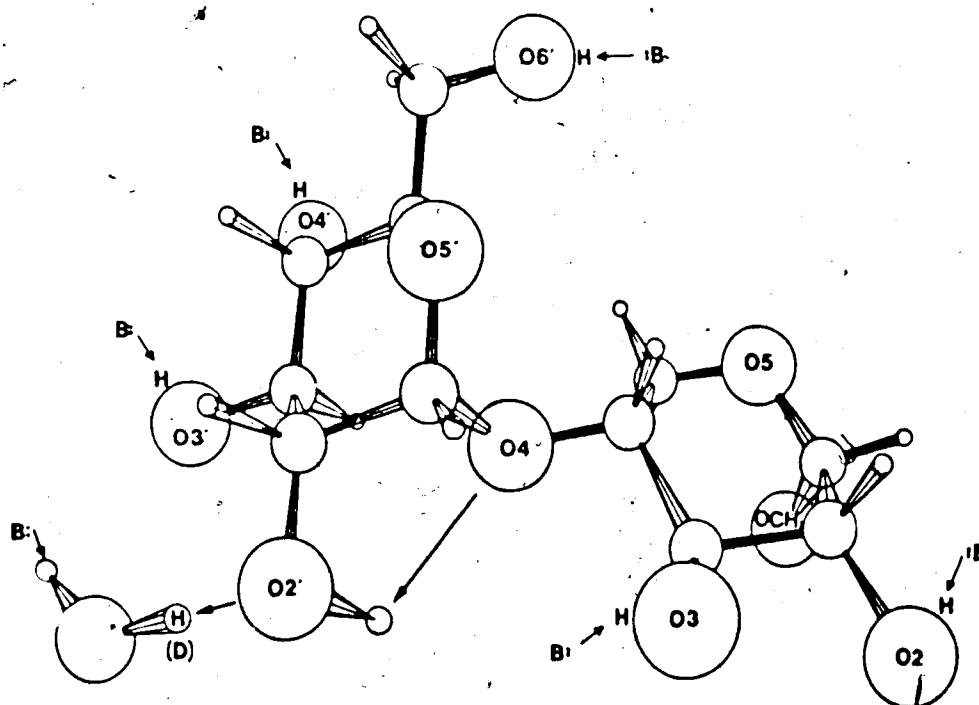


Figure 45. Computer drawn structure for methyl 4-O-( $\alpha$ -D-glucopyranosyl)- $\alpha$ -D-xylopyranoside (12) to display the hydrogen bond O-1'  $\rightarrow$  HO-2'.

## 7. Conclusions

After the nuclear Overhauser enhancements in  $D_2O$  and  $DMSO-d_6$  were determined, and knowing what compounds possess an intramolecular hydrogen bond in DMSO, it was possible to find the conformations that these adopt in solution. In  $DMSO-d_6$  the intramolecular hydrogen bond demands that the distance between O-2' and O-3 be in the range of 2.7 to 3.0 Å which in turn limits the conformations that the molecule can adopt. The allowed conformations correspond to an elliptical area in the conformational map (Figure 46). The measured n.O.e.'s in  $DMSO-d_6$  also restrain the available conformations to a boundary that can be appreciated in Figure 46 where the horizontally shaded area includes the conformations that provide calculated n.O.e.'s (H-4/H-2') close to the experimental value of methyl  $\alpha$ -maltoside ( $1.25 \pm 0.10$ ). Consequently, the conformation in  $DMSO-d_6$  must occur in the intersection, at about  $-10^\circ / -10^\circ$  as indicated in Figure 46.

The smaller n.O.e. ratio (H-4/H-2') for methyl  $\alpha$ -maltoside (13) in  $D_2O$  indicates a conformational preference wherein H-1' and H-4 are more separated on the average than when  $DMSO-d_6$  is the solvent. The torsion angles that provide conformations that have calculated n.O.e.'s in agreement with experiment are displayed in Figure 47, for methyl  $\alpha$ -maltoside (13). The lower energy conformer that satisfies the requirements of the n.O.e. occur at  $-25^\circ / -15^\circ$ , where the distance between O-2' and O-3 (3.33 Å) is too large to allow the formation of the hydrogen bond. Therefore, it is concluded that OH-3 is not hydrogen bonded to O-2' for maltose in water.

These results show an important solvent effect on conformational preference, as was seen to be the case for crystal field forces. As may be expected from other studies of solvent effects on conformational properties<sup>24</sup>,

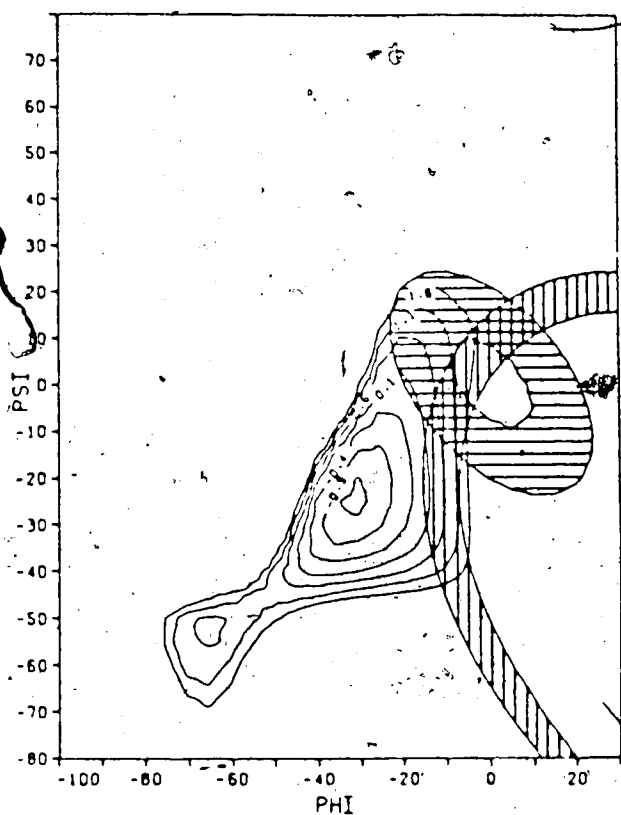


**Figure 46.** Conformational energy contour plot of methyl  $\alpha$ -maltoside (13). The vertically shaded area indicates the range of conformations that would give rise to the occurrence of an intramolecular hydrogen bond between O-2' and O-3 (interatomic distance = 2.7 $\text{\AA}$  - 3.0  $\text{\AA}$ ). The horizontally shaded area encloses the conformations that produce a n.o.e. ratio close to the one found in DMSO- $d_6$  (H-4 / H-2' = 1.15 - 1.35). The intersection shows the region where the conformation of the molecule is expected to occur in DMSO solution.

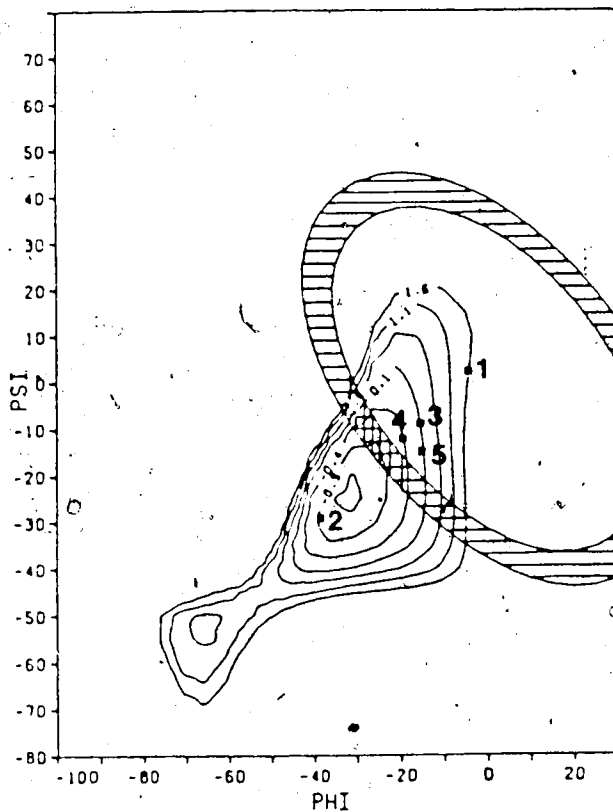


**Figure 47.** Conformational energy contour plot of methyl  $\alpha$ -maltoside (13). The horizontally shaded area shows the conformations that produce a n.O.e. ratio close to the one found in  $D_2O$  ( $H-4 / H-2' = 0.90 - 1.10$ ). The cross-hatched area shows the region where the conformation of the molecule is expected to occur in water. Indicated in the map are the solid state conformations of 1)  $\alpha$ -maltose<sup>13</sup>, 2) methyl  $\alpha$ -maltotrioside<sup>37</sup>, 3)  $V_h$ -amylose<sup>48</sup>, 4) B-amylose<sup>44</sup>, and 5) maltoheptaose<sup>155</sup>.

and which has long been appreciated, references to conformation must include references to the solvent. The problem still remains that HSEA models are determined as if the molecule were in complete isolation, but such models have been found to be in good agreement for the carbohydrate dissolved in water. This appears to mean that intramolecular interactions for the molecule in a vacuum are similar to those when dissolved in water. The results agree with the conformational variation induced upon change of solvent that Pérez and coworkers<sup>69</sup> found for methyl  $\beta$ -maltoside on the basis of  $^{13}\text{C}$  to  $^1\text{H}$  coupling constants. The coupling constants across the glycosidic linkage (see section 1.3.3.2.) measured by these authors in  $\text{D}_2\text{O}$  and  $\text{DMSO}-d_6$  are compared in Table 21 with those calculated (using the method of Pérez and coworkers) for the conformers of methyl  $\alpha$ -maltoside described in the previous paragraphs. It is seen that the experimental coupling constants can be reproduced well (to within 0.6 Hz) by the conformations found in this thesis on the basis of nuclear Overhauser enhancements. These conformers are also in agreement with the different conformational preference that Rees and Thom<sup>58</sup> proposed for methyl  $\beta$ -maltoside in water and in  $\text{DMSO}$  on the basis of optical rotations (see section 1.3.2.).

The conformations that best reproduce the experimental data of all the model compounds were found using a procedure similar to that just described for methyl  $\alpha$ -maltoside and are reported in Table 22. It is seen that the HSEA conformers are in reasonably good agreement with the conformations determined by n.m.r. spectroscopy in  $\text{D}_2\text{O}$ . The internuclear distances between O-3 and O-2' are too large for intramolecular hydrogen bonding in this solvent. The data require different conformations when  $\text{DMSO}-d_6$  is solvent but instead provide conformations for which a strong intramolecular hydrogen bond is possible because the average internuclear distance is between 2.7 and

**Table 21.** Comparison of calculated and experimental linkage coupling constants for methyl  $\alpha$ -maltosides.

Solvent	$J^{\alpha}$ (Hz)		$J^{\beta}$ (Hz)	
	calc. <sup>a</sup>	exp. <sup>b</sup>	calc.	exp.
D <sub>2</sub> O	4.1	4.0	5.1	4.5
DMSO- <i>d</i> <sub>6</sub>	4.7	4.1	5.4	5.1

<sup>a</sup>Calculated using the expression of Thøgersen as applied by Pérez *et al.*<sup>69</sup> for the conformations  $-25^{\circ}/-15^{\circ}$  (D<sub>2</sub>O) and  $-10^{\circ}/-10^{\circ}$  (DMSO-*d*<sub>6</sub>) for methyl  $\alpha$ -maltoside.

<sup>b</sup>Experimental values of Pérez *et al.*<sup>69</sup> for methyl  $\beta$ -maltoside.

3.0 Å. Since an intramolecular hydrogen bond between OH-3 and OH-2' does not form in the case of the xyloside **12**, it seems that the stabilizing energy of such a hydrogen bond does not need to be considered in the conformational analysis of maltose in DMSO. Intramolecular hydrogen bonding is also not important to the conformational preference in aqueous solution since none of the compounds examined provided a conformation suitable for its formation in D<sub>2</sub>O. Therefore, it is clear that hydrogen bond formation occurs only as a consequence of a favorable conformation that is dictated by the *exo*-anomeric effect and non-bonded interactions as previously stated by Lemieux and Bock<sup>51</sup>.

The direction of the conformational change when the solvent is changed from DMSO-*d*<sub>6</sub> to D<sub>2</sub>O, as indicated by the n.O.e.'s, is towards values more favorable to stronger *exo*-anomeric effects. That such conformational change takes place when the solvent is changed is not surprising since it is known<sup>24</sup> that the *exo*-anomeric effect is stronger in aqueous solution due to partial delocalization of the lone electron pair of the ring oxygen with a hydrogen of a



Table 22. Comparison of experimental and calculated nuclear Overhauser enhancements.

Compound	Solvent	Relative n.O.e.'s		n.m.r. conformers <sup>c</sup>		HSEA conformer	
		exp. <sup>a</sup>	calc. <sup>b</sup>	torsion angles (φ/ψ)	distance O3-O2' (Å) <sup>d</sup>	torsion angles (φ/ψ)	distance O3-O2' (Å) <sup>d</sup>
αDGlC(1→4)αDGlCOMe (13)	D <sub>2</sub> O	0.98	0.96	-25°/-15°	3.33	-30°/-25°	3.52
	DMSO-d <sub>6</sub>	1.26	1.21	-10°/-10°	2.80		
1,2-dideoxymaltose (7)	D <sub>2</sub> O	0.91	0.90	-30°/-15°	3.50	-30°/-25°	3.52
	DMSO-d <sub>6</sub>	1.28	1.29	-5°/-5°	2.74		
αDGlC(1→4)-3 deoxy-αDGlCOMe (1)	D <sub>2</sub> O	0.41	0.41	-35°/-35°	N/A	-35°/-35°	N/A
	DMSO-d <sub>6</sub>	0.47	0.50	-30°/-35°	N/A		
6-deoxy-αDGlC(1→4)-6-deoxy-αDGlCOMe (16)	D <sub>2</sub> O	0.70	0.76	-30°/-25°	3.52	-30°/-25°	3.52
	DMSO-d <sub>6</sub>	1.55	1.32	0°/0°	2.70		
αDGlC(1→4)-6-deoxy-βDGlCOMe (2)	D <sub>2</sub> O	0.91	0.90	-30°/-15°	3.50	-30°/-25°	3.52
	DMSO-d <sub>6</sub>	1.17	1.21	-10°/-10°	2.80		
αDGlC(1→4)αDManOMe (3)	D <sub>2</sub> O	0.91	0.94	-30°/-25°	3.44	-35°/-25°	3.61
	DMSO-d <sub>6</sub>	-	-	-	-		
αDGlC(1→4)αDXylOMe (12)	D <sub>2</sub> O	0.81	0.73	-50°/-10°	4.14	-50°/-10°	4.14
	DMSO-d <sub>6</sub>	0.81	0.82	-45°/-10°	3.99		

<sup>a</sup>Ratio of average enhancements of the signals for H4 and H2' upon saturation of H-1'

<sup>b</sup>Calculated relative nOe (H4/H2') that best reproduce the experimental data setting  $\omega = -90^\circ$  and  $\tau = 117^\circ$ .

<sup>c</sup>The conformations that best reproduce the experimental nOe's.

<sup>d</sup>For effective intramolecular hydrogen bonding this internuclear distance should be in the range 2.7-3.0 Å.

water molecule as shown in Figure 48. The *endo*-anomeric effect, which is in competition with the *exo*-anomeric effect is therefore weaker whereas the latter is enforced. The fact that the change is negligible for the 3-deoxy compound **1** and the xyloside **12** suggests that even in DMSO- $d_6$  these have a conformation that meets the demands of the *exo*-anomeric effect to the extent allowed by the non-bonded interactions.

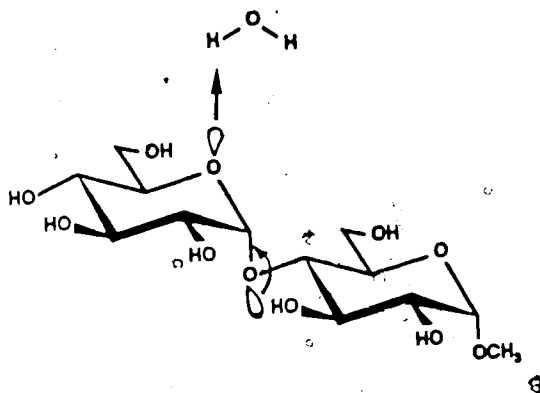


**Figure 48.** Structure of methyl  $\alpha$ -maltoside to illustrate that partial delocalization of the lone electron pair of the ring oxygen of glycosides by way of hydrogen bonding to a molecule of water strengthens the *exo*-anomeric effect.

A comparison of Figures 4 and 47 shows that the conformations found in the solid state for maltosides are not reproduced by the experimental data presented in this thesis. Consequently, the use of crystal structures in the assignment of conformations in solution, not surprisingly, may be misleading. On the other hand, as seen in Figure 47, the conformation of methyl  $\alpha$ -maltoside in  $D_2O$  is similar to those found in the crystal structures of methyl  $\alpha$ -maltotrioside<sup>37</sup>, V<sub>1</sub>-amylose<sup>43</sup> and B-amylose<sup>44</sup>. This fact suggests that the

conformational preference of the higher oligosaccharides is determined, at least in part, by the conformational properties, including the *exo*-anomeric effect, of the building unit; namely, maltose.

In an X-ray crystallographic study of a complex between maltoheptaose and a phosphorylase enzyme specific for glycogen, Fletterick and coworkers<sup>17,155</sup> discovered that the oligosaccharide was bound at an allosteric site present as a shallow groove at the surface of the protein. The authors found it surprising that parts of the maltoheptaose chain showed sufficient rigidity that a helical structure could be discerned that extended into the aqueous phase. On the basis of the electron density map at 2.5 Å resolution, it was concluded that the oligosaccharide exhibits a left-handed helical conformation with average torsion angles  $\phi/\psi = -15^\circ/-15^\circ$ . Goldsmith and Fletterick<sup>17</sup> stated "... all the conformations we observe, with a single exception, retain the O2 - O3' hydrogen bond whether or not they are to the protein. Therefore we might expect the hydrogen bond to have some long term stability in solution also." It should be noted however that the experimental results presented in this thesis prove beyond doubt that this bond does not exist for either methyl  $\alpha$ -maltoside or methyl  $\alpha$ -maltotrioside in aqueous solution where the time-averaged n.m.r. conformer has an O-2' - O-3 internuclear distance of 3.3 Å. Actually, it seems improbable that the X-ray data could reliably distinguish between conformers with  $\phi/\psi = -15^\circ/-15^\circ$  (O-2' - O-3 distance of 3.0 Å) and  $\phi/\psi = -25^\circ/-15^\circ$ . Consequently, the claim by Goldsmith and Fletterick<sup>17</sup> "Our results here show that the intramolecular hydrogen bond is a dominant factor, both for the solution structure of the oligosaccharide and in its interaction with the protein.", must be re-examined as also the use of this postulation for the rejection of a contribution to conformational stability by the *exo*-anomeric effect. Should the intramolecular hydrogen bond observed for

**Table 23.** Comparison of the experimental relative n.O.e. with those calculated for methyl  $\alpha$ -maltoside (13), using the results of Kochetkov *et al.*<sup>a</sup> and of HSEA calculations.

Conformers $\phi^\circ/\psi^\circ$	Conformational energies (kcal/mol)		Conformer populations (mol fractions)		Calculated relative n.O.e.'s <sup>c</sup>
	Kochetkov <i>et al.</i> <sup>a</sup>	HSEA <sup>b</sup>	Kochetkov <i>et al.</i>	HSEA	
-70/-40	-4.2	7.3	0.6	$\sim 10^{-6}$	0.14
-20/-20	-3.1	-0.7	0.3	>0.99	0.98
20/30	-2.4	14.3	0.07	$\sim 10^{-11}$	0.69
-30/-160	-2.6	3.3	0.03	$\sim 10^{-3}$	-0.03

<sup>a</sup>Conformer distribution which was obtained using the parametrization of Scott and Scheraga for the non-bonded interactions and a torsional strain contribution around the glycosidic bond estimated by Tvaroska and Bieha.

<sup>b</sup>Conformational energies produced by HSEA calculations using the  $\omega$  torsion angle =  $-90^\circ$  and  $\tau$  interunit valence angle =  $117^\circ$ .

<sup>c</sup>Calculated ratio of the enhancements of H-4 over H-2' upon saturation of H1' with  $\omega = -90^\circ$  and  $\tau = 117^\circ$ . The statistical average relative n.O.e. expected on the basis of the Kochetkov *et al.* distribution is 0.42 and that by HSEA is 0.98. The experimental relative n.O.e. was 0.98.

maltoheptaose in the oligosaccharide-protein complex actually exist then this result could arise from the glucose units being at least in part in an hydrophobic environment. In this event, the situation would be similar to that for methyl  $\alpha$ -maltoside in DMSO- $d_6$ , where the intramolecular hydrogen bond was found to exist. Regardless of whether or not the O-3 to O-2' distances are within hydrogen bonding range, the evidence that maltoheptaose has a rather restricted conformation is convincing and no longer surprising in view of the

conclusions reached in this thesis. As seen in Figure 47, the conformation of the glucose units in crystalline amylose are similar to those of maltoheptaose but quite different to those for maltose and methyl  $\alpha$ -maltotrioxide. It is apparent, therefore, that once a sufficient number of glucose units are present to describe the left-handed helical structure that interunit interactions occur which tend to stabilize this conformation.

Kochetkov and coworkers<sup>56</sup> recently concluded that methyl  $\alpha$ -maltoside exists in aqueous solution largely as an equilibrium of four conformers (Tables 2 and 23). Two of these conformers, namely,  $-70^\circ / -40^\circ$  and  $-20^\circ / -20^\circ$  were considered to comprise 60% and 30% of the conformer population, respectively. The experimental n.O.e. data presented in Table 17 show that the  $-70^\circ / -40^\circ$  conformer cannot contribute importantly since the relative observed n.O.e. (H-4 / H-2') is 0.98 and that expected for the  $-70^\circ / -40^\circ$  conformer is only 0.14. The  $-20^\circ / -20^\circ$  conformer agrees with the n.O.e. data and indeed is provided by the HSEA calculation. The  $-70^\circ / -40^\circ$  conformer is highly unfavorable. Therefore, it is seen that only HSEA calculations provide conformations that are close to the experimental values. This conclusion should be contrasted to the very recent statement by Tvaroska and Pérez<sup>92</sup> that HSEA calculations should be avoided.

#### IV. REFERENCES

1. D. FRENCH, *MTP Int. Rev. Sci.: Biochemistry, Ser. One* **5**, 267 (1975).
2. C. T. GREENWOOD, *Adv. Carbohydr. Chem.* **11**, 335 (1956).
3. G. S. C. KIRCHOFF, *C. R.* **14**, 389 (1813).  
G. M. DYSON, "A manual of organic chemistry for advanced studies",  
vol. 1, Longmans, Green and Co., London, 1950, p. 812.
4. T. SAUSSURE, *Ann. Chim. Phys.* **11**, 379 (1819).
5. A. P. DUBRUNFAUT, *Ann. Chim. Phys.* **21**, 178 (1847).
6. E. MEISSL, *J. pr. Chem.* **25**, 114 (1882).
7. W. N. HAWORTH AND G. C. LEICHT, *J. Chem. Soc.* 809 (1919).
8. W. N. HAWORTH AND S. PEAT, *J. Chem. Soc.* 3094 (1926).
9. W. N. HAWORTH, C. W. LONG AND J. H. G. PLANT, *J. Chem. Soc.* 2809  
(1927).
10. C. S. HUDSON, *J. Am. Chem. Soc.* **31**, 66 (1909).
11. C. E. BALLOU, S. ROSEMAN AND K. P. LINK, *J. Am. Chem. Soc.* **73**, 1140  
(1951).
12. R. U. LEMIEUX AND S. KOTO, *Tetrahedron* **30**, 1933 (1974).
13. F. TUKUSAGAWA AND R. A. JACOBSON, *Acta Crystallogr.* **B34**, 213 (1978).
14. S. S. C. CHU AND G. A. JEFFREY, *Acta Crystallogr.* **23**, 1038 (1967).
15. IUPAC-IUB COMMISSION ON BIOCHEMICAL NOMENCLATURE, *Arch. Biochem.  
Biophys.* **145**, 405 (1971).
16. IUPAC-IUB COMMISSION ON BIOCHEMICAL NOMENCLATURE, *J. Molec. Biol.*  
**52**, 1 (1970).
17. E. GOLDSMITH AND R. J. FLETTERICK, *Pure and Appl. Chem.* **55**, 577  
(1983).

18. K. BOCK, *Abstr. Int. Carbohydr. Symp. XIIIth, Ithaca* p. 1 (1986).
19. R. U. LEMIEUX, "IUPAC Frontiers of Chemistry", K. J. Laidler, ed., Pergamon Press, New York, 1982, p. 3.
20. D. A. BRANDT, *Q. Rev. Biophys.* **9**, 527 (1976).
21. R. CLEVEN, C. VAN DER BERG AND L. VAN DER PLAS, *Starch/Stärke* **30**, 223 (1978).
22. V. S. R. RAO, P. R. SUNDARARAJAN, C. RAMAKRISHNAN AND G. N. RAMACHANDRAN, in "Conformation of biopolymers", (Ed. G. N. Ramachandran), Academic Press, New York, 1967, Vol. 2, p. 721.
23. D. A. REES AND W. E. SCOTT, *J. Chem. Soc. B* 469 (1971).
24. J. P. PRALY AND R. U. LEMIEUX, *Can. J. Chem.* **65**, 213 (1987).
25. G. M. LIPKIND, V. E. VEROVSKY AND N. K. KOCHETKOV, *Bioorg. Khim.* **9**, 1269 (1983).
26. G. M. LIPKIND, V. E. VEROVSKY AND N. K. KOCHETKOV, *Carbohydr. Res.* **133**, 1(1984).
27. E. A. KABAT, J. LIAO, M. H. BURZYNSKA, T. C. WONG, H. THØGENSEN AND R. U. LEMIEUX, *Mol. Immunol.* **18**, 873 (1981).
28. O. HINDSGAUL, T. NORBERG, J. LEPENDU AND R. U. LEMIEUX, *Carbohydr. Res.* **109**, 109 (1982).
29. U. SPOHR, O. HINDSGAUL AND R. U. LEMIEUX, *Can. J. Chem.* **63**, 2644 (1985).
30. O. HINDSGAUL, D. P. KHARE, M. BACH AND R. U. LEMIEUX, *Can. J. Chem.* **63**, 2653 (1985).
31. U. SPOHR, N. MORISHIMA, O. HINDSGAUL AND R. U. LEMIEUX, *Can. J. Chem.* **63**, 2659 (1985).

32. R. U. LEMIEUX, A. P. VENOT, U. SPOHR, P. BIRD, G. MANDAL, N. MORISHIMA, O. HINDSGAUL AND D. R. BUNDLE, *Can. J. Chem.* **63**, 2664 (1985).
33. G. A. JEFFREY AND M. SUNDARALINGAM, *Adv. Carbohydr. Chem. Biochem.* **43**, 203 (1985).
34. M. E. GRESS AND G. A. JEFFREY, *Acta Crystallogr.* **B33**, 2490 (1977).
35. I. TANAKA, N. TANAKA, T. ASHIDA AND M. KAKUDO, *Acta Crystallogr.* **B32**, 155 (1976).
36. F. BRISSE, R. H. MARCHESSAULT, S. PEREZ AND P. ZUGENMAIER, *J. Am. Chem. Soc.* **104**, 7470 (1982).
37. W. PANGBORN, D. LANGS AND S. PEREZ, *Int. J. Biol. Macromol.* **7**, 363 (1985).
38. B. CASU, M. REGGIANI, G. G. GALLO AND A. VIGEVANI, *Tetrahedron* **22**, 3061 (1966).
39. K. LIDNER AND W. SAENGER, *Acta Crystallogr.* **B38**, 203 (1982).
40. G. J. QUIGLEY, A. SARKO AND R. H. MARCHESSAULT, *J. Am. Chem. Soc.* **92**, 5834 (1970).
41. J. R. KATZ, in "A comprehensive survey of starch chemistry", R. P. Walton, ed., vol. 1, Chemical Catalog Co., New York, p. 68, 1928.
42. A. GUILBOT AND C. MERCIER, in "The polysaccharides", G. O. Aspinall, ed., vol. 3, Academic Press, Orlando, p. 209, 1985.
43. D. A. REES, *MTP Int. Rev. Sci.: Org. Chem. Ser. One* **7**, 251 (1973).
44. J. BLACKWELL, A. SARKO AND R. H. MARCHESSAULT, *J. Mol. Biol.* **42**, 379 (1969).
45. H. C. M. WU AND A. SARKO, *Carbohydr. Res.* **61**, 7 (1978).
46. H. C. M. WU AND A. SARKO, *Carbohydr. Res.* **61**, 27 (1978).
47. K. KAINUMA AND D. FRENCH, *Biopolymers* **11**, 2241 (1972).



48. G. RÄPPENECKER AND P. ZUGENMAIER, *Carbohydr. Res.* **89**, 11 (1981).
49. D. A. REES, *J. Chem. Soc. B*, 877 (1970).
50. J. H. BREWSTER, in "Topics in stereochemistry", ed. N. L. Allinger and E. L. Eliel, Wiley, New York, 1967, vol. 2, p. 1.
51. R. U. LEMIEUX AND K. BOCK, *Arch. Biochem. Biophys.* **221**, 125 (1983).
52. G. A. JEFFREY AND S. TAKAGI, *Acta Crystallogr.* **B33**, 738 (1977).
53. G. A. JEFFREY, R. K. McMULLAN AND S. TAKAGI, *Acta Crystallogr.* **B33**, 728 (1977).
54. R. U. LEMIEUX AND J. T. BREWER, in "Carbohydrates in solution", Advances in chemistry series #117; R. F. Gould, ed., American Chemical Society, Washington, D.C., p. 121, (1973).
55. I. TVAROSKA, *Biopolymers* **21**, 1887 (1982).
56. A. S. SHASHKOV, G. M. LIPKIND AND N. K. KOCHETKOV, *Carbohydr. Res.* **147**, 175 (1986).
57. D. A. REES AND P. J. C. SMITH, *J. Chem. Soc. Perkin II* 836 (1975).
58. D. A. REES AND D. THOM, *J. Chem. Soc. Perkin II* 191 (1977).
59. D. A. REES, E. R. MORRIS, D. THOM AND J. K. MADDEN, in "The Polysaccharides", G. O. Aspinall, ed., vol. 1, Academic Press, New York, p. 195, 1982.
60. J. L. NEAL AND D. A. I. GORING, *Can. J. Chem.* **48**, 3745 (1970).
61. K. BOCK, *Pure and Appl. Chem.* **55**, 605 (1983).
62. R. U. LEMIEUX, D. R. BUNDLE AND D. A. BAKER, *J. Am. Chem. Soc.* **97**, 4076 (1975).
63. R. U. LEMIEUX, K. BOCK, L. T. J. DELBAERE, S. KOTO AND V. S. RAO, *Can. J. Chem.* **58**, 631 (1980).
64. N. K. KOCHETKOV, O. S. CHIZHOV AND A. S. SHASHKOV, *Carbohydr. Res.* **133**, 173 (1984).

65. R. U. LEMIEUX, T. L. NAGABHUSHAN AND B. PAUL, *Can. J. Chem.* **50**, 773 (1972).
66. R. WASYLISHEN AND T. SCHAEFER, *Can. J. Chem.* **50**, 2710 (1972).
67. G. K. HAMER, F. BALZA, N. CYR AND A. S. PERLIN, *Can. J. Chem.* **56**, 3109 (1978).
68. C. A. G. HAASNOOT, F. A. A. M. DE LEEUW AND C. ALTONA, *Tetrahedron* **36**, 2783 (1980).
69. S. PEREZ, F. TARAVEL AND C. VERGELATI, *Nouv. J. Chim.* **9**, 561 (1985).
70. L. EVELYN, L. D. HALL AND J. D. STEVENS, *Carbohydr. Res.* **100**, 55 (1982).
71. J. H. NOGGLE AND R. E. SCHIRMER, "The nuclear Overhauser effect", Academic Press, New York, 1971.
72. R. E. SCHIRMER, J. H. NOGGLE, J. P. DAVIS AND P. A. HART, *J. Am. Chem. Soc.* **92**, 3266 (1970).
73. G. M. CLORE AND A. M. GRONENBORN, *J. Magn. Reson.* **61**, 158 (1985).
74. H. THØGENSEN, R. U. LEMIEUX, K. BOCK AND B. MEYER, *Can. J. Chem.* **60**, 44 (1982).
75. E. ALVARADO, O. HINDSGAUL, R. U. LEMIEUX, K. BOCK AND H. PEDERSEN, *Abstr. Int. Carbohydr. Symp. XIIIth, Utrecht* p. 480 (1984).
76. E. ALVARADO, A. J. RAGAUSKAS AND R. U. LEMIEUX, *Abstr. Int. Carbohydr. Symp. XIIIth, Ithaca* p. 133 (1986).
77. N. L. ALLINGER, *Adv. Phys. Org. Chem.* **13**, 1 (1976).
78. CLARK, "A handbook of computational chemistry", Wiley, New York, 1985.
79. K. RASMUSSEN, "Potential energy functions in conformational analysis", Springer-Verlag, Berlin, 1985.

80. G. A. JEFFREY, J. A. POPLE, J. S. BINKLEY AND S. VISHVESHWARA, *J. Am. Chem. Soc.* **100**, 373 (1978).
81. S. MELBERG, K. RASMUSSEN, R. SCORDAMAGLIA AND C. TOSI, *Carbohydr. Res.* **76**, 23 (1979).
82. B. SHELDRIK AND D. ALDRIGG, *Acta Crystallogr.* **B36**, 1615 (1980).
83. S. ARNOTT AND W. E. SCOTT, *J. Chem. Soc. Perkin II* 324 (1972).
84. L. PAULING, *Proc. Natl. Acad. Sci. U.S.A.* **44**, 211 (1958).
85. L. PAULING, "The nature of the chemical bond", Cornell University Press, Ithaca, New York, 3rd ed. p. 130, 1960.
86. J. M. KLOTZ AND J. S. FRANSEN, *J. Am. Chem. Soc.* **84**, 3461 (1962).
87. R. A. SCOTT AND H. A. SCHERAGA, *J. Chem. Phys.* **44**, 3054 (1966).
88. F. A. MOMANY, L. M. CARRUTHERS, R. F. MCGUIRE AND H. A. SCHERAGA, *J. Chem. Phys.* **78**, 1595 (1974).
89. A. I. KITAIGORODSKY, *Tetrahedron* **14**, 230 (1961).
90. S. MELBERG AND K. RASMUSSEN, *Carbohydr. Res.* **78**, 215 (1980).
91. S. MELBERG AND K. RASMUSSEN, *Carbohydr. Res.* **69**, 27 (1979).
92. I. TVAROSKA AND S. PEREZ, *Carbohydr. Res.* **149**, 389 (1986).
93. C. M. VENKATACHALAM AND G. N. RAMACHANDRAN, in "Conformation of biopolymers", G. N. Ramachandran, ed., Academic Press, New York, vol. 1, p. 83, 1967.
94. R. G. BALL, A. P. VENOT AND R. U. LEMIEUX, unpublished results.
95. R. U. LEMIEUX, T. C. WONG AND H. THØGENSEN, *Can. J. Chem.* **60**, 81 (1982).
96. C. ROUSSEL, A. LIDEN, M. CHANNON, J. METZGER AND J. SANDSTRÖM, *J. Am. Chem. Soc.* **98**, 2847 (1976).
97. D. D. PERRIN, W. L. ARMAREGO AND D. R. PERRIN, "Purification of laboratory chemicals", Pergamon Press, London, 2nd. ed., 1980.

98. G. W. KRAMER, A. B. LEVY AND M. MIDLAND, "Organic synthesis via boranes", McGraw-Hill, New York, chapter 9, 1972.
99. Y. THEIRAULT, Y. MORIO AND G. KOTOVYCH, *Can. J. Chem.* **57**, 165 (1979).
100. R. J. OULLETTE, *Can. J. Chem.* **43**, 707 (1965).
101. J. C. LINDON AND A. G. FERRIGE, *Prog. in NMR Spectroscopy* **14**, 27 (1980).
102. R. L. VOLD, J. S. VAUGH, M. P. KLEIN AND D. E. PHELPS, *J. Chem. Phys.* **48**, 3831 (1968).
103. DISNMR Program: Copyright, Bruker Spectrospin AG, Switzerland.
104. H. KAWAKI, H. BEIERBECK AND G. KOTOVYCH, *J. Biomol. Struct. Dyn.* **3**, 161 (1985).
105. J. H. PAZUR, J. M. MARSH AND T. ANDO, *J. Am. Chem. Soc.* **81**, 2170 (1959).
106. W. N. HAWORTH, E. L. HIRST AND R. J. W. REYNOLDS, *J. Chem. Soc.* 302 (1934).
107. A. THOMPSON AND M. L. WOLFROM, *Methods Carbohydr. Chem.* **2**, 215 (1963).
108. H. J. JENNINGS, *Can. J. Chem.* **49**, 1355 (1971).
109. N. MORISHIMA, S. KOTO, C. KUSUHARA AND S. ZEN, *Bull. Chem. Soc. Jn.* **55**, 631 (1982).
110. R. U. LEMIEUX, K. B. HENDRIKS, R. V. STICK AND K. JAMES, *J. Am. Chem. Soc.* **97**, 4056 (1975).
111. S. L. COOK AND J. A. SECRET III, *J. Am. Chem. Soc.* **101**, 1554 (1979).
112. K. TAKEO, T. SUMIMOTO AND T. KUGE, *Stärke* **26**, 111 (1974).
113. J. C. IRVINE AND I. M. A. BLACK, *J. Chem. Soc.* 862 (1926).
114. D. H. BRAUNS, *J. Am. Chem. Soc.* **51**, 1820 (1929).

115. M. L. WOLFROM, Y. -L. HUNG, P. CHAKRAVARTY, G. U. YUEN AND D. HORTON, *J. Org. Chem.* **31**, 2227 (1966).
116. S. E. ZURABYAN, V. BILIK AND S. BAUER, *Chem. Zvesti* **23**, 923 (1969); *Chem. Abstr.* **75**, 6235a (1971).
117. Y. INOUE, K. ONODERA, I. KARASAWA AND Y. NISHISAWA, *Nippon Nogei Kagaku Kaishi (J. Agr. Chem. Soc. Japan)* **26**, 631 (1952).
118. E. PACSU, J. JANSON AND B. LINDBERG, *Methods Carbohydr. Chem.* **2**, 376 (1963).
119. W. E. DICK, JR., D. WEISLEDER AND J. E. HODGE, *Carbohydr. Res.* **18**, 115 (1971).
120. W. E. DICK, JR., AND J. E. HODGE, *Methods Carbohydr. Chem.* **7**, 15 (1976).
121. P. W. AUSTIN, F. E. HARDY, J. G. BUCHANAN AND J. BADDILEY, *J. Chem. Soc.* 5350 (1963).
122. P. JANDERA AND J. CHURÁČEK, *J. Chromatogr.* **98**, 55 (1974).
123. R. KHAN, *Adv. Carbohydr. Chem. Biochem.* **39**, 213 (1981).
124. S. J. ANGYAL AND K. JAMES, *Aust. J. Chem.* **23**, 1209 (1970).
125. M. BERTOLINI AND C. P. J. GLAUDEMANS, *Carbohydr. Res.* **17**, 449 (1971).
126. P. DESLONGCHAMPS, *Tetrahedron* **31**, 2463 (1975).
127. R. U. LEMIEUX AND S. KOTO, *Tetrahedron* **30**, 1933 (1974).
128. A. J. KIRBY, "The anomeric effect and related stereoelectronic effects at oxygen", Springer-Verlag, Berlin, p. 96, 1983.
129. S. J. ANGYAL AND K. JAMES, *Carbohydr. Res.* **12**, 147 (1970).
130. S. MATSUBARA, *J. Biochem. (Tokyo)* **49**, 226 (1961).
131. K. BOCK AND H. THØGERSEN, *Annu. Rep. NMR. Spectrosc.* **13**, 1 (1983).
132. K. TAKEO, K. MINE AND T. KUGE, *Carbohydr. Res.* **48**, 197 (1976).
133. B. MEYER, *XIth Int. Carbohydr. Symp.*, Vancouver 1982, Abstr. II/25.

134. K. BOCK, personal communication.
135. A. DE BRUYN, M. ANTEUNIS AND G. VERHEGGE, *Bull. Soc. Chim. Belg.* **84**, 721 (1975).
136. A. HEYRAUD, M. RINAUDO, M. VIGNON AND M. VINCENDON, *Biopolymers* **18**, 167 (1979).
137. J. D. MERSH AND J. K. M. SANDERS, *Org. Magn. Reson.* **18**, 122 (1982).
138. L. E. KAY, J. N. SCARDALE, D. R. HARE AND J. H. PRESTEGARD, *J. Magn. Reson.* **68**, 515 (1986).
139. H. LIMBACH, *Stud. Phys. Theor. Chem.* **26**, 410 (1983).
140. M. ST-JACQUES; P. R. SUNDARARAJAN, K. J. TAYLOR AND R. H. MARCHESSAULT, *J. Am. Chem. Soc.* **98**, 4386 (1976).
141. R. U. LEMIEUX AND K. BOCK, *Jpn. J. Antibiot.* **XXXII**, Suppl. S-163 (1979).
142. K. BOCK AND R. U. LEMIEUX, *Carbohydr. Res.* **100**, 63 (1982).
143. P. E. HANSEN, *Annu. Rep. NMR Spectrosc.* **15**, 105 (1983).
144. D. A. FORSYTH, in "Isotopes in Organic Chemistry", E. Buncl and C. C. Lee, eds., vol. 6, Elsevier, p. 1, 1984.
145. L. J. ALTMAN, D. LAUNCONI, G. GUNNARSSON, H. WENNERSTRÖM AND S. FORSEN, *J. Am. Chem. Soc.* **100**, 8264 (1978).
146. J. C. CHRISTOFIDES AND D. B. DAVIES, *J. Chem. Soc. Chem. Commun.* 560 (1982).
147. J. C. CHRISTOFIDES AND D. B. DAVIES, *J. Am. Chem. Soc.* **105**, 5099 (1983).
148. J. REUBEN, *J. Am. Chem. Soc.* **106**, 6180 (1984).
149. J. REUBEN, *J. Am. Chem. Soc.* **107**, 1747 (1985).
150. J. REUBEN, *J. Am. Chem. Soc.* **107**, 1756 (1985).
151. J. C. CHRISTOFIDES, D. B. DAVIES, J. A. MARTIN AND E. B. RATHBONE, *J. Am. Chem. Soc.* **108**, 5738 (1986).

152. J. C. CHRISTOFIDES, D. B. DAVIES, *Magn. Reson. Chem.* **23**, 582 (1985).
153. R. U. LEMIEUX AND A. A. PAVIA, *Can. J. Chem.* **47**, 4441 (1969).
154. J. E. DEL BENE AND J. A. POPLE, *J. Chem. Phys.* **58**, 3605 (1973).
155. E. GOLDSMITH, S. SPRANG AND R. FLETTERICK, *J. Mol. Biol.* **156**, 411 (1982).

\_\_\_\_\_

\_\_\_\_\_

\_\_\_\_\_

\_\_\_\_\_

\_\_\_\_\_